

Washington University in St. Louis

Washington University Open Scholarship

Arts & Sciences Electronic Theses and
Dissertations

Arts & Sciences

Summer 8-15-2017

Identification and Characterization of an Interferon Stimulated Gene That Restricts Alphavirus Infection and Pathogenesis

Subhajit Poddar

Washington University in St. Louis

Follow this and additional works at: https://openscholarship.wustl.edu/art_sci_etds



Part of the [Allergy and Immunology Commons](#), [Immunology and Infectious Disease Commons](#), [Medical Immunology Commons](#), and the [Virology Commons](#)

Recommended Citation

Poddar, Subhajit, "Identification and Characterization of an Interferon Stimulated Gene That Restricts Alphavirus Infection and Pathogenesis" (2017). *Arts & Sciences Electronic Theses and Dissertations*. 1223.

https://openscholarship.wustl.edu/art_sci_etds/1223

This Dissertation is brought to you for free and open access by the Arts & Sciences at Washington University Open Scholarship. It has been accepted for inclusion in Arts & Sciences Electronic Theses and Dissertations by an authorized administrator of Washington University Open Scholarship. For more information, please contact digital@wumail.wustl.edu.

WASHINGTON UNIVERSITY IN ST. LOUIS

Division of Biology and Biomedical Sciences

Immunology

Dissertation Examination Committee:

Michael Diamond, Chair

Jacco Boon

Marco Colonna

Daved Fremont

Deborah Lenschow

Identification and Characterization of an Interferon Stimulated Gene That Restricts Alphavirus
Infection and Pathogenesis

By

Subhajit Poddar

A dissertation presented to
The Graduate School
of Washington University in
partial fulfillment of the
requirements for the degree
of Doctor of Philosophy

August 2017

St. Louis, Missouri

© 2017, Subhajit Poddar

Table of Contents

	Page
Acknowledgements	iii
Abstract	v
Chapter 1: Introduction	1
Chapter 2: Screening for novel antiviral ISGs against alphaviruses and orthobunyaviruses	16
Chapter 3: Characterization of murine Ifitm3 as an antiviral ISG against alphaviruses <i>in vitro</i> and <i>in vivo</i>	59
Chapter 4: Conclusions and Future Directions	98
References	106
Curriculum Vitae	121

ACKNOWLEDGEMENTS

This dissertation would not have been completed without the help and kindness of many fantastic individuals. First and foremost, I would like to thank my mentor Dr. Michael Diamond for allowing me the opportunity to join his lab. His training, guidance and unyielding support have been vital in my growth as scientist. In addition, I have found his focus, drive and enthusiasm to be inspiring, and hope to carry it on to the next stages of my career. I would also like to thank my thesis committee for their support and interest in me and in my dissertation project. Drs. Jacco Boon, Marco Colonna, Daved Fremont, and Deborah Lenschow have all been instrumental in providing advice and insight in both the critical and not so critical times in my Ph.D. journey, and will always be greatly appreciated.

I would also like to thank the many members of the lab, both past and present, with whom I have had the pleasure of being friends and colleagues with. It has been a true honor to be able to work with and learn from so many talented, bright and dedicated people. Everyone's friendliness and willingness to lend an ear, or even a hand, helped make the lab a fantastic environment to work in.

I am also grateful for the many friends that I have made during my time here as a graduate student in Washington University. I am thankful for the support network we all naturally seemed to generate for ourselves, and providing each other a much needed outlet during the high, low and mundane periods of our tenure as trainees.

Last but definitely not least, I thank my family. I would not be the person I am today, with the opportunities I have now, were it not for their constant love, support, dedication and sacrifice.

Subhajit Poddar

Washington University in St. Louis

August 2017

ABSTRACT OF DISSERTATION

Identification and Characterization of an Interferon Stimulated Gene That Restricts Alphavirus

Infection and Pathogenesis

By

Subhajit Poddar

Doctor of Philosophy in Biology and Biomedical Sciences

(Immunology)

Washington University in St. Louis, 2017

Professor Michael Diamond, Chair

Viral infection of host cells induces the Type I interferon (IFN) response, which is characterized by the production of hundreds of IFN-stimulated genes (ISGs). Altogether, these ISGs function to induce an antiviral state, hindering or blocking various steps of the viral lifecycle. Many individual ISGs have potent and broad antiviral functions. However elimination of a single ISG does not completely abrogate protection, suggesting that other ISGs, although moderate or moderate when considered alone, must work cooperatively to provide optimal antiviral activity.

In order to identify and characterize novel ISGs, an attenuated strain of the alphavirus chikungunya (CHIKV-181/25) was tested against an shRNA library of 243 curated murine genes upregulated during IFN treatment. An attenuated CHIKV strain was used with the assumption that ISGs with moderate or low activity may be more easily identified due to the reduced pathogenicity of the virus. In addition, the orthobunyavirus LaCrosse (LACV) was also tested, as

there have been no large scale ISG screens using this pathogen. A total of 21 and 30 novel murine ISGs that putatively restrict infection were identified from the CHIKV-181/25 screen and the LACV screen, respectively.

Although independent confirmation of many candidate antiviral ISG targets using bulk CRISPR lines is still ongoing, we were able to validate and characterize the antiviral role of one of these targets, IFITM3, against alphaviruses *in vitro* and *in vivo*. Alphaviruses, which were previously thought to be unaffected by this ISG, exhibit reduced replication due to restriction by Ifitm3 at the endosomal fusion stage of infection. *Ifitm3*^{-/-} mice infected with CHIKV exhibited greater swelling of the ipsilateral foot at peak days of pathology. Higher viral titers in the spleen, serum and ipsilateral foot were seen at 1 day after infection, coinciding with increased cytokines and chemokines in the ipsilateral foot. Splenic macrophages from *Ifitm3*^{-/-} mice exhibited greater levels of viral antigen at 1 day after infection with CHIKV, and cultured bone marrow derived macrophages lacking Ifitm3 supported enhanced CHIKV replication. To test whether Ifitm3 restricts encephalitic alphaviruses we infected WT and *Ifitm3*^{-/-} mice with VEEV-TC83-A3G, and observed increased mortality and viral burden in *Ifitm3*^{-/-} animals.

Chapter 1: Introduction

THE INNATE IMMUNE RESPONSE TO VIRAL INFECTION

The innate immune system allows for the rapid identification and response to infection in an antigen-independent manner. Through pattern recognition receptors (PRRs), host cells can detect a wide variety of pathogen-associated molecular patterns (PAMPs). PRRs are found on the surface, in endosomes, and the cytosol of host cells, and are activated by PAMPs unique to bacteria, fungi, parasites, or viruses. In the case of viral infection, there are several PRRs which can identify viral or foreign nucleic acids (1). The RIG-I like receptors (RIG-I and MDA-5) recognize viral single-stranded (ssRNA) and double-stranded RNA (dsRNA) in the cytoplasm, while cGAS/STING, IFI16 and DAI detect cytosolic DNA (2). Nucleic acids in the endosome are recognized by the Toll-like receptors TLR3 (ds RNA), TLR7 (ssRNA), and TLR9 (dsDNA) (3). Upon detection of viral nucleic acids, signaling cascades are initiated to activate the transcription factors IRF3, IRF7 and NF- κ B. These transcription factors induce the production of pro-inflammatory cytokines and Type I and III Interferons (IFN) (2).

TYPE I, II AND III IFN

Type I IFNs were first described in 1957 (4). They include IFN α (of which there are 12 subtypes), IFN β , and a series of other poorly defined cytokines such as IFN ϵ , IFN κ and IFN ω (2). Once secreted, IFN functions in an autocrine and paracrine manner, binding to the Type I Interferon receptor (IFNAR), a heterodimer which is expressed transiently on most host cells. This initiates a signal cascade through the JAK/STAT pathway, through which STAT1/STAT2 heterodimers bind to IRF9 and form the IFN-stimulated gene factor 3 (ISGF3) complex. ISGF3 binds to promoters containing IFN stimulated response elements (ISREs) (2), activating the

transcription of hundreds of genes (2). These genes, classified as Interferon Stimulated Genes (ISGs), function to restrict pathogenesis at the different steps of the viral replication cycle, thus inducing a rapid and broad antiviral state in both infected and local naïve host cells.

In addition to Type I IFN, Type III IFN (IFN λ 1, IFN λ 2, IFN λ 3 and IFN λ 4) can also be induced via the detection of viral PAMPs (2, 5), and can promote the induction of ISRE activated ISGs via the IFN λ receptor, albeit not as potently as Type I. However, the expression of the IFN λ receptor is restricted to epithelial cells and some immune cells, leaving most cells in the host unresponsive to Type III IFNs (2, 5).

Type II IFN, consisting only of IFN γ , is not transduced via the direct detection of viral PAMPs, but rather through the detection of the pro-inflammatory cytokine IL-12. Furthermore, IFN γ is only produced in neutrophils, natural killer cells and T cells. IFN γ signals through the Type II IFN receptor (IFNGR), initiating the JAK/STAT pathway and inducing the transcription of pro-inflammatory and apoptotic genes linked to IFN γ activated site (GAS) promoter elements, some of which are also found in the ISGs induced by Type I IFN (6).

INTERFERON STIMULATED GENES

In cell culture, the number of ISGs produced varies with the dosage, duration, type of IFN treatment and cell type tested. By microarray analysis, most cells upregulate between 200-1000 unique ISGs (7). The most potently inhibitory ISGs identified thus far function against a broad spectrum of viruses (7). However, antiviral activity is still seen in mice with targeted deletions of these ISGs (8), suggesting that other ISGs have significant and unique restrictive

functions. It is believed that most ISGs function as weak to moderate inhibitors, and work in a concerted manner to restrict infection.

ISGs preventing entry: IFITMs, which were the first family of antiviral ISGs discovered, appear to prevent the entry via the endocytic pathway of a broad range of viruses, including influenza A virus (IAV) and flaviviruses (9). TRIM5 α binds to the capsid proteins of retroviruses and accelerates uncoating of the virion (10). Mx is another potent ISG with antiviral properties against orthomyxoviruses, bunyaviruses, togaviruses and rhabdoviruses (2, 11). Mx proteins recognize and sequester viral nucleocapsids, preventing their transport to sites of genome amplification or egress. ADAP2 has recently been shown to restrict entry of DENV and VSV by altering endosomal uptake and intracellular trafficking (12).

ISGs preventing viral translation and transcription: Upon recognition of viral dsRNA in the cytosol, 2'-5' oligoadenylate synthetase (OAS) activates RNaseL to initiate nucleic acid degradation (13). APOBECs and ADAR have been shown to directly edit viral RNA, resulting in nucleic acid destabilization and the introduction of lethal mutations. IFITs can block translation of viral RNA by binding to the eIF3 complex. They can also recognize the 5'-ppp motif on viral RNA, or the lack of the 2'-O methylation group normally found in eukaryotic RNA, and prevents translation by directly sequestering them (14). PKR is a prominent ISG, which functions by binding to viral RNA and blocking translation by phosphorylating (and inactivating) the translation initiation factor EIF2 α (13).

ISGs preventing viral protein function, assembly and egress: ISG15 is an ubiquitin like modifier that conjugates viral proteins in a process called ISGylation, thus affecting a plethora of viral protein functions (15–17). Viperin associates with endoplasmic reticulum,

interfering with the assembly of viral proteins and egress of virions at the plasma membrane (18). Finally, tetherin has been shown to prevent the release of viral particles from the plasma membrane (19).

Proviral ISGs: ISGs have also been identified that induce an immunomodulatory response. In a high throughput screen, where ISGs were ectopically expressed *in vitro*, the ISGs *ADAR*, *APOBEC3A*, *LY6E*, *MCOLN*, *IDO1*, and *FAM46C*, increased replication of YFV, WNV, VEEV and CHIKV, though specific mechanisms are as of yet unclear (20). *ASCC3* was identified as a proviral ISG in WNV infection, which dampens Type I IFN dependent signals, possibly through modulating IRF3 and IRF7 (21). Suppressor of cytokine signaling (*SOCS*) is produced early in the Type I IFN response and binds to the phosphorylated tyrosine residues of the IFN receptors or the JAK proteins, thus blocking JAK-STAT signaling (2). USP18 is a potent down-regulator of the Type I IFN response. It binds to the intracellular domain of IFNAR2, altering its conformation and dramatically reducing the binding affinity of IFN α to the receptor (22).

PRIOR SCREENS TO IDENTIFY AND CHARACTERIZE NOVEL ISGS

The antiviral functions of many ISGs are largely unknown. Small-scale studies identified a few key ISGs involved in the restriction of certain viruses. For example, an siRNA screen against influenza A identified IFITM3 as a potent antiviral ISG, and was subsequently confirmed to restrict WNV and dengue virus (9). The first large scale ectopic expression screen was published in 2011. In this study, a lentiviral library expressing 380 human ISGs was used to determine restriction of six different viruses (Hepatitis C Virus (HCV), Human

Immunodeficiency Virus (HIV), YFV, WNV, VEEV, and CHIKV) (20). This ectopic expression based analysis identified ISGs that act broadly, or to only one virus. Most ISGs identified had moderate antiviral activity, and acted as inhibitors of translation. Expression of two different ISGs led to greater restriction of virus replication (20), confirming the notion that IFN based protection requires the additive effect of multiple ISGs.

Another group developed a large-scale screen to identify novel ISGs against WNV (21) by silencing gene targets using a lentiviral shRNA library against 245 human ISGs (23). This allowed investigation of the physiological role of each ISG in the context of an IFN-induced antiviral state. This approach could potentially identify ISGs that required a multicomponent complex to function. The screen against WNV identified 30 ISGs, of which 9 had not been previously identified to have any antiviral effect.

Other groups have performed genome wide siRNA based screens to identify novel ISGs *in vitro* against VSV, MHV-68, and HCV (24–26). An *in vivo* RNA interference screen was developed in which mice were infected with a library of Sindbis viruses (SINV) encoding artificial microRNA (amiRNAs) against murine ORFs. Virions with amiRNAs targeting inhibitory genes were selected for, and the transcription factors like Zfx and Mga were identified (27).

Recently a library of human and macaque ISGs were screened against eleven different retroviruses (28). Of the top antiviral ISGs discovered, around 60% targeted against a single retrovirus, while the remaining 40% were broadly effective. In addition, they also uncovered ISGs that functioned in a species specific manner. For example, human but not macaque

ANGTPL1 inhibited SIV infection. They go on to show that IDO1 (which was identified in a previous screen as proviral for other viruses (20)) and TRIM56 inhibit retroviral replication.

ALPHAVIRUSES

Alphaviruses are enveloped positive-sense ssRNA mosquito-borne viruses of the *Togaviridae* family and can be grouped as arthritogenic or encephalitic based on clinical symptoms. Arthritogenic alphaviruses present with severe polyarthralgia and polyarthritis while the encephalitic alphaviruses produce a severe febrile illness associated with infection and injury to neurons, encephalitis, long-term debilitating neurological sequelae, and death. Arthritogenic alphaviruses include CHIKV, Sindbis virus, O’Nyong-nyong virus, Ross River virus, Mayaro virus, and Semliki Forest virus and the encephalitic alphaviruses, including Venezuelan (VEEV), Eastern, and Western equine encephalitis viruses.

CHIKUNGUNYA VIRUS

CHIKV was originally isolated in 1952 in Tanzania, and has since cause explosive outbreaks worldwide. In fact, its name was derived from the Makonde word meaning “that which bends up”, alluding to the changes in posture and joint inflammation of patients suffering from the arthritic symptoms of infection (29).

Typically, patients infected with CHIKV develop a severe febrile illness marked by polyarthritis, headache, conjunctivitis, and rash that can progress to persistent arthritis that can

last for years after infection. CHIKV has become a growing concern since it emerged in the Caribbean in 2013 and subsequent spread to Central, South and North America, resulting in over 1.8 million cases (30). Currently, there are no approved therapies or vaccines to combat or prevent CHIKV infection.

CHIKV enters host cells via clatherin-mediated endocytosis, and fuses with the endosome in a pH-dependent manner. Replication of genomic RNA and translation of capsid protein occurs in the cytoplasm, which assemble into nucleocapsid cores. The E1 and E2 glycoproteins are translated in the endoplasmic reticulum, and further processed in the Golgi, before going to the plasma membrane. Nucleocapsid cores assemble with the surface glycoproteins at the plasma membrane, leading to budding of mature virions (31).

There are two mouse models of infection, the neonate model which can be used to determine viral dissemination and lethality, and the adult model which is used to better understand the acute symptoms and persistence of CHIKV-induced arthritis (32–34). In wild type mice as young as 4 weeks old, a biphasic pattern of swelling is observed in the inoculated foot. The first, small peak of swelling is seen at day 2 or 3 post infection, and is believed to be the result of viral replication in the fibroblasts, myocytes and osteoblasts, causing cell death, cytokine production and edema. The second, more prominent peak of swelling occurs at day 6-7 post infection, which is largely due to infiltration of immune cells and the subsequent induction of edema, myositis and synovitis. Swelling rapidly drops to near normal levels soon after. Infectious CHIKV can be isolated from the serum, spleen, muscles, liver and ankle joints as early as 1 day post infection, but is rapidly cleared and typically undetectable by 5 to 7 days post infection. However, CHIKV RNA can be detected in the spleen for up to 42 days post infection, and in the joints for essentially the life of the animal (35–37). In addition, studies have shown

that osteoblast infection induces increased osteoclast production in the joints, resulting in possible bone loss (38, 39).

CHIKV-181/25 (TSI-GSD-218) is an attenuated strain developed by the US Army through 18 serial passages of the parental CHIKV 15561 strain (40). While CHIKV-181/25 is immunogenic and protective, 8% of recipients developed chronic joint inflammation (41), and in at least one case symptoms were linked to a genetic reversion of the virus, thus preventing its use as an effective vaccine. The attenuated phenotype is mapped to two mutations in the E2 protein, which disturbs the binding of the virion to heparan sulfate on the cell surface. This reduction in binding affinity reduces the efficiency of infection, and also in turn affects cell spread and tropism *in vivo* (42). CHIKV-181/25 does not cause weight loss or death in WT, or in *IFN γ R^{-/-}* mice, and reduced morbidity in *IFNAR^{-/-}* mice. *Stat1^{-/-}* mice and IFN $\alpha\beta\gamma$ receptor knockout mice both suffer significant weight loss and mortality. Combined with evidence that *IFNAR^{+/-}* mice have reduced morbidity than *IFNAR^{-/-}* mice, it can be inferred that CHIKV-181/25 is susceptible to Type II and Type I IFN responses (43, 44).

IDENTIFIED ISGS AGAINST ALPHAVIRUSES

There are several studies characterizing the effect of ISGs against alphavirus infection. ISG15 protects against SINV *in vivo*, likely via conjugation (ISGylation) to viral proteins (15–17). Zinc finger antiviral protein (ZAP) restricts SINV, Ross River, Semliki Forest, and VEEV by blocking the accumulation of viral genomic content in the cytoplasm (8). Tetherin has recently been shown to prevent egress by tethering virus onto the cell membrane (19), and ZAP

has been shown to work synergistically with 16 other ISGs to enhance restriction, including IFITM3 (45).

In the absence of IFN, SINV is poorly restricted by RNaseL, and strongly inhibited by PKR in the context of replication in DCs (46). However, *PKR*^{-/-} mice are still protected from lethal infection of SINV (8), suggesting that other ISGs can still confer protection. A genetic screen of SINV infected PKR/RNaseL double knockout mice revealed 44 unique ISGs with possible antiviral activity, including *Isg20*, *Ifit1*, *Ifit2*, *Ifit3*, and viperin (also shown to be restrictive against CHIKV) (47). However, in the case of *Ifit1*, which recognizes RNA lacking a 2'O-methylation on the 5'cap structure and prevents translation, alphaviruses subvert this antiviral function via RNA secondary structure motifs that inhibit binding (48). Other ISGs like *HSPE* and *P2RY6* have been identified, though their mechanisms of restriction are currently unknown (7, 20).

LACROSSE VIRUS

LaCrosse (LACV) is an enveloped negative-sense ssRNA orthobunyavirus with a segmented genome. This arthropod-borne virus is endemic to the United States (27, 28), and typically causes disease in children. While most cases are asymptomatic or manifest in febrile illness, a small percentage of children develop seizures, chronic epilepsy, or fatal encephalitis (29).

The replication cycle of bunyaviruses begins upon entry into host cells by clathrin-mediated endocytosis. After pH-dependent fusion with the endosomal membrane and entry into

the cytosol, the encapsidated viral RNA genome segments undergo transcription by viral RNA dependent RNA polymerase (RdRp) to generate mRNA. The mRNA is then used to transcribe structural and nonstructural viral proteins. Structural proteins Gc and Gn dimerize in the ER and are transported to the Golgi. Meanwhile, RdRp generates positive strand antigenomic RNA, which is then used as a template to replicate more genomic copies. Ribonucleoproteins are generated in viral ‘factories’ and then transported to the Golgi for assembly. Virions are secreted via vesicles to the plasma membrane (30). LACV and other orthobunyaviruses can antagonize IFN production responses, particularly through the nonstructural protein NSs, which directly suppresses IFN induction (31). Mice infected with LACV succumb to neurological disease in a dose and age-dependent manner. This is believed to be due to differences in Type I IFN production. Older mice have more myeloid DCs present, which produce more Type I IFN via RLR and TLR3 activation (32). Selectively removing myeloid DCs from older mice increased susceptibility to LACV mediated neurological disease (32).

A few well-known, strongly antiviral genes have been reported to restrict Bunyaviridae family members. Bunyaviruses like LACV and Rift Valley Fever Virus (RVFV) are strongly restricted by MxA, a highly conserved GTPase that prevents virus components from trafficking from the cytosol to the nucleus (33). MxA is potent enough to protect *IFNAR*^{-/-} mice from a lethal dose of Thogoto virus (tick borne orthobunyavirus) and enhance resistance against LACV (34). Viperin (blocks egress), MTAP44 (aggregates microtubules; antiviral function unknown) and PKR (blocks translation) restrict infection by Bunyamwera Virus (35). IFITM2 and IFITM3 were found to restrict RVFV in cell culture, by blocking viral fusion with the endosomal membrane, while IFITM1 had no discernable effect (36). Recent studies have shown that Oropouche and LACV are restricted by Irf3, Irf5 and Irf7 in the mouse, where the deletion of all

three genes leads to increased viral replication in the liver and spleen, and induces early mortality. *Irf5* in particular was found to be required for control of viral replication in bone marrow derived DCs, faster infiltration of into the CNS and death (49, 50). In addition, both murine and human IFIT1 was found to have no discernable effect against Oropouche or LACV *in vitro* and *in vivo* (51).

IFITM

The interferon induced transmembrane (IFITM) family of proteins broadly restricts infection of several families of viruses. These proteins are expressed constitutively in most cell types, but also can be induced by type I, II and III IFNs (52). IFITMs are classified according to sequence similarity and function: Clade 1 contains IFITM1, 2 and 3 (and the mouse orthologs 6 and 7), which participate in viral restriction; Clade 2 contains IFITM5, which is expressed in osteoblasts; and Clade 3 contains IFITM10, which is yet uncharacterized. Only IFITMs in Clade 1 are IFN inducible (14, 52).

Clade 1 IFITMs have 5 conserved domains (9, 52): the N terminal, the intramembrane, the conserved intracellular loop, the transmembrane, and the C terminal. IFITM2 and 3 contain a YXXΦ motif allowing for internalization into endosomes (53). IFITM1 lacks this motif and is believed to associate with the caveolin pathway. Further biochemical studies have identified key regions that affect IFITM function and localization. Lys124 in the N terminal domain is a site for ubiquitination (54), which mediates IFITM degradation. Palmitoylated cysteines in the intermembrane and transmembrane domains are necessary for localization and restriction of viral entry (54), and methylation of K88 appears to counter IFITMs antiviral capacity (55). The

orientation of IFITMs is largely unclear, and in the case of IFITM3, there are three prevailing models. However, the model with the most support has the N terminal domain in the intracellular region, and the C-terminal domain exposed to the extracellular space.

IFITM proteins are basally expressed and localized primarily in late endosomes and lysosomes (52), co-localizing partially with LAMP2 and CD63 (56, 57). In addition, IFITM3 associates with lipid rafts on the plasma membrane (58), and is expressed on the apical membrane and cilia of columnar epithelial cells of the airway (59). IFITM1 appears to co-localize to subcellular compartments separate from IFITM2 and IFITM3 (60, 61). Ectopic expression of IFITMs results in increased expression on the plasma membrane surface. Furthermore, IFITM1 ectopic expressing cells have larger, empty vesicles, and IFITM3 cells develop multivesicular bodies (62).

Antiviral activity of IFITMs was first observed against VSV (52), where infection was restricted in IFITM1 over-expressing cells. IFITM3 was later found to restrict influenza A by blocking entry at the hemifusion stage (9) in the late endosome, and also is protective *in vivo* (59, 63). Since then, the effectiveness of IFITM restriction has been tested *in vitro* against many viruses (64). IFITM genes reportedly restrict infection of flaviviruses (WNV, DENV, ZIKV and JEV), HCV, filoviruses (EBOV and MARV), SARS coronavirus, bunyaviruses (RVFV, LACV), HIV, RSV and reoviruses (56, 60, 61, 64–71). IFITM3 has been shown to prevent HIV-1 infection by incorporating directly into the virion, as well as preventing viral fusion and cell-to-cell spread (72). In addition, HIV-1 has been shown to gain sensitivity to IFITM mediated restriction as the virus population develops mutations on the envelope glycoprotein to evade host neutralizing antibodies (73–75).

IFITMs reportedly do not have significant antiviral activity against Moloney Murine Leukemia Virus (retrovirus), Crimean–Congo Hemorrhagic Fever (CCHFV, a bunyavirus), and arenaviruses (9, 14, 20, 56, 60, 65). In addition, IFITMs do not restrict DNA viruses like Human Papilloma Virus (HPV), and Adenovirus (76), but may restrict Cytomegalovirus (CMV) and African Swine Fever virus (77). It is currently unknown why these viruses escape IFITM restriction, especially since many share common characteristics of entry as restricted ones. Correspondingly, the mechanism of protection by IFITMs also remains unclear. Over-expression of IFITMs has been shown to reduce membrane fluidity, increase cholesterol content and alter the curvature of endosomes, suggesting that IFITM physically alters the properties of the membrane to make viral fusion inefficient (78). For example, Amphotericin B, an antifungal that binds sterols in membranes, abrogates IFITM3 protection from influenza (79).

The human polymorphism rs-12252 results in the deletion of the 21-nucleotide end of the N terminal of IFITM3. This deletion prevents localization to the endosome, restoring influenza (an observation that has been questioned in later publications (80, 81)) but not HIV infection (82). In addition, a recent publication with Hantaan virus suggests that the rs-12252 polymorphism is responsible for increased disease severity and viral load in patients (83). These studies introduce the possibility that IFITM has more than one method of restriction.

In this study, we use a library of murine ISG candidates to identify novel antiviral genes in a high throughput manner. As most ISGs are believed to have a moderate to low potency, we decided to use an attenuated alphavirus (CHIKV-181/25) to try to identify novel targets that may be masked in the context of a more pathogenic strain. In addition, the orthobunyavirus LACV was also used, as this virus has not been previously used in large scale ISG screens. While the initial results still need to be independently verified, the screen identified the ISG *Ifitm3*. Though

Ifitm3 has been characterized as a potent and broad antiviral gene, alphaviruses were considered to be unaffected. Through *in vitro* and *in vivo* studies, we show that both arthritogenic and encephalitic alphaviruses are susceptible to *Ifitm3* mediated restriction.

Chapter 2: Screening for novel antiviral ISGs against alphaviruses and orthobunyaviruses

ABSTRACT

The identification and characterization of novel antiviral interferon-stimulated genes (ISGs) can help elucidate functions of viral replication and pathogenesis *in vitro* and *in vivo*. In addition, identifying novel mechanisms of restriction can provide new avenues of therapeutics for many viral diseases, including arboviruses like chikungunya and LaCrosse virus. Using a shRNA library targeting 243 unique ISG candidates, a total of 21 and 30 novel genes were determined to be antiviral against the attenuated strain CHIKV-181/25 and LACV, respectively. However, the efficacy of the screen was called into question, as only 1 of every 3 shRNA constructs against a particular gene was guaranteed to produce significant knockdown, and off-target effects were never assessed. Independent assessment of the top hits against CHIKV-181/25 using a transducible system to generate bulk CRISPR knockout cell lines has proven ineffective, and would require the generation of clonal lines before proper analysis can be done. Verification of certain target ISGs through readily available knockout cell lines and mouse models led us to identify *Ifitm3* as having antiviral mechanisms against alphaviruses.

INTRODUCTION

Of the hundreds to thousands of ISGs that are upregulated upon infection, the functions of only a small handful have been identified and further studied. An antiviral response is still seen in cell culture systems with the most potent ISGs removed, suggesting that the remaining uncharacterized ISGs have some protective functions. Most of these ISGs likely have mild to moderate antiviral activity on their own, and likely work synergistically to provide stronger restriction. Other ISGs may only be effective against a particular strain or family of viruses. Given the sheer number of ISGs, it is also likely that these genes have redundant functions, acting as a countermeasure against viruses that have evolved a means of avoiding restriction by other ISGs with a similar, but not exact mechanism of action.

Prior large scale screens for ISGs have focused on human targets (9, 20, 21, 24–26, 28, 84), and used non-attenuated viruses. Although identifying novel antiviral human ISGs could direct a path toward targeted therapeutics, validation studies in animals would likely still be required. Some ISGs (like IFI6) identified from human screens against WNV did not have apparent mouse orthologs in part due to gene duplication and diversification, limiting their potential for further pathogenesis studies *in vivo*. Non-attenuated viruses may have the disadvantage of having mechanisms for antagonizing the function of specific ISGs or the IFN signaling response in general. In this case, moderate or weakly potent antiviral ISGs might be masked in a screen. Some attenuated or vaccine strains show impaired virulence due to their greater sensitivity to IFN, like WNV-Kunjinn (85), making them a useful tool to reveal new antiviral ISGs. Furthermore, ISGs that are effective only against attenuated viruses can suggest novel viral immune evasion mechanisms. As an example, a virulent strain of WNV commonly used for pathogenesis studies exhibited no phenotype in IFIT1^{-/-} mice or primary cells; the role of

IFIT1 as an antiviral effector was revealed with an attenuated genetic mutant virus that lacked 2'-O methylation on its viral RNA (86, 87).

In this study, we employed a library of 756 unique shRNAs (targeting 243 unique murine ISGs) to screen against the attenuated alphavirus vaccine strain of chikungunya virus CHIKV-181/25. In addition, we also used the library against the orthobunyavirus LACV, which has not been subject to a large, high-throughput ISG screen. As a segmented negative-stranded RNA virus, La Crosse is a unique encephalitic arbovirus and may thus be restricted by a distinct set of ISGs. By using a gene knockdown approach, this screen has the additional advantage of identifying antiviral ISGs in the context of physiological doses of IFN, and can be used to recognize ISGs that require a multi-component complex to function. From our initial screens, we identified 21 and 30 novel candidate antiviral ISGs against CHIKV-181/25 and LACV, respectively. While the results included ISGs of known antiviral function, providing evidence that the screen was successful, subsequent analysis of individual shRNAs against a particular gene target suggested that many of our results could be due to off-target effects. Independent assessment of select targets using bulk CRISPR lines has been so far incomplete, and further optimization of the system needs to be done.

MATERIALS AND METHODS

Cells. Vero, 293T, NIH 3T3 cells and MEFs were cultured in complete DMEM, which was supplemented with 10% fetal bovine serum, and 10 mM each of GlutaMAX, sodium pyruvate, non-essential amino acids and HEPES (pH 7.3). MEFs from $\beta 2mK^{bD^b}$ triple knockout mice were provided by Ken Murphy (Washington University in St Louis).

Viruses. The CHIKV-181/25 strain was provided by the World Reference Center for Arboviruses (R. Tesh, University of Texas Medical Branch). The CHIKV-LR (La Reunion OPY1 p142) strain was a gift from S. Higgs (Kansas State University). LACV (original strain) was provided by Andrew Pekosz (Johns Hopkins University, Baltimore, MD) Virus propagation and titration was performed in Vero cells.

Lentiviral packaging and transduction of shRNA. The shRNA library targeting murine ISGs was purchased commercially (Open Biosystems), and uses the lentiviral pGIPZ vector. This plasmid co-expresses shRNA and GFP downstream of the CMV promoter. Individual plasmids from the library were co-transfected in a 96 well format into 293T cells with the packaging plasmids pSPAX.2 and pMD2G using the FuGENE HD (Roche) transfection reagent, following manufacturer's instructions. After 48 hours, lentiviral supernatants were harvested and transferred onto NIH-3T3 cells in a 96 well format with a final concentration of 10ug/ml polybrene. Cells were spinoculated at 1000 x g at room temperature for 30 minutes before being placed in the 37°C incubator. Supernatant was replaced with complete DMEM 24 hours later and returned to 37°C for 48 more hours to allow for efficient expression of GFP reporter and knockdown of the target genes.

ISG screening. The NIH-3T3 cells transduced with the lentiviral library for 72 hours were then treated with commercial mouse IFN β (PBL) (2.5 IU/ml for CHIKV-181/25 or 1 IU/ml for LACV) for 6 hours, washed, and then infected with virus (MOI 5 of CHIKV-181/25 or MOI 200 of LACV). These MOIs were chosen to facilitate 2-5% infection in the presence of IFN treatment or 70-80% infection in the absence of IFN treatment. After 14 hours (CHIKV-181/25) or 48 hours (LACV), cells were trypsinized, fixed in 1% PFA and permeabilized with a 0.1% saponin solution in HBSS and 10mM HEPES. CHIKV infected cells were stained with CHK11, a mouse monoclonal antibody specific to the E2 protein, and LACV infected cells were stained with supernatants from the hybridomas 807:31 and 807:33, kindly provided by Andrew Pekosz. Following secondary antibody staining with goat-anti mouse IgG-Alexa Fluor 647 (Life Technologies), cells were analyzed by flow cytometry using the FACSArray Flow Cytometer (BD Biosciences). Transduced populations were identified by GFP, and infected populations were identified by Alexa Fluor 647 staining.

Generation of bulk CRISPR lines. Single guide RNAs (sgRNA) were identified using the online algorithm developed by the lab of Feng Zheng and the Broad Institute (www.broadinstitute.org/gpp/public/analysis-tools/sgrna-design). Briefly, the algorithm determined a series of possible guides that could bind to the gene of interest and ranked them according to predicted specificity and efficacy. The top three ranked guides were chosen, flanked with the correct nucleotide sequences (Oligo 1: 5'-CACCG; Oligo 2: 5'-C and 3'-AAAC) to accommodate ligation into the LentiCRISPRv2 vector, and commercially produced (IDT). Guides are provided in Table 1.

LentiCRISPRv2 (Addgene 52961) is a lentiviral plasmid with Cas9 and the puromycin resistance gene expressed under the EFS promoter, and a U6 promoter just upstream of a 2kb

filler region flanked by BsmBI restriction sites. The filler region was removed via BsmBI digestion and gel purification, and then replaced with sgRNAs via T4 DNA Ligase. The plasmids were then transformed, collected via Qiagen's MiniPrep kit, and sequence verified using the following primer: U6 Fwd 5'-GAGGCCTATTTCCCATATTCC-3'.

The LentiCRISPRv2 library was packaged in 293T cells in 6 well plates with pSPAX2 (Addgene 12260) and pMD2.G (Addgene 12259), using the FuGENE HD (Roche) transfection reagent. After 48 hours, lentiviral supernatant was removed and collected. Low passage NIH-3T3 cells plated in 12 well plates were then spinoculated with lentivirus and 10ug/ml polybrene for 30 minutes at room temperature at 1000 x g. The next day, cells were split 1:4 and given fresh complete DMEM with 2µg/ml puromycin to select for transduced cells. After 7 days of selection, cells were aliquoted and frozen down.

IFN treatment, infection with CHIKV-181/25 and analysis were optimized to provide a consistent 4-6 fold difference between negative control, scrambled sgRNA, and STAT1 sgRNA bulk CRISPR lines. At 14 hours post infection, cells were harvested, fixed, stained and analyzed by flow cytometry as described above.

Western Blotting. Negative control scrambled and *Ifitm3* bulk CRISPR lines were lysed in RIPA and electrophoresed under reducing conditions on a 4-12% Bis-Tris NuPAGE gel with MES buffer according to the manufacturer's instructions (Thermo Fisher). After transfer onto PVDF membranes (Thermo Fisher) using an iBlot apparatus (Thermo Fisher), proteins of interest were detected with mouse anti-β-actin (CST, 8H10D10), Polyclonal rabbit anti-Ifitm3 (Proteintech, 11714-1-AP), HRP-conjugated anti-mouse IgG (Sigma Chemical), and HRP-conjugated anti-rabbit IgG (Sigma Chemical).

Mice. *Lamp3*^{-/-} mice were generated by CRISPR, deleting 11 or 335 nucleotide deletions in exon 2 of the *Lamp3* gene, both of which result in a frame shift and a premature stop codon. Both alleles were backcrossed twice to C57BL/6J mice to remove potential off-target effects and then generated mouse lines using brother by sister mating. *Ifit2*^{-/-} mice were made commercially (Taconic) in the C57BL/6 background, wherein exons 2 and 3 of the *Ifit2* gene were flanked by flt sites and then excised via Flt recombinase. Mice were either infected in the footpad with CHIKV-LR at a final volume of 10ul, or with LACV with a final volume of 50ul, diluted in PBS. Viral burden of tissues or serum harvested were done by a focus forming assay.

Viral growth kinetics. For viral yield assays, cells were plated (10⁵ cells per well in a 12-well plate) and in some experiments pretreated with specified doses of IFN β for 12 hours. Cells then were infected with CHIKV at 37°C. One hour later, the plates were rinsed twice with warm PBS, and replaced with fresh DMEM supplemented with 10% FBS. Supernatants were collected at specific time points, and viral titers were determined by focus forming assay on Vero cells, as described (37, 48).

Measurement of viral burden by qRT-PCR. Mouse tissue homogenates were processed for RNA using the Qiagen RNeasy kit. Serum samples were prepared using the Qiagen QIAmp Viral RNA kit. Viral titers were quantified to a standard curve of CHIKV and normalized to tissue weight or ml of serum. CHIKV RNA was detected using an E1 specific primer and probe set.

Data and Statistical analysis. Flow cytometry data was analyzed using FloJo software. Analysis of the shRNA ISG screen and Z-score calculations were done on Microsoft Excel.

Student t-tests, Mann-Whitney or Dunnet's multiple comparison ANOVA tests were performed with Prism Software (GraphPad, San Diego, CA).

RESULTS

Screening for novel antiviral ISGs. A library comprised of 756 unique shRNAs, targeted against 243 putative murine ISGs was obtained commercially from Open Biosystems. These putative ISGs were identified from a collection of published microarray analyses of genes upregulated *in vitro* after treatment with Type I IFN. Each shRNA arrived inserted into the bicistronic pGIPZ lentiviral vector, which includes a GFP reporter (**Fig 2.1A**). Individual plasmids from the library were packaged into lentiviruses and transiently transduced into NIH-3T3 cells in a 96 well format. Each plate contained negative scrambled controls and positive Stat1 shRNA transduced controls. After 72 hours, successful transduction was determined by GFP expression. Cells were then treated with IFN β for 6 hours and infected with either CHIKV-181/25 (MOI 5) or LACV (MOI 200) (**Fig 2.1B**). The administration of IFN and virus was optimized to obtain a low percentage of infectivity in the presence of IFN and a high percentage in the absence of IFN (3-7% and 70-80% in all transduced cells, respectively) in an attempt to skew towards the detection of antiviral ISGs. After 14 hours (CHIKV) or 48 hours (LACV), cells were processed and analyzed by flow cytometry (**Fig 2.1C**). The transduced (GFP⁺) cell population was analyzed to determine the percentage of infected cells (GFP⁺ Alexa Fluor 647⁺) in each well, and subsequently normalized to the percentage calculated in the scrambled controls. These ratios were then ranked by Z-score. Any shRNA construct with a Z-score of 1.5 (one and a half standard deviations above the mean) was considered a ‘hit’ in these screens.

In the CHIKV-181/25 screen, a total of 33 shRNAs, corresponding to 28 unique ISG targets were identified (**Fig 2.2A**). These included shRNAs targeting the positive control (*Stat1*) ISGs with well characterized antiviral function (*Stat2* and *Ifit1*), transcription factors (*Irf8*), and proteins involved in antigen presentation (*β 2m* and *H2-T*). After manually eliminating genes that

were already characterized, deemed difficult to characterize (such as transcription factors, or genes canonically involved in the adaptive immune response), a final list of 21 candidate ISGs was generated. In the LACV screen, a total of 49 shRNAs, corresponding to 46 unique ISG targets were identified (**Fig 2.2B**). Like the CHIKV screen, ISGs with known antiviral potency and mechanism were included. Manual curation of these targets resulted in a final list of 30 unique ISG targets, three of which were also found in the CHIKV screen (*Agt*, *Ifi47*, *Lypla1*). A table of the final ISGs targets and their known functions are included in **Table 2.1**.

Independent assessment of the top candidate ISG targets. To better understand the efficiency of knockdown and potential off-target effects of the library, the Z-scores of all the shRNAs against the top ISG target hits were directly compared (**Fig 2.3**). Strikingly, for most of the gene targets, the majority of the corresponding shRNAs had a Z-score well below 1.5. Even for the positive control, Stat1, only 3 of the 6 shRNAs had a Z-score greater than 1.5, suggesting only 50% efficiency of this library at best. Combined with the manufacturer's claim that "at least one of three constructs is guaranteed to reduce target mRNA levels by 70% or more," (Open Biosystems) the reliability of the shRNA screen is put into question.

To independently verify the top hits, we decided to use the gene editing technology CRISPR to generate targeted knockout cell lines. We prioritized targets identified in the CHIKV-181/25 screen over the LACV screen because there are more reagents available to evaluate CHIKV pathogenesis. An sgRNA library was first developed using the online designer tool from the Broad Institute (www.broadinstitute.org/gpp/public/analysis-tools/sgrna-design). The top 3 guides were picked for each ISG target (**Table 2.2**) and ligated into the LentiCRISPRv2 plasmid (**Fig 2.4**), which also expresses Cas9 and the puromycin resistance gene. After packaging, the CRISPR library was transduced into NIH-3T3 cells and maintained under 2 μ g/ml of puromycin

selection for 7 days. After selection, the cell lines were aliquoted and frozen down. Efficacy of gene editing was tested by treating the scrambled negative control and *Stat1* targeted lines with increasing doses of murine IFN β for 6 hours and then infecting with different MOIs of CHIKV-181/25 for 14 hours. By flow cytometry, all 3 *Stat1* bulk CRISPR lines were more susceptible to infection than scrambled controls, especially as the concentration of IFN was increased (**Fig 2.5**). However, analysis of the bulk CRISPR library yielded no clear antiviral phenotype, with only a few individual lines attaining a 2-fold change increase in infection compared to the scrambled controls (**Fig 2.6**). A closer analysis was performed of six ISG targets that had at least one bulk CRISPR line infected higher than 1-fold. After treating cells with increasing doses of IFN and virus, only the *Ccng1* bulk CRISPR lines had a consistent, increased fold change in infection compared to scrambled controls. Furthermore, the *Ccng1* bulk CRISPR lines showed differences in infection without IFN treatment, suggesting that the *Ccng1* phenotype may not be IFN dependent (**Fig 2.7**).

Since the CRISPR screen only validated one gene identified in the shRNA screen, an additional positive control was included. Even though *Stat1* has been used consistently and successfully for similar ISG screens as a positive control, adding a known, less potent antiviral ISG could assist in fine tuning the IFN dosage and infection conditions to tease out the effects of the more moderately acting antiviral genes. The ISG *Ifitm3* was chosen, as we had recently published its antiviral effects on alphaviruses (discussed in Chapter 3 of this dissertation). Unfortunately, no variation in IFN dosage or MOI tested could induce a satisfactory difference in infectivity between the *Ifitm3* bulk CRISPR lines and the negative controls (**Fig 2.8A**). By Western blot, *Ifitm3* can still be detected in all three lines, and expression increased if the cells

were pre-treated with IFN β (**Fig 2.8B**). This is likely due to the genetic heterogeneity of the bulk cells.

Alternative approaches to independently assess target ISGs. Knockout mice were available for four of the ISGs identified in our shRNA screens. *Ifitm3* and *Lamp3* were identified in both the CHIKV and LACV screens, while *Ifit2* and *β 2m* were identified in the LACV screen only. As *Ifitm3* had previously been described to restrict orthobunyaviruses *in vitro*, we decided to follow up on its potential role in CHIKV instead, using *Ifitm3*^{-/-} and *Ifitm* locus deletion MEFs. Further discussion of these experiments will be in Chapter 3 of this dissertation.

Ifit2 is a potent antiviral ISG that has been shown to restrict viral replication by binding to subunits eIF3, which is required for initiation and translation (14). In the context of WNV infection, it was shown that *Ifit2* restricts viral replication in the CNS, and only functions in a subset of primary cells, like cerebellar granule cells and macrophages, but not MEFs (88). The lack of restriction was also observed in growth kinetics studies with LACV in MEFs (data not shown). In addition, no significant differences weight in loss and death were observed in 8 to 10 week old *Ifit2*^{-/-} and WT mice infected with 10⁵ FFU of LACV in the footpad (**Fig 2.9**).

β 2m, or beta-2-microglobulin, is canonically known for its role in stabilizing the structure of MHCI, which is required for presentation of cellular antigen to CD8⁺ T cells (89). Due to its importance in adaptive immunity, studying its potential role as an antiviral ISG *in vivo* would be difficult. Instead, β 2mK^bD^b triple knockout MEFs were infected with CHIKV after treatment with IFN. Interestingly, we noticed that the triple knockout cells were less prone to infection after 14 hours than MEFs from WT littermate controls (**Fig 2.10**). Although an interesting

observation, additional experiments were not performed, and due to the foreseeable difficulty of properly studying the non-canonical properties of β 2m.

Lamp3 is an endosomal-lysosomal associated protein that is highly expressed in the cells of the airway, and in macrophages and dendritic cells (90), though there has been no extensive study on its upregulation in other tissues upon IFN stimulation. Recent unpublished observations have shown that Lamp3 is highly protective against MERS-Coronavirus pathogenesis. One study in A549 cells suggest that Lamp3 is actually proviral, and is required for the IAV nucleoprotein and titers (91). In the context of CHIKV infection, no differences were seen after 14 hours by flow cytometry, nor were any differences seen by growth kinetics (**Fig 2.11A-B**). When infected subcutaneously with 10^4 FFU, WT and *Lamp3*^{-/-} mice had comparable levels of titer in the spleen, ankle joints and serum at day 1 and 2 post infection by focus forming assay (**Fig 2.12**). To determine if Lamp3 had a possible role in maintaining or clearing the chronic viral RNA seen in the feet and spleen, infected mice were assayed by qPCR at 21 days post infection. Again, no differences in viral RNA titer were observed (**Fig 2.13**). The role of Lamp3 in LACV pathogenesis has not been studied.

DISCUSSION

To identify novel antiviral ISGs, a murine shRNA library targeting 243 genes was tested against the attenuated alphavirus CHIKV-181/25 and the orthobunyavirus LACV. Using shRNAs to knockdown target genes *in vitro* allowed for the identification of genes with antiviral function in the context of physiological response to IFN treatment. In addition, the attenuated alphavirus and orthobunyavirus were used in an attempt to find antiviral ISGs whose functions were either likely masked by pathogenic strains, or to identify completely novel, virus specific gene targets. From the shRNA screen, a total of 28 and 46 unique ISGs were identified that were deemed antiviral against CHIKV-181/25 and LACV, respectively. These genes included known antiviral ISGs like *Stat 2*, *Ifit1 and Ifit2*, *Ifitm3*, and *Mx1*, as well as transcription factors like *Irf8* and *Irf9*. However, a lack of reliability of knockdown by the shRNA library led to a concern that the unique ISGs in these top hits were the result of off-target effects.

Independent assessment of these targets using bulk CRISPR edited NIH-3T3 cells have thus far proven to be incomplete, and further optimization is needed before the hits can be properly analyzed. The current conditions of the CRISPR screen are unable to identify novel antiviral ISGs less potent than *Stat1* or as effective as *Ifitm3*. Since CRISPR acts by inducing breaks and random repair of genomic DNA, we cannot guarantee that enough alleles in the bulk population of cells have been knocked out to see an appreciable change in phenotype. This issue is compounded by the fact that NIH-3T3 cells are hypertriploid, increasing the likelihood that some CRISPR targeted cells have at least one functioning target allele. In fact, by Western blot analysis of the *Ifitm3* bulk CRISPR lines, the protein could still be detected, especially in samples where the cells were stimulated with IFN.

To salvage the CRISPR screen, we would have to generate and validate (by DNA sequencing and, if reliable antibodies are available, by protein detection) clonal knockout lines for each ISG target from the bulk populations. This way, we can cleanly assess the role of each target ISG without background noise from partially affected or unaltered alleles. Furthermore, any potential *trans* functions an ISG may have will no longer be a factor. Positive hits should be re-assessed on other cell lines (such as MEFs, BV2s, and human lines like HeLas and 293Ts) to address the possibility that the phenotype observed is unique only to NIH-3T3s.

A better approach for this screen or for future high throughput screens could be to try CRISPR interference (CRISPRi), which represses gene expression at the transcriptional level, physically blocking the progress of RNA polymerase. Using this knockdown method, which can be stably transduced, heterogeneity of mutations at the genomic level can be avoided while we can take advantage of the specificity of the sgRNA-dCas9 system. Validation can be done by RT-PCR (presence or lack of mRNA) and by Western blot. One caveat is that the efficiency of knockdown decreases the further the target is from the transcription start site, which may limit the number of possible sgRNA candidates per gene.

Another option would be to step away from the CRISPR lines and see if ectopic expression of the ISG targets yields any results. This approach is beneficial because we can theoretically track the cells that have incorporated the expression vector by flow cytometry, and determine the antiviral potency of each target ISG in the absence of IFN stimulation. However, this runs contrary to the spirit of the original screen, which was designed to understand a target ISGs importance in a physiological antiviral environment.

In summary, we attempted to identify novel antiviral ISGs in a high-throughput manner using a gene knockdown system and viruses that are either attenuated or not previously tested in prior, similar studies. This shRNA based screen identified a series of novel and previously described ISG targets. Due to the unreliability of the knockdown system, the validity of these hits is questionable at best. However, by using available knockout reagents for a select number of the top ISGs, Ifitm3 was found to restrict CHIKV infection.

Figure 2.1

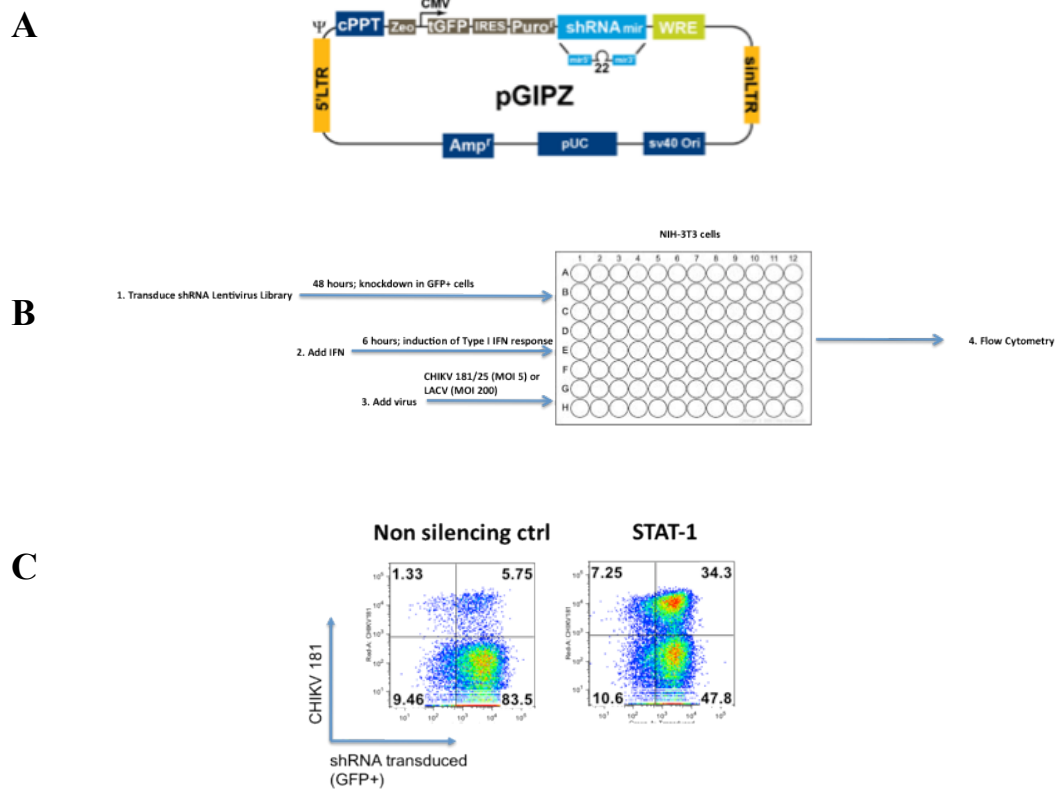
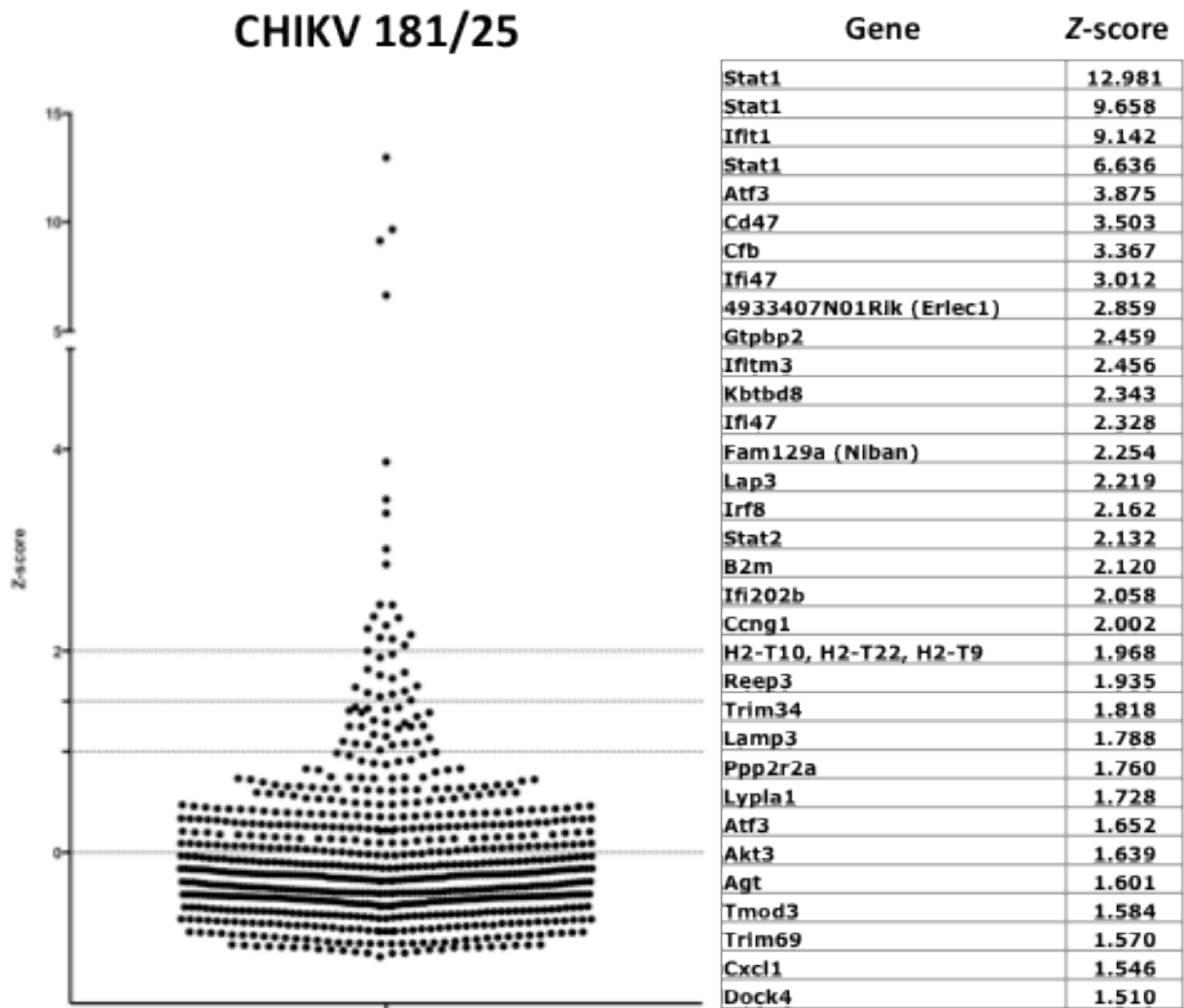


Figure 2.1. Lentiviral based shRNA screen for ISGs that restrict alphavirus or orthobunyavirus infection. (A) Plasmid map of the pGIPZ plasmid containing the shRNA oligo and the IRES GFP reporter. **(B)** The shRNA library targeting ISGs were packaged and transduced into NIH-3T3 cells. 72 hours later, cells were treated with IFN β (2.5 IU/ml for CHIKV and 1 IU/ml for LACV) for 6 hours then infected with CHIKV-181/25 or LACV at MOI 5 or MOI 200, respectively. After 14 hours (CHIKV) or 48 hours (LACV), cells were processed for flow cytometry. **(C)** Representative flow plots of non-silencing control (NSC) transduced cells or Stat1 shRNA transduced control cells infected with CHIKV-181/25. Transduction efficiency is determined by the expression of GFP on the x-axis and infection efficiency is shown by viral envelope staining on the y-axis.

Figure 2.2

A



B

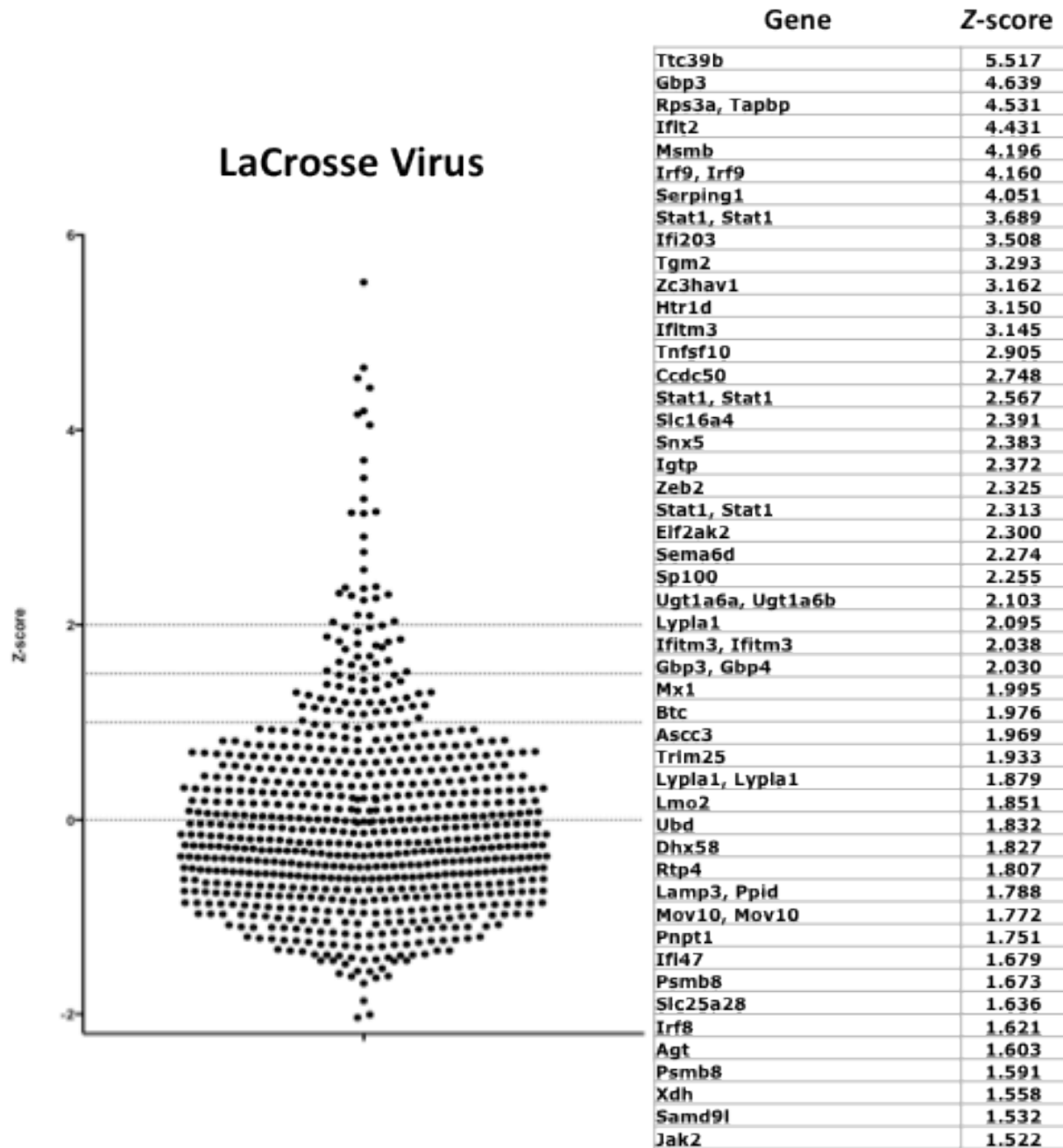


Figure 2.2. Analysis of the ISG screen. After flow cytometry, the percentage of infected cells of the total transduced population for every well was normalized to that of the non-silencing control. This ratio was normalized by Z-score and ranked for **(A)** CHIKV-181/25 and for **(B)** LACV. The top hits with a Z-score of 1.5 and above are listed on the table to the right. Each dot represents a single shRNA in the library.

Figure 2.3

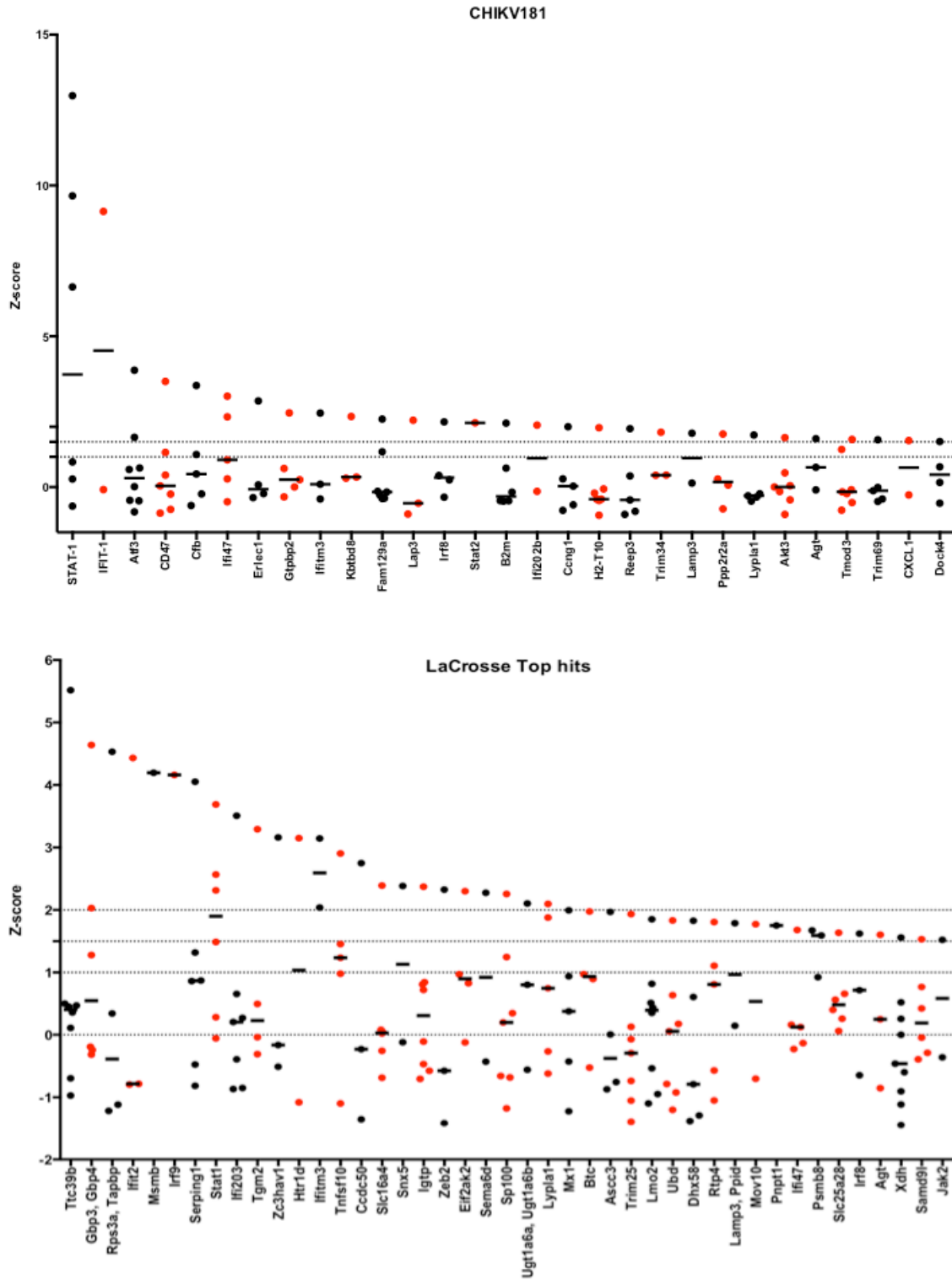


Figure 2.3. Efficacy of the shRNA library. The Z-scores of all the shRNAs targeting the top ranked ISGs from the CHIKV (top) and the LACV (bottom) screens were directly compared. Dotted lines mark Z-score at 1 and 1.5 for the CHIKV graph, and 0, 1, 1.5 and 2 for the LACV graph. Dashed lines represent the the median value. Z-score threshold for both screens was 1.5 (1.5 standard deviations above the mean).

Figure 2.4

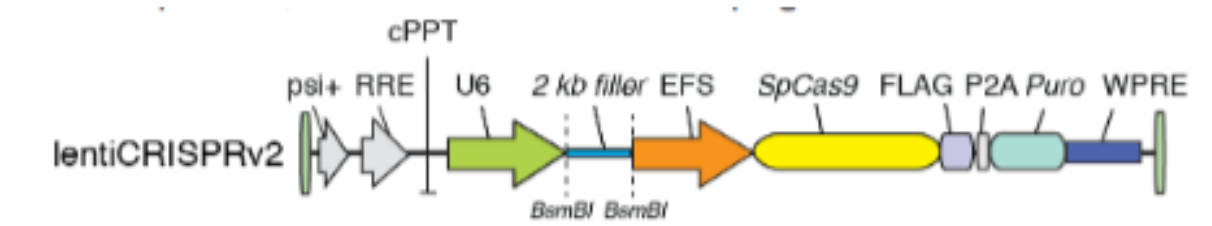


Figure 2.4. CRISPR knockout of select ISGs. Plasmid map of the LentiCRIPSRv2 vector, which contains a 2kb filler space under the U6 promoter. This spacer is replaced by the sgRNA oligo. The Cas9 and puromycin resistance gene cassette are under the EFS promoter.

Figure 2.5

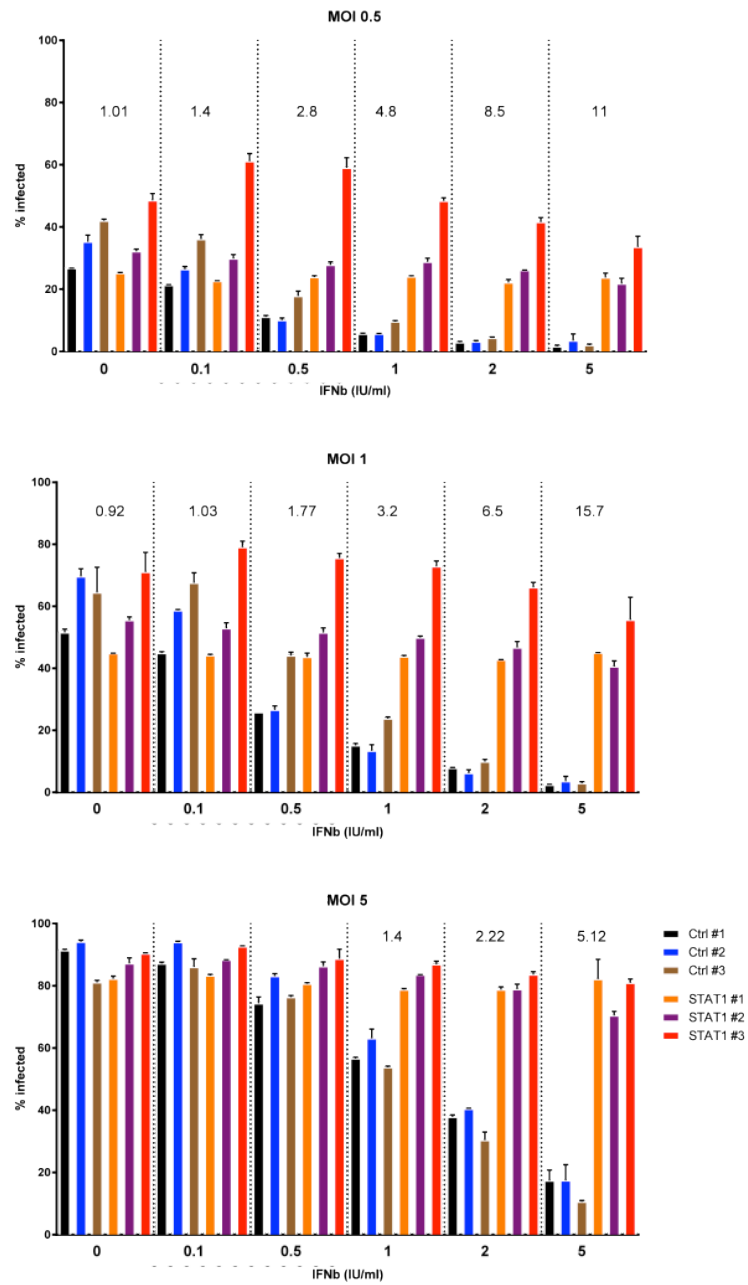


Figure 2.5. Demonstration of the efficacy of the CRISPR gene editing system. Non-silencing control lines and Stat1 bulk CRISPR lines were pretreated with the indicated concentration of IFN β for 6 hours before being infected for 14 hours with CHIKV 181/25 at an MOI of 0.5, 1 or 5. Percentages of infection were then determined by flow cytometry. The numbers above indicate the average fold-difference in infection between the control and the Stat1 bulk CRISPR lines.

Figure 2.6

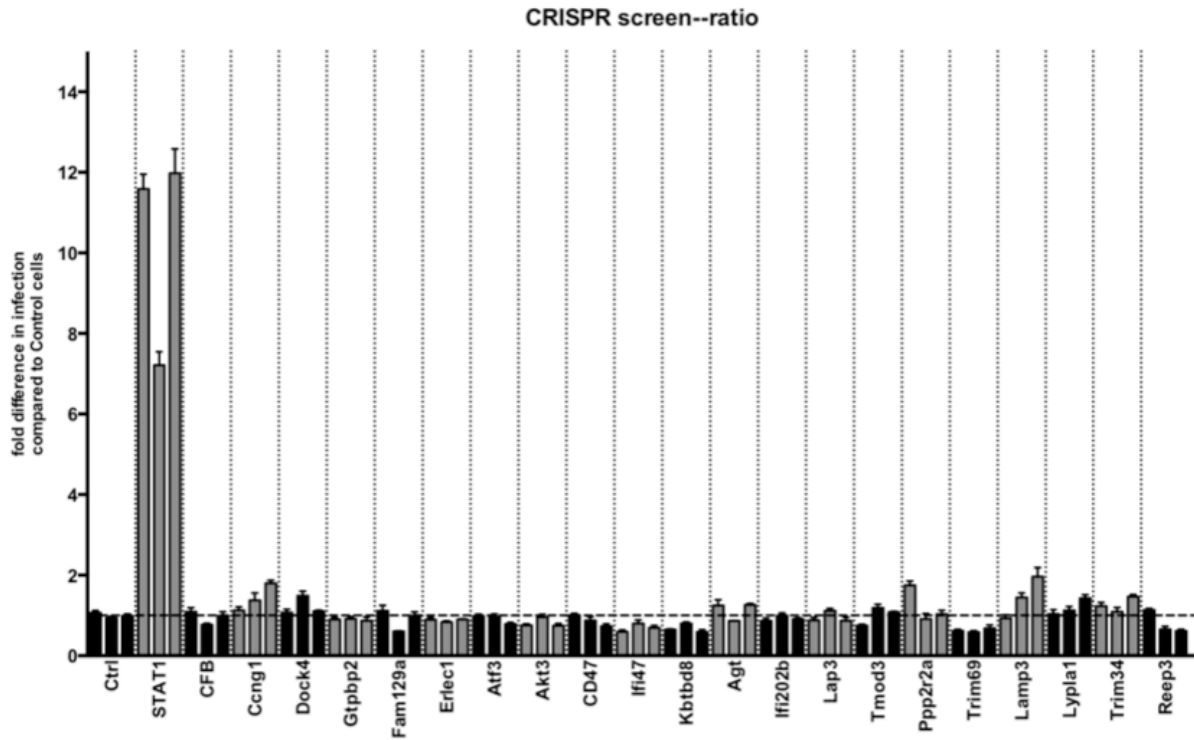


Figure 2.6. Attempt at validating the antiviral phenotype of select ISGs using bulk CRISPR lines. NIH-3T3 bulk CRISPR lines were treated with IFN β (3 IU/ml) for 6 hours, then infected with CHIKV 181/25 at MOI 1 for 14 hours. Cells were then analyzed by flow cytometry. Fold-differences in infection versus control lines are shown here. The dotted line indicates a one-fold change.

Figure 2.7

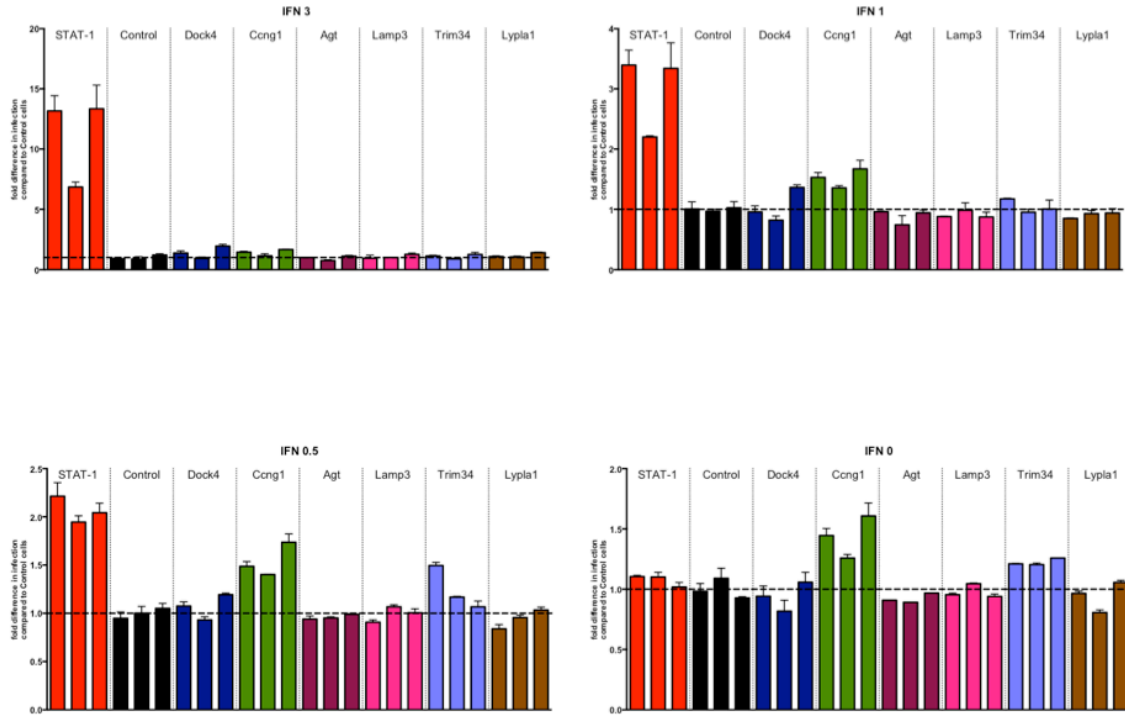


Figure 2.7. Analysis of select bulk CRISPR lines. The bulk CRISPR lines of six ISG targets from the initial screen were further tested to verify the presence of an antiviral phenotype. Cell lines were pretreated at the indicated concentrations of IFN β for 6 hours before being infected with MOI 1 of CHIKV 181/25 for 14 hours. Cells were analyzed by flow cytometry and the fold differences in infection compared to controls are graphed. The dotted line indicates a one-fold difference.

Figure 2.8

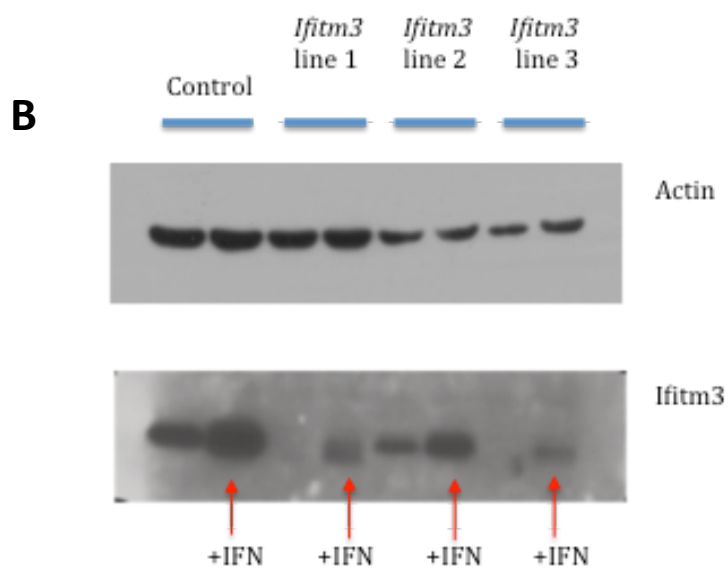
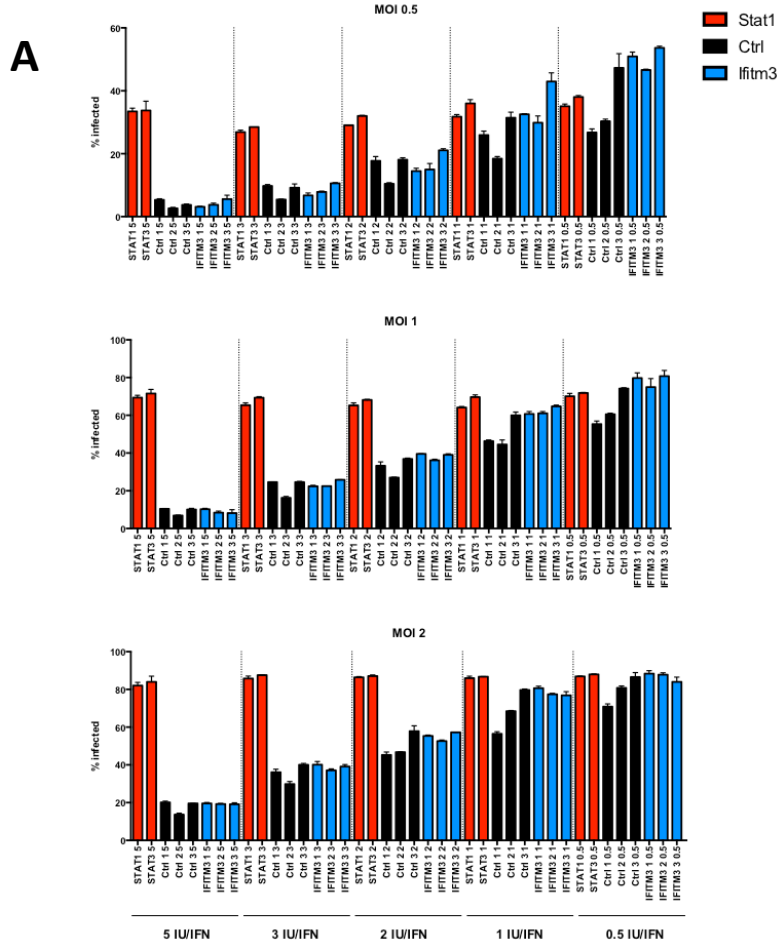


Figure 2.8. Attempt at showing an antiviral phenotype with Ifitm3 bulk CRISPR lines. (A) NIH-3T3 bulk CRISPR lines were treated with the indicated dose of IFN β for 6 hours and then infected with various MOIs of CHIKV 181/25 for 14 hours before being analyzed by flow cytometry. **(B)** Western blot of control and Ifitm3 bulk CRISPR lines with or without 3 IU/ml IFN β treatment for 6 hours.

Figure 2.9

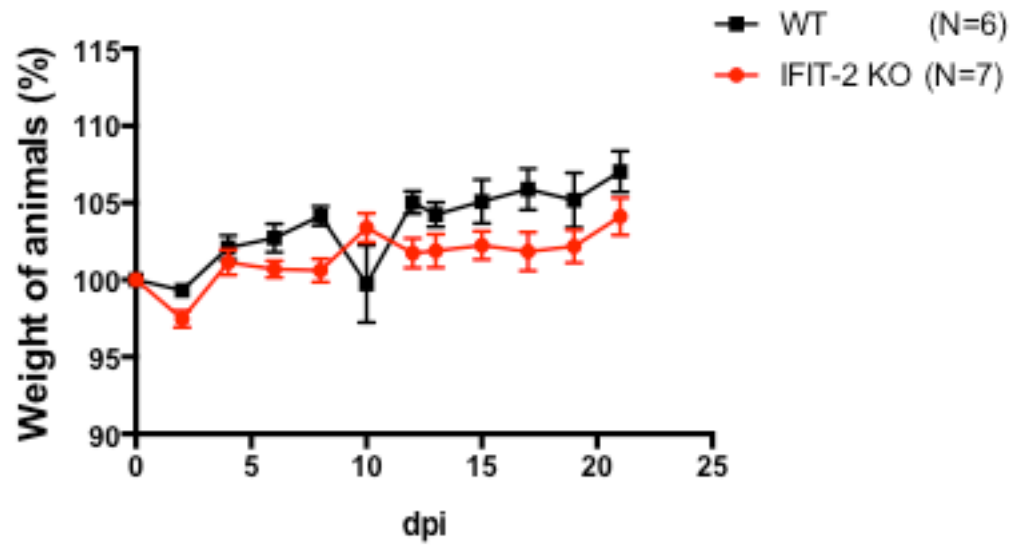


Figure 2.9. Pathology of LACV in *Ifit2*^{-/-} mice. 8 week old WT and *Ifit2*^{-/-} mice were infected with 10^5 FFU into the footpad and followed for weight loss. No mortality was seen during the course of infection.

Figure 2.10

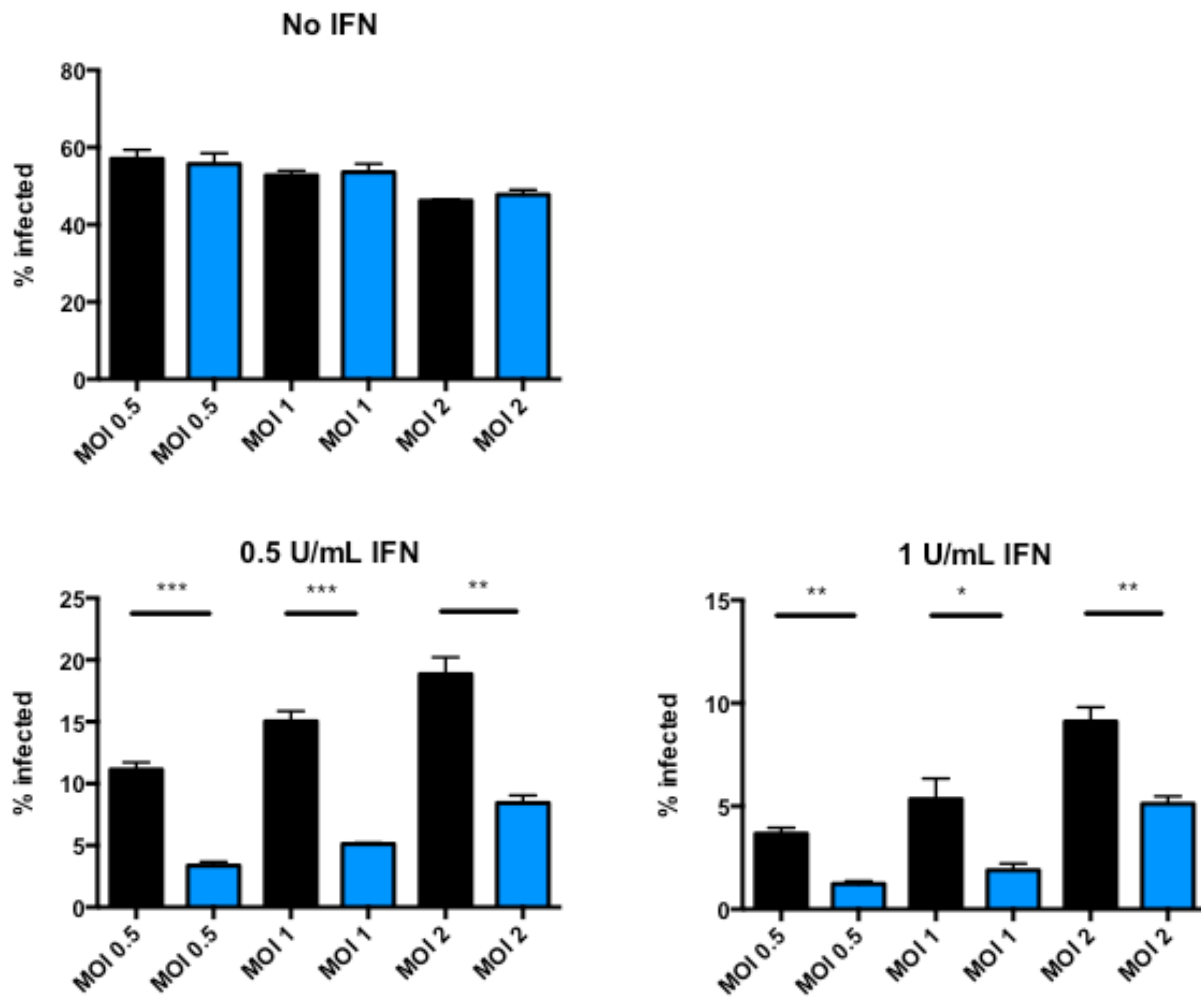


Figure 2.10. Susceptibility of $\beta 2mK^{bD^b}$ triple knockout MEFs to infection by CHIKV 181/25. MEFs were treated with the indicated concentration of IFN β for 6 hours before being infected with various MOIs of CHIKV 181/25 for 14 hours. Cells were analyzed by flow cytometry. Means were compared by Student t-test. (*, $P < 0.05$; **, $P < 0.01$; ***, $P < 0.001$).

Figure 2.11

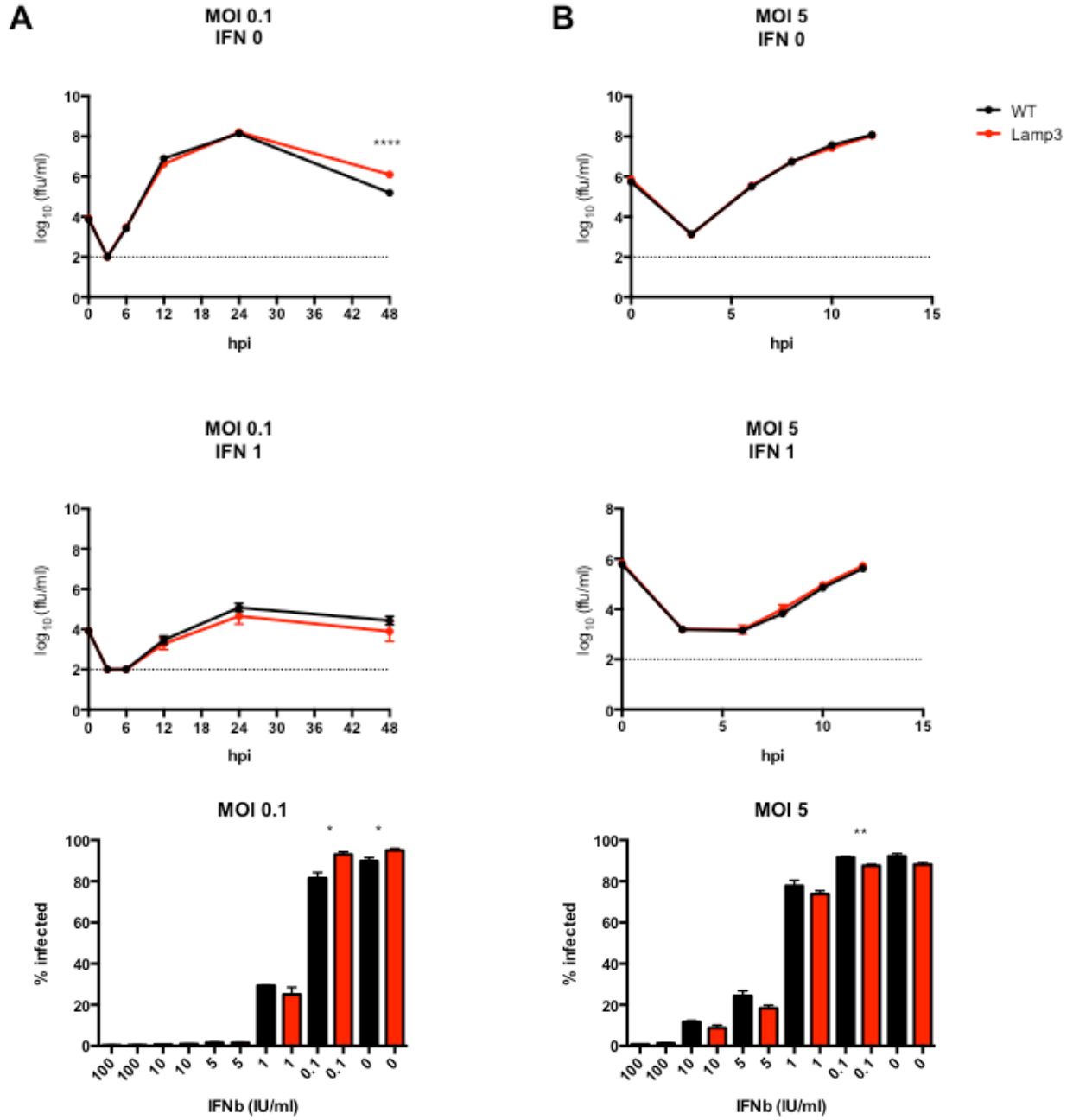


Figure 2.11. CHIKV infection is not enhanced by Lamp3 *in vitro*. WT and *Lamp3*^{-/-} MEFs were treated with IFN β and then infected with either **(A)** MOI 0.1 or **(B)** MOI 5 of CHIKV 181/25. Virus Statistically significant but inconsequential differences were observed in the multistep growth kinetics **(A)** of CHIKV in the absence of IFN, as well as in percent infection of MEFs at low dose of IFN. No differences were seen in viral growth kinetics at **(B)** high MOI, nor do we see a notable difference in infection of MEFs after 14 hours. Means were compared by Student t-test. (*, $P < 0.05$; **, $P < 0.01$; ***, $P < 0.001$).

Figure 2.12

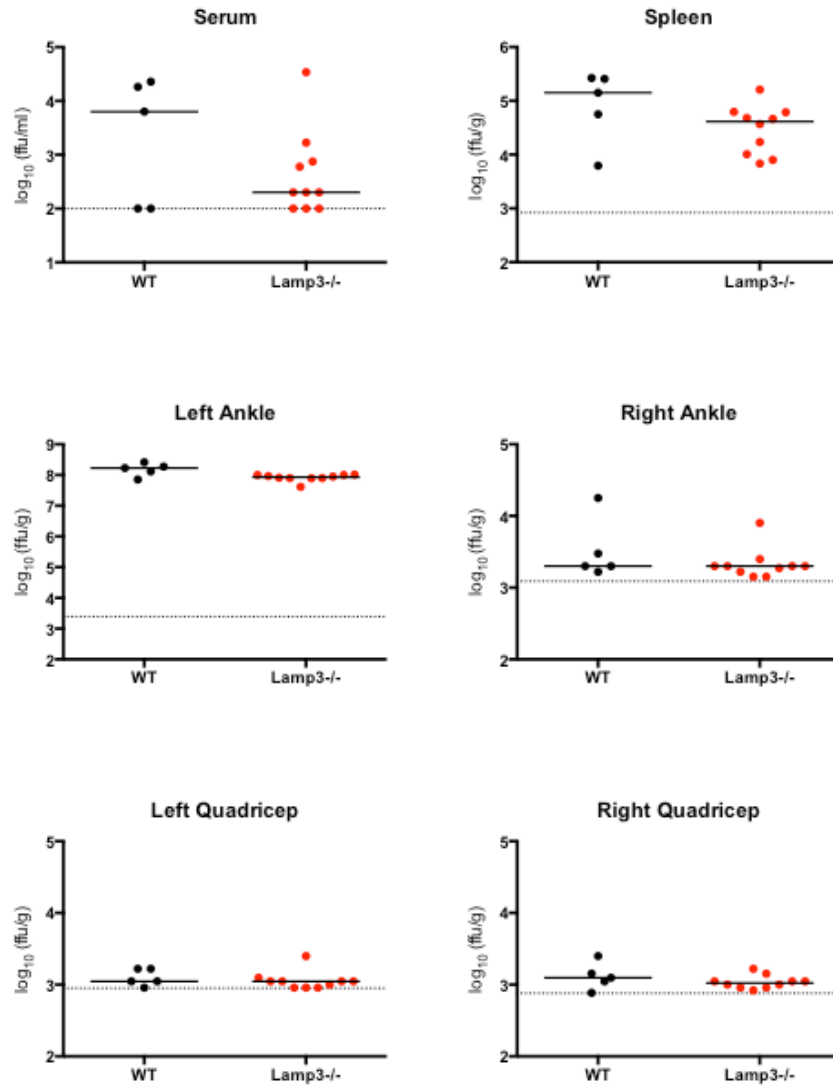


Figure 2.12. Lamp3 does not protect against early viral CHIKV titers in the tissues. 4 week old WT and Lamp3^{-/-} mice were injected with 1000 FFU of CHIKV-LR and were sacrificed at 1 day post infection. Viral burdens in the serum, spleen, ankles, and quadriceps were analyzed by focus forming assay. No statistical differences were identified by Mann-Whitney.

Figure 2.13

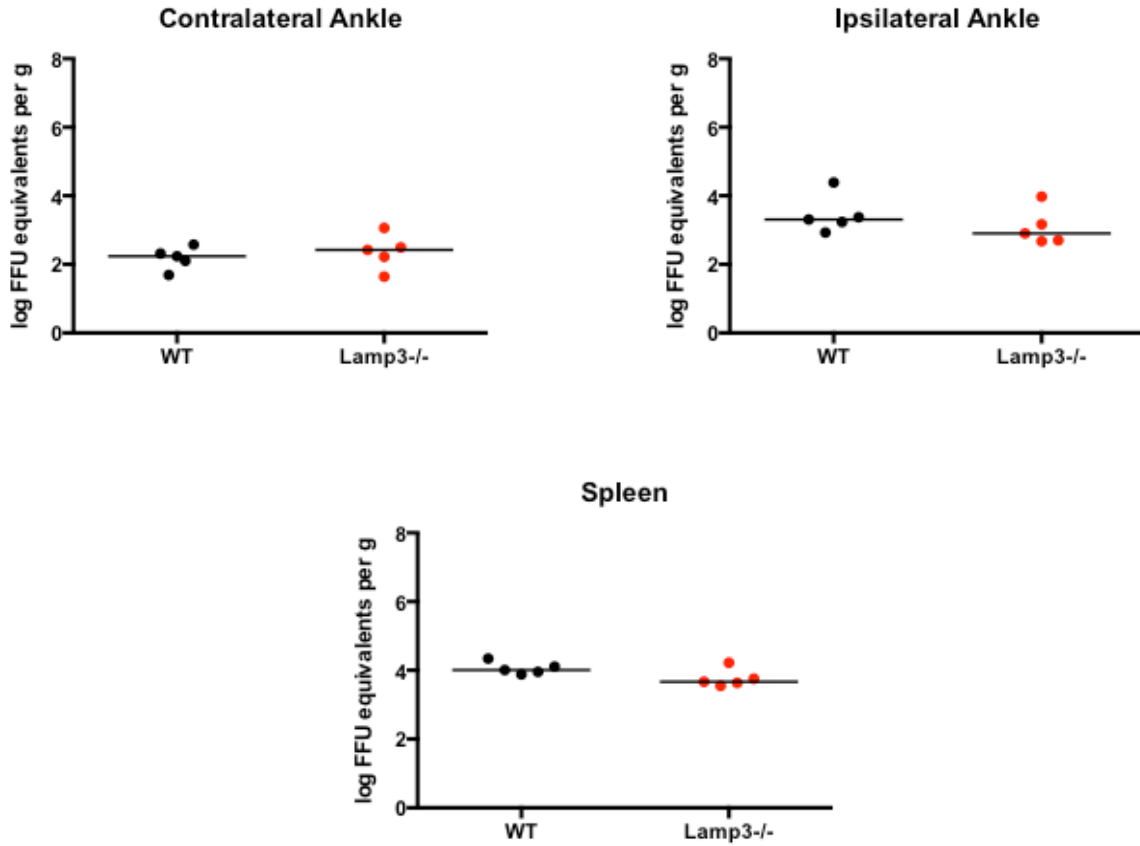


Figure 2.13. Lamp3 does not affect the chronic burden of CHIKV in mice. 4 week old mice were infected with 1000 FFU of CHIKV-LR and harvested at 21 days post infection. Viral burden in the ankles and the spleen were determined by quantitative PCR. No statistical difference was observed by Mann-Whitney.

Table 2.1. Final list of CHIKV and LACV antiviral ISGs identified from the shRNA screen

CHIKV targets		
Symbol	Full Name	Known functions (NCBI)
Agt	Angiotensinogen	Cleaved by renin in response to lowered blood pressure to form angiotensin-1.
Akt3	Thymoma viral proto-oncogene 3	Serine/threonine kinase that plays a key in regulating cell survival, insulin signaling, angiogenesis and tumor formation. Akt is a downstream mediator of the PI 3-K pathway, which results in the recruitment of Akt to the plasma membrane.
Atf3	Activating transcription factor 3	Binds cAMP. Represses transcription from promoters with ATF sites.
Ccng1	Cyclin G1	May play a role in growth regulation. Is associated with G2/M phase arrest in response to DNA damage. May be an intermediate by which p53 mediates its role as an inhibitor of cellular proliferation
Cd47	CD47 antigen	Cell adhesion receptor on platelets. Modulation of integrins. May be involved in membrane permeability changes induced following virus infection.
Cfb	Complement factor B	Component of the alternative complement pathway.
Dock4	Dedicator of cytokinesis 4	Involved in regulation of adherens junction between cells. Plays a role in cell migration. Functions as a guanine nucleotide exchange factor (GEF), which activates Rap1 small GTPase by exchanging bound GDP for free GTP.
Erlec1	RIKEN cDNA 4933407N01	N-glycan recognition in the ER and may regulate glycoprotein traffic
Fam129a	Family with sequence similarity 129, member A	Regulates phosphorylation of a number of proteins involved in translation regulation including EIF2A, EIF4EBP1 and RPS6KB1. May be involved in the endoplasmic reticulum stress response
Gtpbp2	GTP binding protein 2	Upregulated in mouse peritoneal macrophages.
Ifi202b	Interferon activated gene 202B	Unknown function
Ifi47	Interferon gamma inducible protein 47	Unknown function
Kbtbd8	Kelch repeat and BTB (POZ) domain containing 8	Unknown function
Lamp3	Lysosomal-associated membrane protein 3	May play a role in dendritic cell function and in adaptive immunity.
Lap3	Leucine aminopeptidase 3	Presumably involved in the processing and regular turnover of intracellular proteins. Catalyzes the removal of unsubstituted N-terminal amino acids from various peptides.
Lypla1	Lysophospholipase 1	Hydrolyzes fatty acids from S-acylated cysteine residues in proteins such as trimeric G alpha proteins or HRAS. Has depalmitoylating activity toward KCNMA1. Has low lysophospholipase activity
Ppp2r2a	Protein phosphatase 2, regulatory subunit B, alpha isoform	one of the four major Ser/Thr phosphatases, and it is implicated in the negative control of cell growth and division
Reep3	Receptor accessory protein 3	Microtubule-binding protein required to ensure proper cell division and nuclear envelope reassembly by sequestering the endoplasmic reticulum away from chromosomes during mitosis. Probably acts by clearing the endoplasmic reticulum membrane from metaphase chromosomes.
Tmod3	Tropomodulin 3	Blocks the elongation and depolymerization of the actin filaments at the pointed end. The Tmod/TM complex contributes to the formation

		of the short actin protofilament, which in turn defines the geometry of the membrane skeleton
Trim34a	Tripartite motif-containing 34a	Unknown function
Trim69	Tripartite motif-containing 69	The mouse ortholog of this gene is specifically expressed in germ cells at the round spermatid stages during spermatogenesis and, when overexpressed, induces apoptosis. Alternatively spliced transcript variants encoding distinct isoforms have been described.

LACV targets

Symbol	Full Name	Known functions (NCBI)
Agt	Angiotensinogen	Cleaved by renin in response to lowered blood pressure to form angiotensin-1.
Btc	Betacellulin	Growth factor that binds to EGFR, ERBB4 and other EGF receptor family members. Potent mitogen for retinal pigment epithelial cells and vascular smooth muscle cells.
Ccdc50	Coiled-coil domain containing 50	Involved in EGFR signaling. Mutations cause hearing loss in mice.
Dhx58	DEHX box polypeptide 58	Acts as a regulator of DDX58/RIG-I and IFIH1/MDA5 mediated antiviral signaling. Cannot initiate antiviral signaling as it lacks the CARD domain required for activating MAVS/IPS1-dependent signaling events.
Gbp3	Guanylate binding protein 3	Specifically bind guanine nucleotides (GMP, GDP, and GTP) and contain two of the three consensus motifs found in typical GTP-binding proteins. Exhibits antiviral activity against influenza virus.
Gbp4	Guanylate binding protein 4	Binds GTP, GDP and GMP. Hydrolyzes GTP very efficiently; GDP rather than GMP is the major reaction product. Plays a role in erythroid differentiation
Htr1d	serotonin receptor 1D	G-protein coupled receptor for 5-hydroxytryptamine (serotonin). Also functions as a receptor for ergot alkaloid derivatives, various anxiolytic and antidepressant drugs and other psychoactive substances. May play a role in vasoconstriction
Ifi203	Interferon activated protein 203	Unknown function
Ifi47	Interferon gamma inducible protein 47	Unknown function
Igtp	Interferon gamma induced GTPase	Unknown function
Lypla1	Lysophospholipase 1	Hydrolyzes fatty acids from S-acylated cysteine residues in proteins such as trimeric G alpha proteins or HRAS. Has depalmitoylating activity toward KCNMA1. Has low lysophospholipase activity
Mov10	Moloney leukemia	Probable RNA helicase. Required for RNA-mediated gene silencing by the RNA-induced silencing complex (RISC). Required for both

	virus 10	miRNA-mediated translational repression and miRNA-mediated cleavage of complementary mRNAs by RISC. Also required for RNA-directed transcription and replication of the human hepatitis delta virus (HDV).
Pnpt1	Polyribonucleotide protein nucleotidyltransferase 1	RNA-binding protein implicated in numerous RNA metabolic processes.
Psmb8	Proteasome subunit, beta type 8	Replacement of PSMB5 by PSMB8 increases the capacity of the immunoproteasome to cleave model peptides after hydrophobic and basic residues. Acts as a major component of interferon gamma-induced sensitivity. Plays a key role in apoptosis via the degradation of the apoptotic inhibitor MCL1. May be involved in the inflammatory response pathway.
Rps3a	Ribosomal protein S3A	May play a role during erythropoiesis through regulation of transcription factor DDIT3
Rtp4	Receptor transporter protein 4	Probable chaperone protein which facilitates trafficking and functional cell surface expression of some G-protein coupled receptors (GPCRs). Promotes functional expression of the bitter taste receptor TAS2R16
Samd9l	Sterile alpha motif domain containing 9-like	Unknown function
Sema6d	Semaphorin 6D	Shows growth cone collapsing activity on dorsal root ganglion (DRG) neurons in vitro. May be a stop signal for the DRG neurons in their target areas, and possibly also for other neurons. May also be involved in the maintenance and remodeling of neuronal connections.
Serping1	Complement 1 inhibitor	forms a proteolytically inactive stoichiometric complex with the C1r or C1s proteases. May play a potentially crucial role in regulating important physiological pathways including complement activation, blood coagulation, fibrinolysis and the generation of kinins.
Slc16a4	Solute carrier family 16, member 4	Proton-linked monocarboxylate transporter. Catalyzes the rapid transport across the plasma membrane of many monocarboxylates such as lactate, pyruvate, branched-chain oxo acids derived from leucine, valine and isoleucine, and the ketone bodies acetoacetate, beta-hydroxybutyrate and acetate
Slc25a28	Solute carrier family 25, member 28	Mitochondrial iron transporter that mediates iron uptake.
Snx5	Sorting nexin 5	Involved in several stages of intracellular trafficking.
Sp100	Nuclear antigen Sp100	involved in a large number of physiological processes including cell growth, differentiation and apoptosis.
Tgm2	Transglutaminase 2	Catalyzes the cross-linking of proteins and the conjugation of polyamines to proteins.

Trim25	Tripartite motif-containing 25	Expression of the gene is upregulated in response to estrogen, and it is thought to mediate estrogen actions in breast cancer as a primary response gene.
Ttc39b	Tetratricopeptide repeat domain 39b	Unknown function
Ubd	Ubiquitin D	Constitutively expressed in mature dendritic cells and B-cells. Mostly expressed in the reticuloendothelial system (e.g. thymus, spleen), the gastrointestinal system, kidney, lung and prostate gland
Ugt1a6a	UDP glycosyltransferase	UDPGT is of major importance in the conjugation and subsequent elimination of potentially toxic xenobiotics and endogenous compounds. This isoform has specificity for phenols. Isoform 3 lacks transferase activity but acts as a negative regulator of isoform 1
Xdh	xanthine dehydrogenase	Key enzyme in purine degradation. Catalyzes the oxidation of hypoxanthine to xanthine. Catalyzes the oxidation of xanthine to uric acid. Contributes to the generation of reactive oxygen species. Has also low oxidase activity towards aldehydes
Zeb2	Zinc finger E-box binding homeobox 2	Transcriptional inhibitor that binds to DNA sequence 5-CACCT-3 in different promoters. Represses transcription of E-cadherin.

Table 2.2. sgRNAs for select ISGs to generate bulk CRISPR knockout cell lines.

Gene Name	CRISPR line	Sequence 5'-->3'	Gene Name	CRISPR line	Sequence 5'-->3'
Stat1	1	caccgGGATAGACGCCAGCCACTG aaacCAGTGGCTGGGCGTCTATCCc	Kbtbd8	1	caccgCCTGTGACGATATCTAGACA aaacTGTCTAGATATCGTCACAGGc
	2	caccgTGTGATGTTAGATAAACAGA aaacTCTGTTTATCTAACATCACAc		2	caccgAGACAGTGACGATTTAAATG aaacCATTAAATCGTCACTGTCTc
	3	caccgCGGCTGTCGTTCTACCACGA aaacTCGTGGTAGAACGACAGCCGc		3	caccgAAGACTCCAATAGAATTCTG aaacCAGAATTCATTGGAGTCTTc
Cngl	1	caccgGGATCAAATCAGTCGCCAGT aaacACTGGCGACTGATTTGATCCc	Lamp3	1	caccgAGAGTAGGCCTAGGAACTAG aaacCTAGTTCTTAGGCCTACTCTc
	2	caccgGGAGTCTAGATGTCAGCCAA aaacTTGGCTGACATCTAGACTCCc		2	caccgCCCAGTTATATAGTTGACAA aaacTTGTCAACTATATAACTGGGc
	3	caccgACGACACCTTGCCATTGAG aaacCTCAAATGGCAAGGTGTCTGtc		3	caccgTCATCTACTGACGATACCAT aaacATGGTATCGTCAGTAGATGAc
Erlec1	1	caccgCCAGGCCAGTTGACTCGGAA aaacTTCCGAGTCAACTGGCCTGGc	Ifi202b	1	caccgGGGAAACCAATATTACACTC aaacGAGTGTAATATTGGTTTCCCCc
	2	caccgACTTCCACTTGTGACAAGTG aaacCACTTGTCACAAGTGGAAGTc		2	caccgCCAAAAAAGAACATTAGCAA aaacTTGCTAATGTTCTTTTTTTGGc
	3	caccgTCCAACGTCTTAGTGTGAG aaacCTCACACTAAGACAGTTGGAc		3	caccgTGGCCAGATGAATCACTGGA aaacTCCAGTGATTCATCTGGCCAc
Atf3	1	caccgCCAGCGCAGAGGACATCCGA aaacTCGGATGTCCTCTGCGCTGGc	Ifi47	1	caccgGGTCTAGATAAGCGTCTGCG aaacCGCAGACGCTTATCTAGACCc
	2	caccgTCCTCAAATACCACTGACCC aaacGGGTCACTGGTATTTGAGGAc		2	caccgTTGGAGATCAGGAAGATGCA aaacTGCATCTTCTGATCTCCAAc
	3	caccgTACCGTCAACAACAGACCCC aaacGGGGTCTGTTGTTGACGGTAc		3	caccgCTGATTAATGCAGAGTACTG aaacCAGTACTCTGCATTAATCAGc
Fam129a	1	caccgATTGTAACCTACTCCAAACC	Lypla1	1	caccgTTCACGGATTGGGAGATACA

		aaacGGTTTGGAGTAAGTTACAATc			aaacTGTATCTCCCAATCCGTGAAc
	2	caccgACGGAGCTTAACCTTCTCGA aaacTCGAGAAGGTTAAGCTCCGtc		2	caccgCGGGCGGTGGCCCTTCGGG aaacCCCGGAAGGCCACCGCCGc
	3	caccgCAGACCTCAAACCGCCATG aaacCATGGCGGTTTTGAGGTCTGc		3	caccgTGGACAGATGTATTTGATGT aaacACATCAAATACATCTGTCCAac
Gtpbp2	1	caccgCCAGTTCCTAGATCTCCGTG aaacCACGGAGATCTAGGAACTGGc	Lap3	1	caccgGGGGTGCCTCGGTTGCATTG aaacCAATGCAACCGAGGCACCCc
	2	caccgACTGGACAGTGTAATATAG aaacCTATATTTACTGTCCAGTc		2	caccgGTCCACCGCAGACATGACGA aaacTCGTCATGTCTGCGGTGGACc
	3	caccgCCTGTGTGCTAAGACCACAG aaacCTGTGGTCTTAGCACACAGGc		3	caccgAAGTGCCAGTAGTAAAACCA aaacTGGTTTTACTACTGGCACTTc
Dock4	1	caccgCCATATTGGAGATCACTAGT aaacACTAGTGATCTCCAATATGGc	Ppp2r2a	1	caccgAAAAGAGGAACACTTACCGT aaacACGGTAAGTGTTCCTCTTTTc
	2	caccgGGTAGCGGGTAGTATCCTGA aaacTCAGGATACTACCCGCTACCc		2	caccgCAAACGTGTTACAGCTGTTG aaacCAACAGCTGTAACACGTTTGc
	3	caccgATGAAATCCTCGATCTGCCA aaacTCGCAGATCGAGGATTTCAc		3	caccgGATGTGATAAGTGTGGGCGT aaacACGCCACACTTATCACATCc
CFB	1	caccgTATGACGGTTACTCTCCG aaacCGGAGAGTGTAACCGTCATAc	Trim69	1	caccgCGGAACCAGTCGTTACACAG aaacCTGTGTAACGACTGGTTCCGc
	2	caccgCATGTACGACACCCTCAAG aaacCTTGAGGGGTGTCGTACATGc		2	caccgAAGAAGTTACCCTGCTCAA aaacTTGAGCAGGGGTAACCTCTTc
	3	caccgTCTGCAGGATTGCACAACAT aaacATGTTGTGCAATCCTGCAGAc		3	caccgAGGATGCACGGTTGTCTATG aaacCATAGACAACCGTGCATCTc
Agt	1	caccgGGAAGGGGTGGATGTATACG aaacCGTATAACATCCACCCCTTCCc	Tmod3	1	caccgTTCGGTTAGCACCGACCTCG aaacCGAGGTGCGGTGCTAACCGAAc
	2	caccgTGGATAAATCCAGAGAGCGT aaacACGCTCTCTGGATTTATCCAac		2	caccgTGTAGGGCACATAATCGTCC aaacGGACGATTATGTGCCCTACAc

	3	caccg CTCCCGACTAGATGGACACA aaac TGTGTCCATCTAGTCGGGAGc		3	caccg GATGTGCTGGGAAGTAGTAA aaac TTACTACTTCCCAGCACATCc
Akt3	1	caccg CCGTAGCCGACCGATTGCAG aaac CTGCAATCGGTCGGCTACGGc	Reep3	1	caccg CGTGAAGACGAAAAACGTCA aaac TGACGTTTTTCGTCTTCACGc
	2	caccg AATTTGATGCTAGATAAGGA aaac TCCTTATCTAGCATCAAATCc		2	caccg GCTGTGCCCTACACTAGAG aaac CTCTAGGTAGGGCGACAGCc
	3	caccg CTGCACCATAGAAACGTGTG aaac CACACGTTTTCTATGGTGCAGc		3	caccg ATCTTCAGCTCATAGTACAG aaac CTGTACTATGAGCTGAAGATc
CD47	1	caccg ATCAGCCTGTTCTTACGAGG aaac CCTCGTAAGAACAGGCTGATc	Trim34a	1	caccg GACAGGCTTGGCATAACAGG aaac CCGTGTATGCCAAGCCTGTCc
	2	caccg GGATAAGCGCGATGCCATGG aaac CCATGGCATCGCGCTTATCCc		2	caccg GAGAATCTAGTACCACACAC aaac GTGTGTGGTACTAGATTCTCc
	3	caccg CACTTCATGCAATGAAACTG aaac CAGTTTCATTGCATGAAAGTc		3	caccg GCTTAGAAGAATCCTGGACA aaac TGTCCAGGATTCTTCTAAGCc
negative control	1	caccg ACGGAGGCTAACGTCGCAA aaac TTGCGACGTTAGCCTCCGTCc	Ifitm3	1	caccg CTGACAGAAGCCGATCCGTG aaac CTCGGATCGGCTTCTGTCCAGc
	2	caccg CGCTTCCGCGCGGCCCGTTCAA aaac TTGAACGGGCGCGCGGAAGCGc		2	caccg AATCAAGGAAGAATATGAGG aaac CCTCATATTCTTCTTGATTc
	3	caccg ATCGTTTCCGCTTAACGGCG aaac CGCCGTTAAGCGGAAACGATc		3	caccg GTCTAGGGATCGGAAGATGG aaac CCATCTCCGATCCCTAGACc

Sequences in bold correspond to the sgRNA oligo. Nucleotides in lower case correspond to the flanking sequence required to ligate the oligos to the LentiCRISPRv2 vector.

Chapter 3: Characterization of murine Ifitm3 as an antiviral ISG against alphaviruses *in vitro* and *in vivo*

This chapter is essentially as published in Journal of Virology:

“The Interferon-Stimulated Gene IFITM3 Restricts Infection and Pathogenesis of Arthritogenic and Encephalitic Alphaviruses” Poddar S, Hyde JL, Gorman MS, Farzan M and Diamond MS. October 2016, vol 90, no.19 8780-8794.

ABSTRACT

Host cells respond to viral infections by producing type I interferon (IFN), which induces the expression of hundreds of interferon stimulated genes (ISGs). Although ISGs mediate a protective state against many pathogens, the antiviral functions of the majority of these genes have not been identified. IFITM3 is a small transmembrane ISG that restricts a broad range of viruses including orthomyxoviruses, flaviviruses, filoviruses, and coronaviruses. Here, we show that alphavirus infection is increased in *Ifitm3*^{-/-} and *Ifitm* locus deletion (*Ifitm-del*) fibroblasts, and reciprocally, reduced in fibroblasts trans-complemented with *Ifitm3*. Mechanistic studies showed that *Ifitm3* did not affect viral binding or entry, but inhibited pH-dependent fusion. In a murine model of chikungunya virus arthritis, *Ifitm3*^{-/-} mice sustained greater joint swelling in the ipsilateral ankle at days 3 and 7 post infection, and this correlated with higher levels of pro-inflammatory cytokines and viral burden. Flow cytometric analysis suggested that *Ifitm3*^{-/-} macrophages from the spleen were infected at greater levels than observed in wild-type (WT) mice, results that were supported by experiments with *Ifitm3*^{-/-} bone marrow derived macrophages. *Ifitm3*^{-/-} mice also were more susceptible than WT mice to lethal alphavirus infection with Venezuelan equine encephalitis virus, and this was associated with greater viral burden in multiple organs. Collectively, our data define an antiviral role for *Ifitm3* in restricting infection of multiple alphaviruses.

INTRODUCTION

The type I interferon (IFN) response is a critical factor that orchestrates innate protection against viral pathogens. Upon detection of pathogen-associated molecular patterns (PAMPs), host cells produce type I IFN, which in turn induces expression of hundreds of IFN stimulated genes (ISGs). ISGs can inhibit multiple steps of the viral life cycle (e.g. entry, protein translation, assembly, or egress) or modulate the immune response, such as by enhancing the recruitment of leukocytes or promoting B and T cell maturation (14).

IFN-induced transmembrane (IFITM) proteins 1, 2 and 3 were among the first IFN-stimulated genes (ISGs) to be identified (92), and initially were studied for their roles in germ cell homing and maturation. IFITM proteins are approximately 130 amino acids in length, and are conserved in most vertebrate species (93). IFITMs have no catalytic subunit, but share similar domain architectures consisting of a short N-terminal domain, two antiparallel domains, a conserved intracellular loop, and a hydrophobic C-terminal domain (94, 95). The topology of IFITM3 has been clarified by electron paramagnetic and nuclear magnetic resonance analyses; the N-terminal is located inside the cell, whereas the antiparallel domains reside as intramembrane α -helices, followed by the transmembrane C-terminal domain (96). Although IFITM1, 2, and 3 all have reported antiviral activity, IFITM3 exhibits the greatest protection against the broadest range of viruses including influenza A virus (IAV), flaviviruses (Dengue, West Nile, and Japanese encephalitis viruses), hepaciviruses (hepatitis C virus), filoviruses (Ebola and Marburg viruses), bunyaviruses (Rift Valley Fever and La Crosse viruses), rhabdoviruses (vesicular stomatitis virus), coronaviruses (SARS-CoV), paramyxoviruses (respiratory syncytial virus, RSV), and reoviruses (9, 56, 60, 61, 64, 66, 68–70, 97, 98). Despite a wealth of *in vitro* data, the antiviral effects of IFITM3 *in vivo* are less well characterized. To

date, only IAV and RSV have been shown to have enhanced pathogenesis in *Ifitm3*-deficient (*Ifitm3*^{-/-}) mice (59, 63, 64). In humans, the allelic polymorphism rs12252-C, which results in a splice variant of IFITM3 lacking the first 21 amino-terminal amino acids, correlates with increased morbidity and mortality following IAV infection (63, 99, 100). However, some studies have questioned the significance of this truncated IFITM3 allele in the susceptibility to IAV and other viral infections (80, 81).

The mechanisms by which IFITM3 restrict viral infection are not fully elucidated. Studies have shown that IFITM3 affects pH dependent fusion in the late endosome, which potentially traps entering virions in a hemifusion state (57, 78, 101). IFITM3 expression also can modulate the efficiency of cathepsin-mediated proteolysis in an as yet undefined manner, which is required for the cleavage of the fusion proteins of reoviruses, filoviruses, and coronaviruses, and release of the viral genome from the endolysosome into the cytosol (56, 69). Additionally, IFITM3 is incorporated into the plasma membrane of budding HIV particles, which restricts their fusogenic capability (72). Finally, ectopic expression of IFITMs appears to alter the physical characteristics of the endosome, resulting in increased size, reduced membrane fluidity, and increased cholesterol content, which subsequently impact the efficiency of viral fusion (52, 78, 79).

Alphaviruses are enveloped single-stranded positive sense RNA viruses of the *Togaviridae* family, many of which are transmitted by mosquitoes. The binding, entry, and pH-dependent fusion of alphaviruses are directed by the structural glycoproteins E1 and E2 (102, 103). E1 and E2 are arranged as heterodimers, and assembled into trimeric spikes on the surface of the virion (104). E1 is classified as a type II membrane fusion protein, whereas E2 contains the putative receptor binding site (102).

Chikungunya virus (CHIKV) has emerged rapidly over the last decade, causing outbreaks in the islands of the Indian Ocean, in Southern Europe, and in Southeast Asia. In 2013, CHIKV spread to the Western Hemisphere and by the end of 2015 had infected more than 1.8 million people in North, Central, and South America (30). Other arthritogenic alphaviruses have a more limited distribution in parts of Oceania, Africa, and South America, whereas outbreaks of encephalitic alphaviruses occur sporadically in North, Central, and South America (105). Infection by arthritogenic alphaviruses, including CHIKV, Sindbis, Ross River, and Mayaro viruses, results in a febrile illness associated with rash, myalgia, and moderate to severe joint pain (41). The musculoskeletal disease caused by these viruses is associated with direct infection of myocytes, synovial fibroblasts and osteoblasts (32, 34, 38, 39, 41) and the ensuing infiltration of inflammatory cells. Infection by encephalitic alphaviruses, including Venezuelan (VEEV), Eastern, and Western equine encephalitis viruses, causes a severe febrile illness associated with infection and injury to neurons, encephalitis, long-term debilitating neurological sequelae, and death (105). To date, there are no licensed alphavirus vaccines available for use in humans.

Several ISGs have been characterized as restriction factors against alphavirus infection, including *ISG15*, *PKR*, *ZAP* and *BST-2*; these genes target viral protein translation and virion egress, respectively (15–17, 19, 46). Ectopic expression-based screens against alphaviruses also have revealed putative inhibitory genes, including *Isg20*, *Ifit1*, *Ifit2*, *Ifit3*, and *Rsad2* (47). However, in the case of *Ifit1*, which recognizes RNA lacking a 2'-*O* methylation on the 5' cap structure and prevents translation, alphaviruses subvert its antiviral function via RNA secondary structure motifs that inhibit binding (48). Recent studies suggest that ectopic expression of IFITM genes in cell culture can restrict infection of Sindbis (SINV) and Semliki Forest (SFV) viruses in cell culture by inhibiting viral fusion with cellular membranes (106). Other ISGs (e.g.,

HSPE and *P2RY6*), have been identified, with little information regarding their mechanism of restriction (7, 20). Finally, ISGs can act in synergy to inhibit alphavirus infection (45).

In this study, we evaluated the antiviral activity of IFITM3 against several alphaviruses by comparing infection of IFN-treated wild-type (WT), *Ifitm3*^{-/-}, and *Ifitm* locus deletion (*Ifitm-del*) mouse fibroblasts with CHIKV, SFV, SINV, O'nyong nyong (ONNV), and VEEV viruses. In the absence of *Ifitm3* gene expression we observed an increase in alphavirus replication *in vitro*, which was inhibited following trans-complementation with *Ifitm3*. *In vivo*, *Ifitm3*^{-/-} mice inoculated with CHIKV sustained higher viral burden in the spleen, serum, and joint tissues at early times after infection. This was associated with higher levels of pro-inflammatory cytokines and increased joint swelling along with greater replication in macrophages in some tissues. Consistent with this latter observation, bone marrow derived macrophages from *Ifitm3*^{-/-} mice sustained higher levels of CHIKV infection than WT cells. Analogous to our observed phenotypes with CHIKV *in vivo*, *Ifitm3*^{-/-} mice infected with VEEV exhibited greater weight loss and mortality, and supported greater replication in the liver, spleen, spinal cord, and brain. Collectively, our data suggest that *Ifitm3* contributes to an early host defense response against multiple alphaviruses of global concern.

MATERIALS AND METHODS

Ethics statement. This study was carried out in accordance with the recommendations in the Guide for the Care and Use of Laboratory Animals of the National Institutes of Health. The protocols were approved by the Institutional Animal Care and Use Committee at the Washington University School of Medicine (Assurance Number: A3381-01). Dissections and injections were performed under anesthesia that was induced with ketamine hydrochloride and xylazine.

Mice. WT C57BL/6 mice were obtained commercially from Jackson Laboratories. *Ifitm-del* and *Ifitm3^{-/-}* mice have been reported previously (107). *Ifitm2^{-/-}* mice will be described in a forthcoming manuscript (M. Gorman and M. Diamond, unpublished data). All transgenic mice were backcrossed to 99% purity using speed congenic analysis (108). Four week-old mice were inoculated in the left footpad with 10^3 FFU of CHIKV-LR in 10 μ l of PBS. Ankles were measured (width x height) for joint swelling on days 3 and 7 post infection. On selected days after infection, mice were sacrificed for the collection of serum and tissues. After intracardiac perfusion with PBS, organs were harvested, weighed and homogenized to determine viral titers by a focus forming assay. For studies with VEEV, a vaccine-derived recombinant strain with a point mutation (TC83-A3G) was used; this mutation confers partial virulence in WT mice as it restores the capacity to antagonize the inhibitory actions of the ISG, *Ifit1* (48). Four week-old mice were inoculated in the left footpad with 10^6 FFU of VEEV-TC83-A3G in 10 μ l of PBS. Mice were followed daily for survival and weighed every two days. On selected days, infected mice were sacrificed and organs were harvested as described above.

Flow cytometric analysis of CHIKV-infected splenocytes. Spleens of CHIKV-infected mice were harvested after perfusion with PBS. Splenocytes were obtained by generating a single cell suspension, passaging through a 70 μ m filter, and lysis of red blood cells with ACK buffer (Invitrogen). Splenocytes were maintained on ice in PBS supplemented with 2% FBS and 1 mM EDTA. After blockade of Fc γ receptors with anti-CD16/32 (eBioscience Clone 93), staining for viability (eBioscience FVD eFluor 506), and cell surface antigens CD45, CD3, CD19, CD3, Ly6G, Ly6C, CD11b, CD11c, MHC class II, and F4/80 was performed. Viral antigen (E1 and E2 proteins on the surface of cells) was detected using biotinylated humanized CHK-152 and murine CHK-166 (37), with biotinylated humanized WNV E16 and murine WNV E60 (109, 110) serving as isotype controls, respectively. Secondary staining was followed with streptavidin conjugated Alexa 647 (Invitrogen). Cells were fixed subsequently using the eBioscience FoxP3 Fixation Buffer Set and processed for flow cytometry with the BD LSRII. Data were analyzed with FloJo software.

Bioplex cytokine assay. To measure cytokine levels, a BioPlex Pro Assay was performed according to the manufacturer's protocol (BioRad) on homogenized ankle tissues isolated at day 1 and 2 post infection. The cytokine screen included IL-1 α , IL-1 β , IL-2, IL-3 IL-4, IL-5, IL-6, IL-9, IL-10, IL-12p40, IL-12p70, IL-13, IL-17, Eotaxin, G-CSF, GM-CSF, IFN- γ , KC, MCP-1 MIP-1 α , MIP-1 β , RANTES (CCL5), and TNF- α .

Cells and viruses. Primary WT, *Ifitm-del*, *Ifitm2^{-/-}* and *Ifitm3^{-/-}* derived mouse embryonic fibroblasts (MEFs) and bone marrow derived macrophages were generated according to published methods (111). Transformed MEFs were generated by transfection of the SV2 plasmid, which encodes for the large T antigen of SV2 polyoma virus (112), and passaged ~10 times. All MEFs were cultured in complete DMEM, which was supplemented with 10% fetal

bovine serum, and 10 mM each of GlutaMAX, sodium pyruvate, non-essential amino acids and HEPES pH 7.3. MEFs that ectopically express c-Myc-tagged firefly luciferase or c-Myc-tagged *Ifitm3* were generated via lentiviral transduction of the pFCIV vector, which contains an IRES-GFP (113, 114). Lentivirus was produced by transfecting 293T cells with pSPAX.2 (Addgene 12260), pMD2G (Addgene 12259) and pFCIV. Supernatants were harvested at 48 to 72 h post transfection. WT, *Ifitm-del* and *Ifitm3^{-/-}* transformed MEFs were incubated with lentiviral supernatants and 10 µg/ml of polybrene and spinoculated (300 x g) at room temperature for 30 min. The inoculum was replaced with complete DMEM 24 h later and incubated at 37°C. Transduction efficiency was determined by expression of GFP, and sorting of GFP⁺ cells was performed on a FACS AriaII (Becton-Dickinson). After repeated passages to ensure stable expression, the MEFs were tested for GFP and protein expression by flow cytometry and Western blotting, respectively. Vero and 293T cells were cultured and passaged in complete DMEM.

The CHIKV-LR (La Reunion OPY1 p142) strain was a gift from S. Higgs (Kansas State University). SINV (Toto) was a gift from C. Rice and P. MacDonald (Rockefeller University). VEEV-TC83 was a gift from W. Klimstra (University of Pittsburgh). These strains were produced from infectious cDNA clones (115, 116). CHIKV 181/25, ONNV (MP30), SFV (Kumba), were provided by the World Reference Center for Arboviruses (R. Tesh, University of Texas Medical Branch). Virus propagation and titration was performed in Vero cells.

Genotyping of MEFs. Genomic DNA was extracted from MEFs with the Qiagen DNeasy Blood and Tissue kit, and was characterized by PCR. *Ifitm2* WT allele or the knockout construct was genotyped using the following primers: *Ifitm2* WT F: 5'-ATGTGGTCTGGTCCCTGTTC-3', *Ifitm2* WT R: 5'-AGGTGCTCTGGCTCCATTTTC-3'; WT

band = 520 bp. *Ifitm2* KO F: 5'-TCATTCTCAGTATTGTTTTGCC-3', *Ifitm2* KO R: 5'-TGGAGACCAGAAGCCTGAC-3'; KO band = 373 bp. PCR reaction conditions for both *Ifitm2* WT and KO alleles were as follows: 94°C for 3 min, 94°C for 45 s, 55°C for 30 s, 70°C for 1 min 30 s, 35 cycles, and 70°C for 10 min. The *Ifitm3*^{-/-} mouse can be identified by the in-frame insertion of GFP within the *Ifitm3* allele (C Bailey, unpublished)(107). WT allele or the knockout construct was genotyped using the following primers: WT *Ifitm3* F: 5'-ATCCTTTGCCCTTCAGTGCT-3' and WT *Ifitm3* R: 5'-ACTCATACTCGGTGCCATC-3'; WT band = 355 bp, KO band = 1321 bp. PCR reaction conditions for both *Ifitm3* WT and KO were as follows: (a) 94°C for 1 min 30 s, 94°C for 25 s, 60°C for 30 s, reducing temperature by 0.1°C per cycle, 72°C for 1 min 30 s, 35 cycles, and 72°C for 5 min. The IFITM-del allele was determined using the following primers (107): IFITM-del WT F: 5'-AACATGCCTTGCATCCCTGGAGTTCCTTCTAAAGGA-3', IFITM-del WT R: 5'-CCCTAAAACACTTAGCAGTGACCCCTCACAAGCC-3'; WT band = 500bp. *Ifitm-del* KO F: 5'-ACTCTAGCCAGAGTCTTGCATTTCTCAGTCCTAAAC-3', IFITM-del KO R: 5'-TCTAGTACAGTCGGTAAGAACAAAATAGTGTCTATC A-3'; KO band = 600bp. PCR reaction conditions for *Ifitm-del* alleles were as follows: 95°C for 30 s, 54°C for 30 s, 68°C for 1 min 30 s, 29 cycles, and 68°C for 5 min.

qRT-PCR measurement of *Ifitm* genes. WT, *Ifitm2*^{-/-}, *Ifitm3*^{-/-} and *Ifitm-del* MEFs (10⁴ cells per condition) were seeded in a 96-well plate. After a 6 h incubation with IFN-β at varying doses, MEFs were lysed and total RNA was extracted with the Qiagen RNeasy Kit. *Ifitm2* and *Ifitm3* were detected using qRT-PCR and normalized to *Gapdh* expression, using the following PrimeTime assays (IDT) according to the manufacturer's instructions: *Ifitm2*: Mm.PT.58.33172327.g, *Ifitm3*: Mm.PT.51.6979575.g, and *Gapdh*: Mm.PT.39a.a.

Western blotting. MEFs were lysed in RIPA and electrophoresed under reducing conditions on a 12% Bis-Tris NuPAGE gel with MES buffer according to the manufacturer's instructions (Thermo Fisher). After transfer onto PVDF membranes (Thermo Fisher) using an iBlot apparatus (Thermo Fisher), proteins of interest were detected with mouse anti- β -actin (CST, 8H10D10), mouse anti-c-Myc (Sigma, 9E10), goat anti-Ifitm3 (R & D, AF337), HRP-conjugated anti-mouse IgG (Sigma Chemical), and HRP-conjugated anti-goat IgG (Santa Cruz, sc2304). For quantification of protein, secondary donkey anti-mouse IRDye 680 (Li-Cor 925-68072) and anti-rabbit- IRDye 800CW (Li-Cor, 926-32214) were used instead of HRP conjugates, and visualized on the Odyssey Imager (Li-Cor). Polyclonal rabbit anti-Ifitm3 (Proteintech, 11714-1-AP) was used for Ifitm3 detection in these experiments. Quantification was performed with Li-Cor Odyssey software.

Virus infection of cells. MEFs were plated (10^4 cells per well) in a 96-well plate, and in some experiments pretreated for 6 h with recombinant mouse IFN β (PBL Assay Science) at concentrations from 5 to 0.1 IU/ml, as indicated in the Figure Legends. The cells were inoculated with a given alphavirus (multiplicity of infection (MOI) of 5) and incubated at 37°C. At selected time points, cells were trypsinized, fixed with 1% paraformaldehyde (PFA), and permeabilized with Hank's Balanced salt solution (HBSS) containing 0.1% saponin and 10 mM HEPES. Infection was determined after sequentially staining cells with mouse or human mAbs (CHIKV, CHK-11; SFV, 2B4; TC83, 1A4A-1; ONNV, 4J21) (37, 117) against the E2 glycoprotein. SINV infection was detected using murine anti-SINV ascites (ATCC, VR-1248AF). Alexa 647 conjugated goat-anti mouse or human IgG antibody (Life Technologies) was used for secondary antibody staining. Samples were processed by flow cytometry using a BD FACSAArray. Data were analyzed with FloJo software.

For viral yield assays, cells were plated (10^5 cells per well in a 12-well plate) and in some experiments pretreated with specified doses of IFN β for 12 hours. Cells then were infected with CHIKV at 37°C. One hour later, the plates were rinsed twice with warm PBS, and replaced with fresh DMEM supplemented with 10% FBS. Supernatants were collected at specific time points, and viral titers were determined by focus forming assay on Vero cells, as described (37, 48). After fixation, infected cell foci were detected with CHK-11 and HRP-conjugated anti-mouse IgG (Sigma Chemical), and quantified with an ImmunoSpot (Cellular Technologies, Ltd.).

Binding and internalization assays. MEFs were plated (10^5 cells/well in a 24 well plate) the night before use. Cells were chilled on ice for 10 min, exposed to CHIKV-LR at an MOI of 5, and incubated on ice for 1 h. Unbound virus was removed with repeated washes of chilled media or PBS. To determine binding efficiency of virus, MEFs were lysed with RLT buffer and RNA was extracted using the Qiagen RNeasy Mini Kit, and analyzed for CHIKV RNA by qRT-PCR. To determine the efficiency of virus internalization, warm complete DMEM was added to MEFs and incubated at 37°C for 1 hr. Medium was removed and cells were placed on ice. Proteinase K (500 μ g/ml) in ice cold PBS was added for 1 h to digest any surface bound virus (118). MEFs were then transferred to eppendorf tubes and washed with PBS before lysing with RLT buffer and extracting RNA for qRT-PCR. Primer probe sets were ordered from IDT were CHIKV (F: 5'-TCGACGCGCCCTCTTTAA-3', R: 5'-ATCGAATGCACCGCACACT-3', Probe: 5'-/56-FAM/ACCAGCCTGCACCCATTCCTCAGAC/36-TAMSp/-3') and the GAPDH Primetime Assay Mm.PT.39a.a.

Fusion from without (FFWO) assay. MEFs were rinsed and then incubated with DMEM, supplemented with 0.2% FBS, 10 mM HEPES pH 7.3 and 20 mM NH $_4$ Cl on ice for 15 min. Virus (MOI of 100) was added to MEFs on ice for one hour to allow binding. Unbound

virus was removed after several rinses with chilled medium. Subsequently, pre-warmed acidic (DMEM, 0.2% FBS, 10 mM HEPES, 30 mM succinic acid pH 5.5) or neutral (DMEM, 0.2% FBS, 10 mM HEPES, pH 7.4) medium was added for 2 min at 37°C. Medium then was removed and replaced with warmed DMEM, 10% FBS, 10 mM HEPES supplemented with 20 mM NH₄Cl to inhibit endosomal viral fusion and *de novo* infection via the endosomal pathway. At 6 h after infection, MEFs were fixed with PFA, permeabilized, and analyzed for viral antigen by flow cytometry, as described above.

Statistical analysis. All data was analyzed using Prism software (GraphPad6, San Diego, CA). Viral infection assays in cell culture were analyzed by one-way ANOVA with Dunnett's multiple comparisons test, or Student's t-test. Viral kinetics assays were analyzed by two-way ANOVA with Dunnett's or Sidak's multiple comparisons. Viral burden assays were analyzed by the Mann-Whitney test. Quantitative RT-PCR assays were analyzed by Student's t-test. Kaplan-Meier survival curves were analyzed by the log rank test.

RESULTS

Restriction of alphaviruses by Ifitm proteins in cell culture. Although expression of IFITM genes inhibits infection of several different genera of viruses (9, 56, 60, 61, 64, 66, 68–70, 97), their antiviral activities against alphaviruses have yet to be established. To test whether Ifitm genes restrict alphavirus infection, we developed MEF lines lacking Ifitm2 (*Ifitm2^{-/-}*), Ifitm3 (*Ifitm3^{-/-}*), and Ifitm1, 2, 3, 5, and 6 (*Ifitm-del*) (**Fig 3.1A**). To assess their effects on CHIKV replication, MEFs were first pretreated with 1 IU/ml of recombinant mouse IFN β to induce *Ifitm* gene expression (**Fig 3.1B**). Ifitm3 protein induction was confirmed by Western blotting in WT and *Ifitm2^{-/-}* MEFs after IFN β treatment, whereas, as expected, *Ifitm3^{-/-}* and *Ifitm-del* MEFs lacked Ifitm3 protein (**Fig 3.1C**). IFN pretreated MEFs were then infected with a high viral dose (MOI of 5) of pathogenic (CHIKV-La Reunion 2006 (LR)) or attenuated (CHIKV 181/25) strains of CHIKV. Fourteen hours later, cells were harvested, and viral antigen was analyzed by flow cytometry. Whereas *Ifitm3^{-/-}* and *Ifitm-del* MEFs supported greater CHIKV infection (3-fold, $P < 0.01$ and 4-fold, $P < 0.001$ for CHIKV 181/25; 4.5-fold, $P < 0.0001$ and 6.5-fold, $P < 0.0001$ for CHIKV-LR) than WT cells, no increase in viral antigen expression was observed in *Ifitm2^{-/-}* MEFs (**Fig 3.1D-F**). Correspondingly, IFN β pre-treated *Ifitm3^{-/-}* and *Ifitm-del* MEFs infected with CHIKV produced higher titers of infectious virus compared to WT or *Ifitm2^{-/-}* cells (**Fig 3.1G**, CHIKV 181/25: 28-fold for *Ifitm3^{-/-}* ($P < 0.01$), and 12-fold for *Ifitm-del* ($P < 0.05$); **Fig 3.1H**, CHIKV-LR: 147-fold for *Ifitm3^{-/-}* ($P < 0.0001$), and 36-fold for *Ifitm-del* ($P < 0.0001$)) at 14 h post-infection. These data suggest that Ifitm3 has a dominant antiviral effect on CHIKV infection compared to Ifitm2.

We next tested whether Ifitm3 exhibited antiviral activity against other alphaviruses. Analogous to experiments with CHIKV, WT and Ifitm-deficient MEFs were pre-treated with varying doses of IFN β , infected at a high MOI, and assayed by flow cytometry. Notably, *Ifitm3*^{-/-} and *Ifitm-del* MEFs pre-treated with IFN β supported enhanced infection by SFV, ONNV, VEEV (strain TC-83), and SINV compared to WT cells ($P < 0.05$, **Fig 3.2**).

To corroborate our findings, we trans-complemented WT, *Ifitm3*^{-/-} and *Ifitm-del* MEFs with c-myc tagged to the N-terminal of Ifitm3 or firefly luciferase protein as a control. After confirmation of ectopic protein expression by flow cytometry and Western blotting (**Fig 3.3A and B**), MEFs were infected with CHIKV 181/25 (MOI of 5) in the absence of IFN β treatment and analyzed at 6 h post-infection. MEFs trans-complemented with Ifitm3 showed less CHIKV replication than firefly luciferase expressing controls (**Fig 3.3C and D**). This data suggests that Ifitm3 inhibits multiple alphaviruses *in vitro* and does not require expression of Ifitm1, Ifitm2, Ifitm5, and Ifitm6 proteins to exert its antiviral activity.

Ifitm3 inhibits pH-dependent fusion of alphaviruses. Studies with IAV have shown that IFITM3 prevents fusion of virions from the late endosome, which is required for release of viral genomic material into the cytosol (57, 101). Correspondingly, IFITM3 is expressed preferentially on membranes of intracellular vesicles including endosomes (56). However, following gene upregulation, such as after IFN induction or ectopic expression, IFITM3 can accumulate on the plasma membrane (59, 62, 119), which independently could restrict attachment of viruses to the cell surface. To define the stage in the alphavirus lifecycle that Ifitm3 inhibits, we assessed its effect on binding, internalization, and fusion.

To determine if expression of *Ifitm3* alters binding of alphaviruses to the cell surface, trans-complemented MEFs were incubated with CHIKV at 4°C for 1 h, washed extensively to remove unbound virus, and assayed by quantitative RT-PCR (qRT-PCR). As no differences in levels of bound CHIKV genomic RNA were detected between *Ifitm3* expressing MEFs and their corresponding controls (**Fig 3.4A**), we concluded that binding efficiency was not appreciably affected. To assess whether *Ifitm3* affected internalization, CHIKV was pre-bound to trans-complemented MEFs for 1 h on ice, followed by incubation at 37°C for 1 h. MEFs then were treated with proteinase K to remove residual surface bound virus before recovery of cellular RNA. Similar to cell surface binding assays, we observed no difference in the levels of internalized viral RNA (**Fig 3.4B**). As anticipated, in control binding experiments performed at 4°C, proteinase K treatment significantly decreased (11-fold, $P < 0.0001$) the level of cell-bound viral RNA (**Fig 3.4C**).

As we did not observe effects of *Ifitm3* on attachment or internalization, we next evaluated pH-dependent fusion. Alphaviruses can be induced to fuse at the plasma membrane in the presence of an acidic solution (acid-bypass or fusion from without (FFWO)) (120), albeit at low efficiency; this required us to infect at a high multiplicity of infection. To test whether FFWO is affected by ectopic expression of *Ifitm3*, MEFs were pre-incubated with CHIKV at 4°C, washed to remove unbound virus, and then incubated with pre-warmed medium at pH 7.4 or pH 5.5. Subsequently, medium was replaced with normal pH culture medium supplemented with 20 mM NH_4Cl , which prevents alphavirus maturation and fusion (120), was added to inhibit productive infection of progeny virions. Fourteen hours later, MEFs were analyzed for viral antigen by flow cytometry. *Ifitm3* trans-complemented MEFs had lower levels of CHIKV antigen than luciferase expressing controls in WT, *Ifitm3*^{-/-} and *Ifitm-del* MEFs (**Fig 3.4D and**

E). Consistent with results with IAV (101), expression of Ifitm3 also inhibits pH-dependent fusion of alphaviruses.

Ifitm3 inhibits alphavirus infection *in vivo*. To determine whether Ifitm3 has a protective role against alphaviruses *in vivo*, we used an established mouse model of CHIKV infection and arthritis (36). We inoculated 4-week old WT and *Ifitm3*^{-/-} mice with CHIKV-LR in the left footpad and measured joint swelling on days 3 and 7 after infection, which correspond to the peaks of tissue edema and cellular infiltrates, respectively (36, 37). Whereas no difference was seen in viral titers at these time points (**Fig 3.5A**), greater swelling was observed in ipsilateral ankle joints of *Ifitm3*^{-/-} compared to WT mice on both days, (**Fig 3.5B and C**, $P < 0.001$ and $P < 0.01$). Because of the disparity between clinical signs and virological data, we analyzed viral burden in different tissues (serum, spleen, ankles, wrists, and quadriceps muscles) at earlier time points (days 1 and 2 after inoculation) (**Fig 3.5D-K**). At day 1 after inoculation, the serum, spleen, and ipsilateral ankle (**Fig 3.5D-F**) of *Ifitm3*^{-/-} mice had higher viral titers compared to WT mice (20-fold in serum $P < 0.0001$; 160-fold in spleen, $P < 0.0001$; and 2.5-fold in ipsilateral ankle, $P < 0.01$). In comparison, at day 2, the titers in the spleen, serum and ipsilateral ankle were similar but levels in the contralateral ankle and quadriceps muscle (**Fig 3.5G and I**) were somewhat higher (4.5-fold, $P < 0.001$; and 5-fold $P < 0.01$, respectively). However, by day 3, no differences in viral titer were observed in any tissues between WT and *Ifitm3*^{-/-} mice.

The early higher viral burden in *Ifitm3*^{-/-} mice corresponded to higher levels of inflammatory chemokines and cytokines in the ipsilateral ankle (**Table 3.1**). The mean concentrations of several chemokines and cytokines (e.g., IL-2, MCP-1, TNF- α , IL-1 α , IL-12p40, G-CSF, and GM-CSF, $P < 0.05$) were higher in ankles from CHIKV-infected *Ifitm3*^{-/-}

than WT mice at days 1 and/or 2 after infection. These data suggest that in the context of CHIKV infection *in vivo*, *Ifitm3* contributes to restriction of early viral infection and spread, which impacts cytokine induction and the development of clinical disease.

Given the increase in viral titers in the spleen of *Ifitm3*^{-/-} mice on day 1, we hypothesized that *Ifitm3* might affect the cellular tropism of CHIKV. To identify the cell subsets that were more susceptible to CHIKV infection, we performed flow cytometric analysis on spleens of infected WT and *Ifitm3*^{-/-} mice (**Fig 3.6A-C**). Splenocytes were stained for CHIKV envelope (E1 and E2) proteins using specific MAbs (37) and compared to isotype control MAbs. Inflammatory monocytes (CD11b⁺Ly6G⁺), macrophages (CD11b^{hi}F4/80^{lo}), and red pulp macrophages (CD11b^{lo}F4/80^{hi}) expressed high levels of viral antigen (50%, 50% and 25%, respectively), with no difference in the fraction of infected cells from WT and *Ifitm3*^{-/-} cells (**Fig 3.6B** and data not shown). Nonetheless, greater numbers of CHIKV antigen-positive CD11b^{hi}F4/80^{lo} and CD11b^{lo}F4/80^{hi} macrophages were detected in the spleens of *Ifitm3*^{-/-} compared to WT mice (1.3 fold, *P* < 0.05; 1.7 fold, *P* < 0.05; and 2.2 fold, *P* < 0.05, respectively; **Fig 3.6C**). An increased number of *Ifitm3*^{-/-} neutrophils expressed CHIKV antigen (1.6 fold, *P* < 0.05), but the overall number of neutrophils was substantially lower compared to other myeloid cell populations. No differences in viral antigen-positive inflammatory monocytes were observed between the *Ifitm3*^{-/-} and WT controls, and neither *Ifitm3*^{-/-} nor WT CD4⁺, CD8⁺, CD19⁺, or NK1.1⁺ cells exhibited detectable viral protein staining (data not shown). To determine if *Ifitm3*^{-/-} macrophages can support greater replication of CHIKV, bone marrow derived macrophages were cultured from WT and *Ifitm3*^{-/-} mice, and infected at an MOI of 0.1. Viral supernatants were collected up to 72 h post infection and analyzed by focus forming assay. *Ifitm3*^{-/-} macrophages produced more virus at 24 and 48 h post infection compared to WT cells (**Fig 3.6D**, 12.5-fold, *P* < 0.01 and 10-fold, *P*

< 0.01, respectively). These data suggest that a lack of Ifitm3 allows for enhanced CHIKV infection in macrophages.

To assess whether Ifitm3 had a protective effect against other alphaviruses *in vivo*, we infected 4 week-old WT and *Ifitm3*^{-/-} mice with a previously described moderately pathogenic encephalitic alphavirus strain (VEEV TC83-A3G), which is resistant to the antiviral effects of another ISG, Ifit1 (48). *Ifitm3*^{-/-} mice exhibited greater mortality (**Fig 3.7A**) and morbidity (as judged by weight loss, **Fig 3.7B**) after VEEV TC83-A3G infection compared to WT mice. Consistent with the clinical phenotypes, higher VEEV titers were observed at day 1 after infection in the liver and spinal cord (3-fold, $P < 0.05$; 8-fold, $P < 0.01$, respectively, **Fig 3.7C**) and day 2 after infection in the spleen, brain, and liver of *Ifitm3*^{-/-} compared to WT mice (2.5-fold, $P < 0.05$; 250-fold, $P < 0.05$; and 10-fold, $P < 0.01$, respectively, **Fig 3.7C**). These data confirm that Ifitm3 restricts alphavirus infection *in vivo* and prevent early dissemination.

DISCUSSION

To evaluate the potential antiviral role of Ifitm3 in restricting alphaviruses *in vitro*, we infected WT, *Ifitm3*^{-/-} and *Ifitm-del* MEFs with CHIKV, SFV, ONNV, VEEV and SINV. All alphaviruses tested exhibited some degree of enhanced infection in *Ifitm3*^{-/-} cells. In contrast, studies with CHIKV and *Ifitm2*^{-/-} MEFs showed comparable infection to WT MEFs, suggesting that Ifitm2 is not the predominant Ifitm gene responsible for the inhibiting alphaviruses in the context of an intact type I IFN response. The antiviral function of Ifitm3 against alphaviruses was validated using trans-complemented MEFs that ectopically express Ifitm3. Analogous to how IFITM3 inhibits IAV infection (78, 101), our mechanism of action studies suggest that Ifitm3 does not affect the binding or internalization of CHIKV, but instead prevents pH-dependent fusion events.

We also observed greater CHIKV infection and disease pathogenesis *in vivo* in animals lacking Ifitm3 expression. *Ifitm3*^{-/-} mice developed greater ankle swelling compared to WT animals, and this difference correlated with an increased in viral burden and inflammatory chemokine and cytokine levels at early times post inoculation. Notably, at later time points, titers became equivalent in WT and *Ifitm3*^{-/-} mice, suggesting possible immune evasion of Ifitm3 by CHIKV, which could occur by several previously identified mechanisms including host transcriptional shut-off (121) or antagonism of IFN signaling (122). To assess possible effects of Ifitm3 on cellular tropism, we assessed CHIKV antigen staining using flow cytometric analysis of splenocytes at day 1 post infection. These cells were chosen because they were easily profiled, and exhibited substantial (160-fold) difference in viral yield at this time point. Although the overall percentage of CHIKV-positive myeloid cells was similar in the spleens of *Ifitm3*^{-/-} and WT mice, a higher number of macrophages were positive for CHIKV antigen, suggesting a

possible role for Ifitm3 in controlling viral growth in these cell types. One limitation of the flow cytometry experiments is that we cannot be certain that CHIKV antigen-positive staining defines *bona fide* infection, as it remains possible that we are detecting bound/opsonized virus on the surface of cells rather than E1 and E2 proteins prior to budding. To address this issue, we tried infection studies in WT and *Ifitm3*^{-/-} mice with double subgenomic reporter gene viruses (e.g., CHIKV-GFP); however the fluorescence staining was too dim for conclusive results, possibly because of the attenuation of these viruses. Nonetheless, our studies with bone marrow derived macrophages support a role for Ifitm3 restriction of CHIKV infection in this cell type, as increased titers were observed in cells from *Ifitm3*^{-/-} mice.

Our *in vivo* findings were not limited to CHIKV, as we also observed greater mortality, weight loss, and viral burden following VEEV infection of *Ifitm3*^{-/-} mice. These data suggest an important role for Ifitm3 in restricting alphavirus pathogenesis *in vivo*, by limiting replication and dissemination early during infection. Future studies using analogous flow cytometric approaches and conditional gene deletions are planned to define the cell-type specific antiviral effect of Ifitm3 in the context of VEEV pathogenesis.

A possible antiviral role of IFITM proteins against alphaviruses has not been extensively analyzed. Studies with pseudotyped virions (alphavirus structural proteins and retroviral RNA) initially suggested that IFITMs had little antiviral activity against CHIKV, SINV, and VEEV (M. Farzan, unpublished observations (52)). It remains uncertain why *Ifitm3* would not inhibit pseudotyped alphavirus virions although the icosahedral display of E1 and E2 may be altered in these viruses, which could affect entry and fusion of virus particles. *Ifitm3* has been implicated although not definitively demonstrated as a restriction factor for alphaviruses. Karki et al identified *IFITM3* as one of 31 human ISGs that functioned synergistically with zinc finger

antiviral protein (ZAP) to enhance restriction of SINV infection (45). Schoggins et al reported that IFITM3 moderately reduced CHIKV and ONNV infection in human cells ectopically expressing IFITM3 (20, 84). Consistent with these observations, a recent paper reported an inhibitory effect of IFITM3 and IFITM1 against SFV and SINV when ectopically expressed in human A549 cells (106). These data support our findings of an antiviral activity of Ifitm3 against multiple alphaviruses.

The characterization of Ifitm3 as an antiviral ISG against alphaviruses adds to the known host defense genes that block alphavirus infection. ISG15 protects against SINV *in vivo*, likely via conjugation (ISGylation) to viral proteins (15–17), ZAP restricts SINV, Ross River, SFV, and VEEV by blocking the accumulation of viral genomic content in the cytoplasm (8), and BST-2 (tetherin) prevents CHIKV egress by retaining budding virus on the plasma membrane (19). SINV also is strongly inhibited by PKR in the context of replication in DCs (46). Finally, a separate genetic screen revealed several unique ISGs with possible antiviral activity, against SINV including Isg20, Ifit1, Ifit2, Ifit3, and Rsad2 (viperin) (47).

In studies with other viruses, IFITM3 appears to restrict early steps in the viral lifecycle, particularly fusion into the cytoplasm (57, 78, 101). This is supported by data from our FFWO experiments in the context of CHIKV infection and by recent studies with SFV (106). However, it remains possible that IFITM3, akin to effects on HIV, could restrict alphavirus infection in a pH insensitive manner by integrating into the viral membrane, which we are currently exploring using mass spectrometric analysis of alphavirus virions derived from cells expressing or lacking Ifitm3. An additional mechanism that warrants investigation is the possible role for Ifitm3 in preventing viral budding and/or egress. IFITM3 can be detected at the plasma membrane, and its expression and localization is enhanced upon IFN stimulation (59, 62, 119).

In summary, we have shown that Ifitm3 can restrict several alphaviruses both *in vitro* and *in vivo*. Our data in mice suggest that Ifitm3 may function to restrict early replication and dissemination of alphaviruses, thereby preventing pathogenesis. Further investigation into additional mechanisms of Ifitm3 mediated restriction of alphaviruses is warranted as well as effects of gene polymorphisms, which could contribute to relative disease susceptibility in humans. Indeed, a common human allelic IFITM3 variant, rs12252-C, encodes for a 21 amino acid deletion of the N terminal part of the protein that appears to be associated with susceptibility to IAV infection (63, 99, 100). It remains to be determined whether this or other polymorphisms in the *IFITM3* gene can be linked to more severe or persistent alphavirus infection.

Figure 3.1

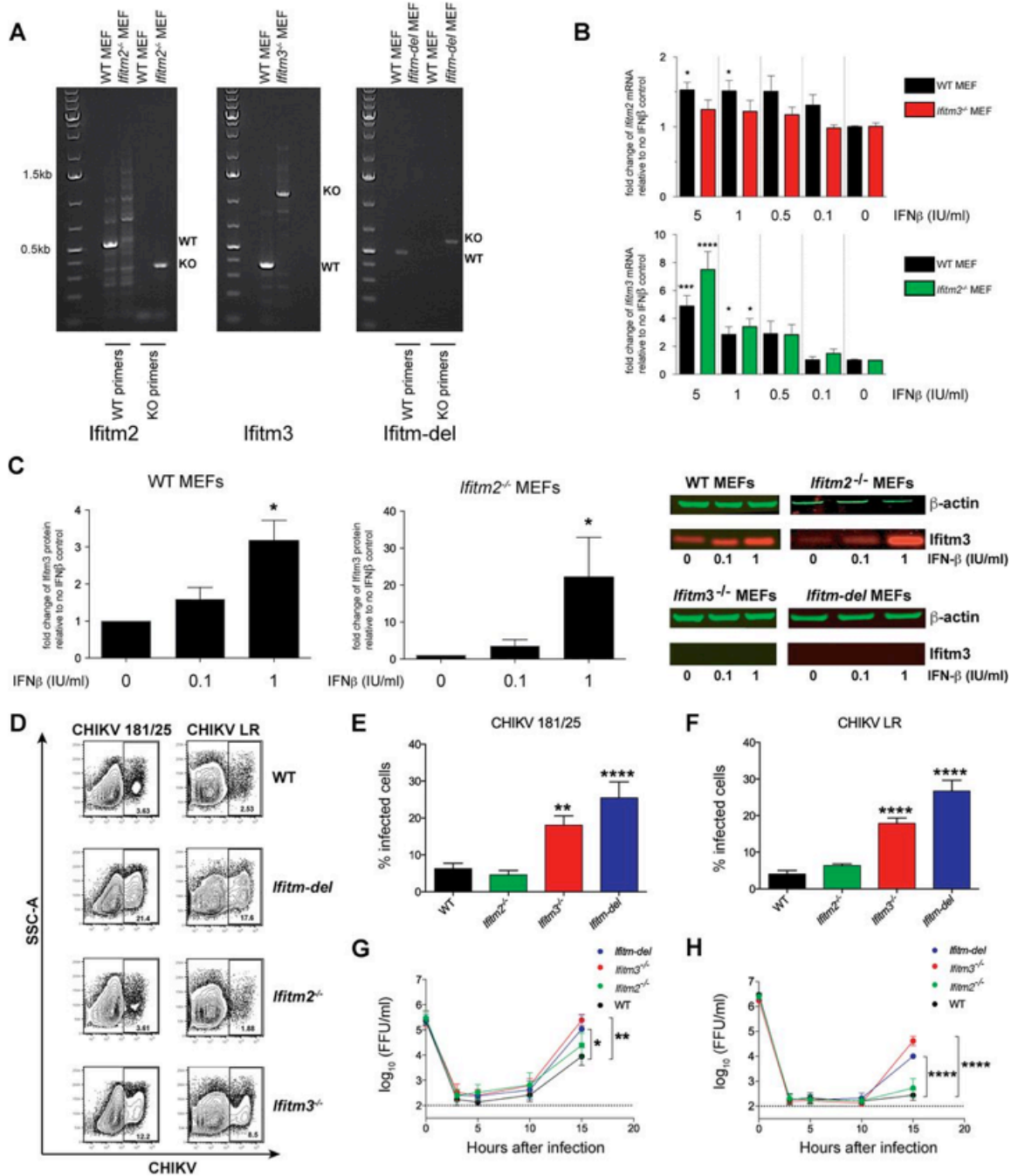


Figure 3.1. CHIKV infection is enhanced in cells lacking *Ifitm3* expression.

WT, *Ifitm2*^{-/-}, *Ifitm3*^{-/-}, and *Ifitm-del* MEFs were generated from WT and gene-targeted mice.

(A) Genotyping of MEFs was performed by PCR and agarose electrophoresis. Bands corresponding to WT and KO alleles are indicated to the right of each gel. (B) MEFs were

pretreated with various doses of IFN β and tested for *Ifitm2* and *Ifitm3* gene induction by qRT-PCR. *Ifitm2* expression was not detected in *Ifitm2*^{-/-} and *Ifitm-del* MEFs, and *Ifitm3* expression was not detected in *Ifitm3*^{-/-} and *Ifitm-del* MEFs. Bars show the means and standard errors of the means from three independent experiments performed in duplicate. Means were compared between control and IFN β -treated cells using a nonparametric one-way ANOVA with Dunn's multiple comparisons (*, $P < 0.05$; ***, $P < 0.001$; ****, $P < 0.0001$). **(C)** MEFs were pretreated with the indicated doses of IFN β and tested for *Ifitm3* expression by quantitative Western blotting. (Left) Means from three independent experiments were compared between control and IFN β -treated cells using a nonparametric one-way ANOVA with Dunn's multiple comparisons (*, $P < 0.05$). (Right) A representative Western blot with loading controls (β -actin) is shown. **(D to H)** The indicated MEFs were pretreated with 1 U/ml of IFN β and subsequently infected with CHIKV 181/25 or CHIKV-LR at an MOI of 5. **(D)** At 14 h postinfection, MEFs were stained for viral E2 protein and analyzed by flow cytometry. **(E and F)** Cumulative flow cytometry data for CHIKV 181/25 and CHIKV-LR. Bars show the means and standard errors of the means (SEM) from five independent experiments performed in quadruplicate or duplicate. Means were compared between WT and deficient cell lines using one-way ANOVA with Dunnett's multiple comparisons (*, $P < 0.05$; **, $P < 0.01$; ***, $P < 0.001$; ****, $P < 0.0001$). **(G and H)** Kinetics of CHIKV 181/25 and CHIKV-LR replication in IFN β -pretreated WT, *Ifitm3*^{-/-}, and *Ifitm-del* MEFs infected at an MOI of 5. Supernatant was harvested at indicated time points, and virus titers were determined. Curves show the means and standard errors of the means from the pooled data of two or three independent experiments performed in triplicate. Means at each time point were compared between WT and knockout cell lines using two-way ANOVA with Dunnett's multiple comparisons (*, $P < 0.05$; **, $P < 0.01$; ***, $P < 0.001$; ****, $P < 0.0001$).

Figure 3.2

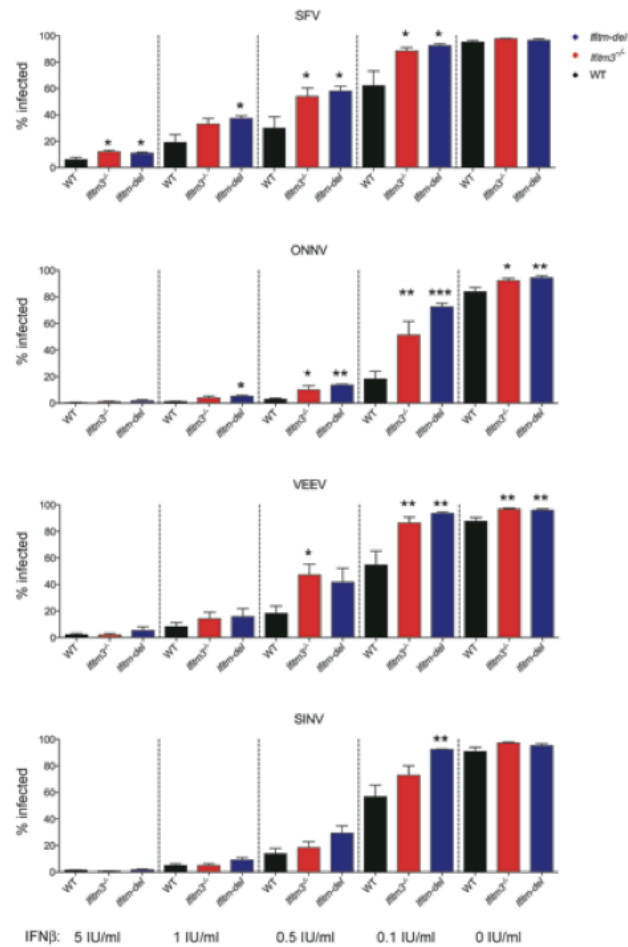


Figure 3.2. Infection of other alphaviruses is enhanced in cells lacking *Ifitm3* expression.

WT, *Ifim3*^{-/-}, and *Ifitm-del* MEFs were pretreated with the indicated concentrations of IFN β and subsequently infected with SFV (A), ONNV (B), VEEV-TC83 (C), or SINV (D) at an MOI of 5. At 14 h postinfection, MEFs were stained for viral E2 proteins and analyzed by flow cytometry. Bars represent the means and standard errors of the means from three independent experiments performed in duplicate. For each concentration of IFN β , means between WT and knockout cells were compared using one-way ANOVA with Dunnett's multiple comparisons (*, $P < 0.05$; **, $P < 0.01$; ***, $P < 0.001$).

Figure 3.3

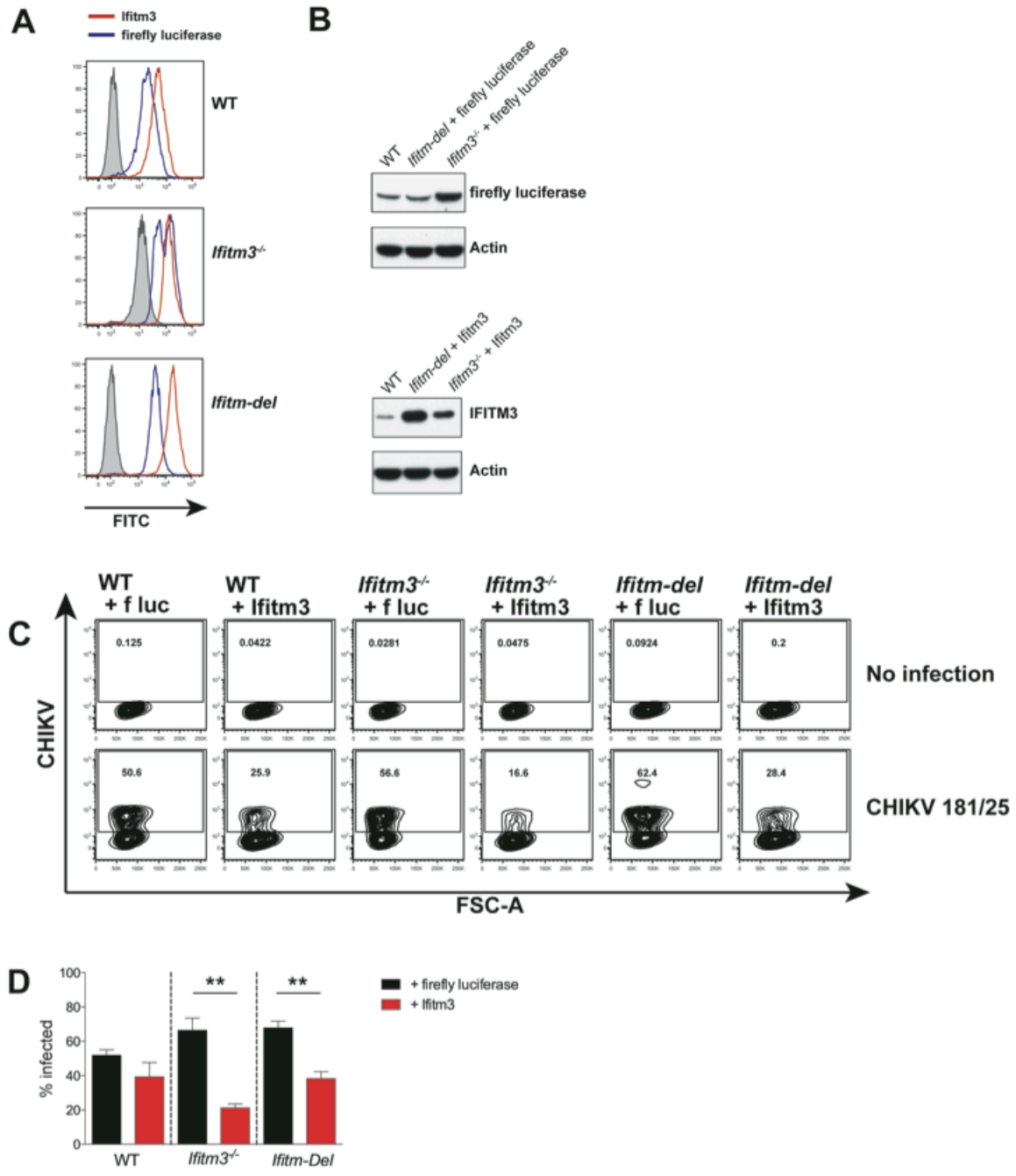


Figure 3.3. Ectopic expression of IFITM3 inhibits CHIKV infection. c-Myc-tagged firefly luciferase and Ifitm3 were cloned into the pFCIV vector and introduced into WT, *Ifitm3*^{-/-}, and *Ifitm-del* MEFs via lentiviral transduction. **(A and B)** Successful transduction was determined by staining for c-Myc tag by flow cytometry (gray-filled are negative control; black lines, anti-c-Myc) **(A)** and Western blotting for firefly luciferase (detected with anti-c-Myc antibody) and Ifitm3 (detected with anti-Ifitm3 antibody) in transcomplemented MEFs **(B)**. β -Actin loading controls are provided below each gel. Results are representative of three independent experiments. **(C)** Flow cytometry contour plots of CHIKV infection in transcomplemented MEFs. Cells were infected for 6 h in the absence of IFN β with CHIKV 181/25 at an MOI of 5. Infection was determined by flow cytometry of E2-positive cells. **(D)** Pooled data from CHIKV infection. Bars represent the means and standard errors of the means from three independent experiments done in triplicate. Means were compared by Student's *t* test (**, $P < 0.01$).

Figure 3.4

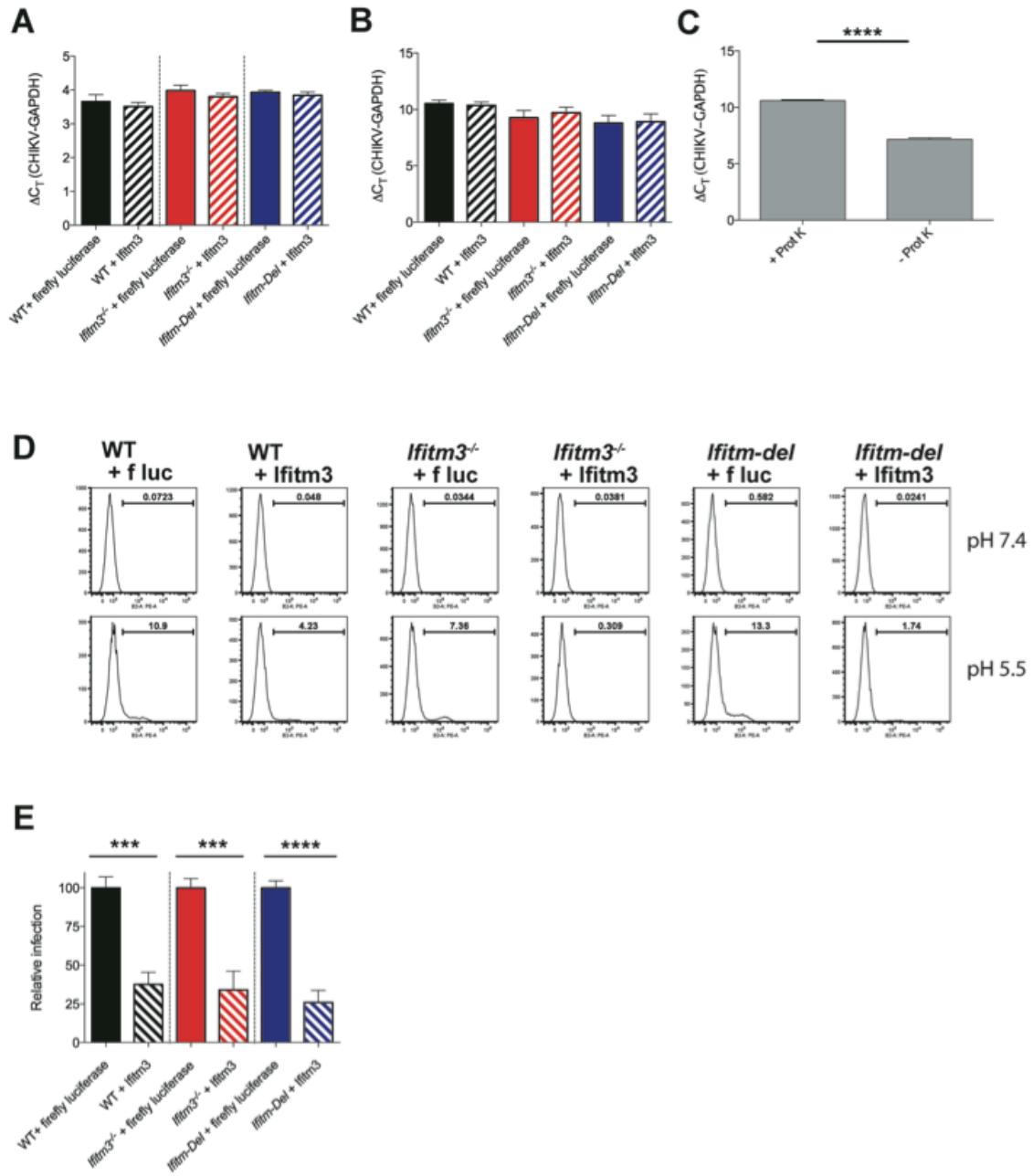


Figure 3.4. Role of Ifitm3 in restricting CHIKV binding, entry, and pH-dependent fusion.

(A) CHIKV-LR was bound to firefly luciferase or Ifitm3-transcomplemented MEFs for 1 h on ice. After repeated rinses with chilled PBS, total RNA was isolated and analyzed for CHIKV RNA by qRT-PCR. Pooled data from 3 independent experiments done in duplicate are shown.

(B) After CHIKV-LR binding and washing, MEFs were incubated at 37°C for 1 h to allow for virus internalization. MEFs were then treated with proteinase K on ice for 1 h to digest any bound but not internalized virions, followed by washing, RNA extraction, and analysis by qRT-PCR. Data are representative of three independent experiments performed in duplicate. **(C)** As a control, we confirmed the efficiency of proteinase K for removing surface-bound (at 4°C) but not internalized CHIKV. MEFs treated with proteinase K had lower levels of CHIKV RNA as detected by qRT-PCR (higher threshold cycle [C_T] values, $P < 0.0001$).

(D and E) FFWO assay of CHIKV 181/25 on transcomplemented MEFs. CHIKV (MOI of 100) was bound to cells on ice for 2 h, followed by treatment with neutral (pH 7.4) or acidic (pH 5.5) medium at 37°C for 2 min to induce fusion. Medium was replaced with neutral culture medium supplemented with NH_4Cl and incubated at 37°C for 14 h before analysis of CHIKV antigen-positive cells by flow cytometry. Data represent the means and standard errors of the means from three independent experiments done in triplicate. Means were compared by Student's *t* test (***, $P < 0.001$; ****, $P < 0.0001$).

Figure 3.5

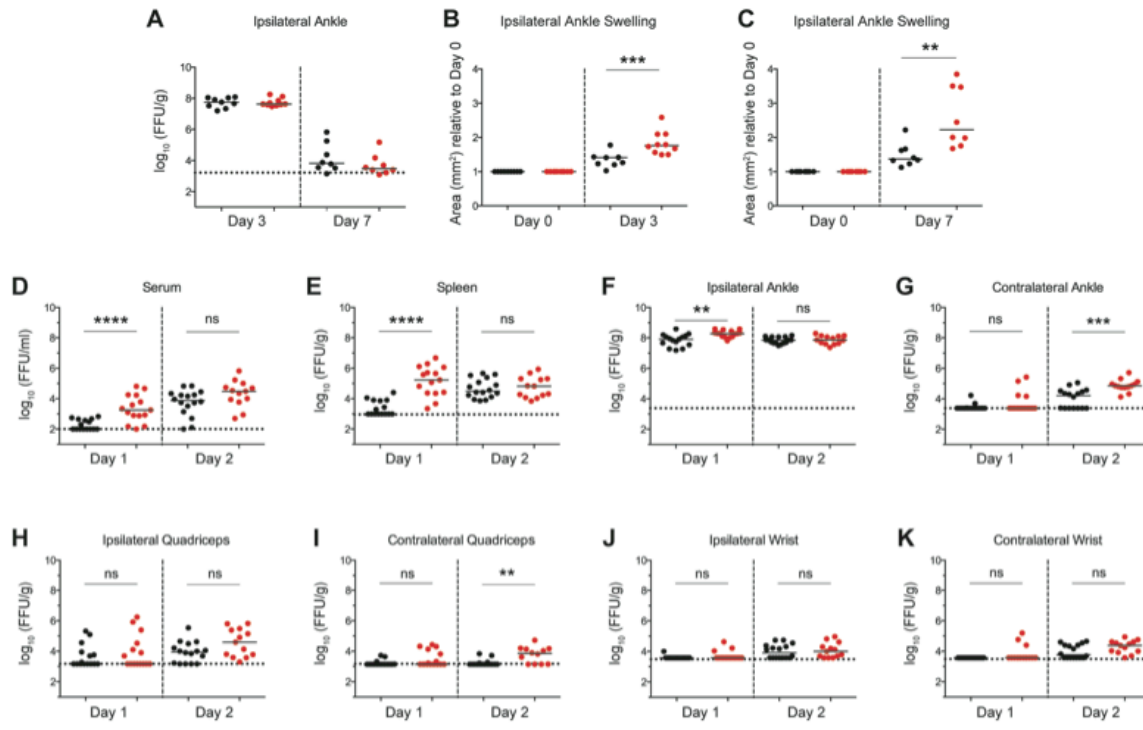
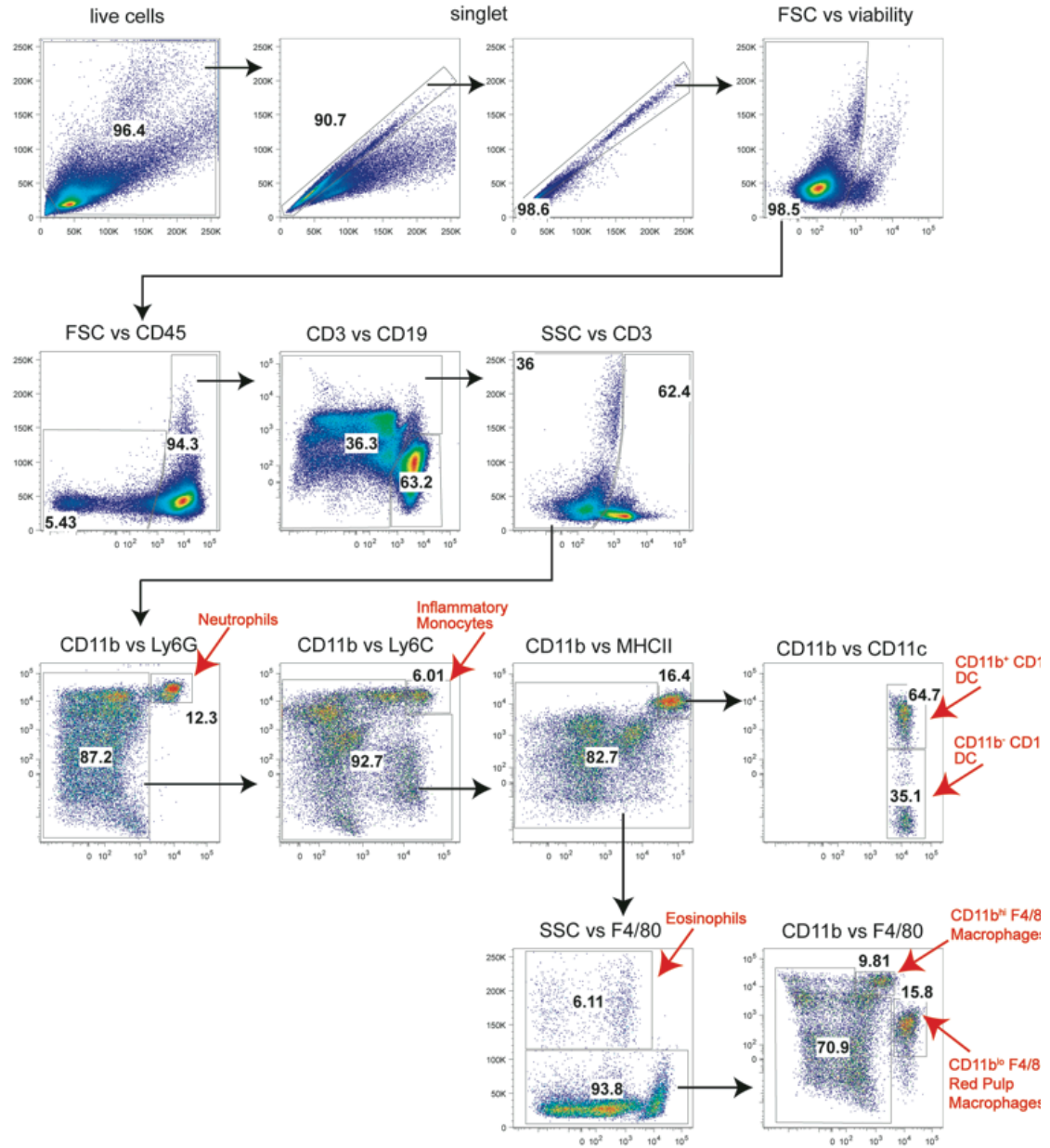


Figure 3.5. Ifitm3 restricts CHIKV pathogenesis *in vivo*. Four-week-old WT and *Ifitm3*^{-/-} mice were inoculated with 10³ FFU of CHIKV-LR in the left footpad. **(A)** Viral titers in the ipsilateral ankle at days 3 and 7 postinfection. Data were pooled from two independent experiments, and each point represents one mouse ($n = 8$ to 10). The dotted line represents the limit of detection. No statistical difference was seen by the Mann-Whitney test. **(B and C)** Swelling of the ipsilateral ankle of infected WT and *Ifitm3*^{-/-} mice at days 3 and 7 postinfection. Area was determined by measuring the width and height of the ankle using digital calipers. Data are pooled from two independent experiments and are normalized to the measured area of the ankles just prior to infection. Each dot represents one mouse ($n = 8$ to 10). Asterisks indicate statistical differences by the Mann-Whitney test (**, $P < 0.01$; ***, $P < 0.001$). **(D to K)** Four-week-old WT and *Ifitm3*^{-/-} mice were inoculated with 10³ FFU of CHIKV-LR in the left footpad. Viral burdens in the serum (D), spleen (E), ankles (F and G), muscles (H and I), and wrists (J and K) at days 1 and 2 postinfection were determined by focus-forming assay. Dotted lines represent the limit of detection. Data are pooled from three independent experiments, and each dot represents one mouse ($n = 13$ to 16). Asterisks indicate statistical differences by the Mann-Whitney test (**, $P < 0.01$; ***, $P < 0.001$; ****, $P < 0.0001$).

Figure 3.6

A



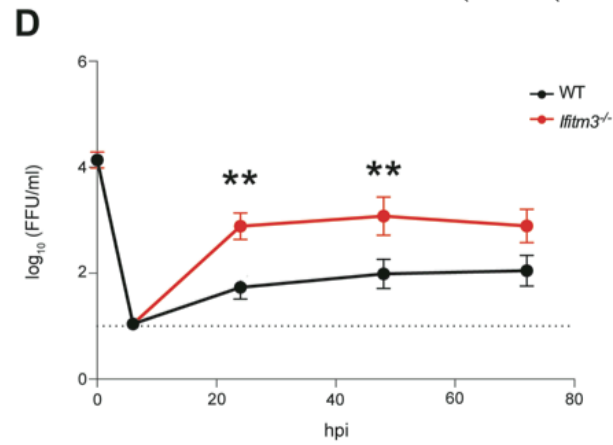
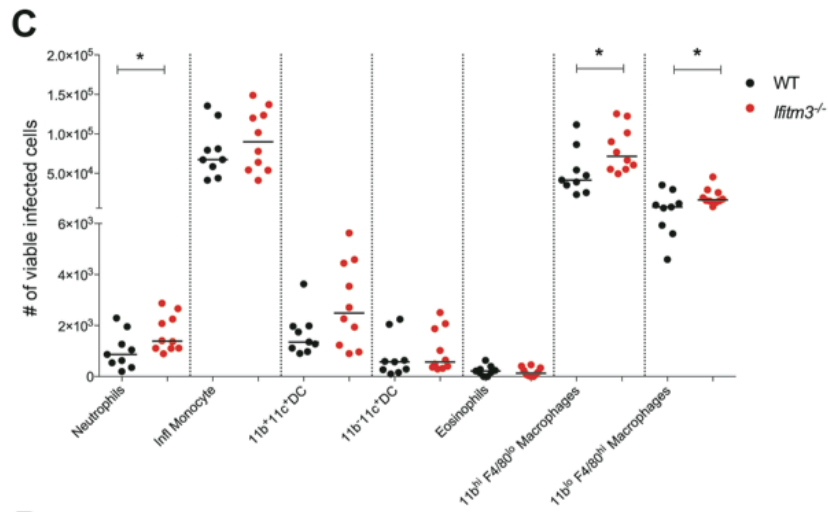
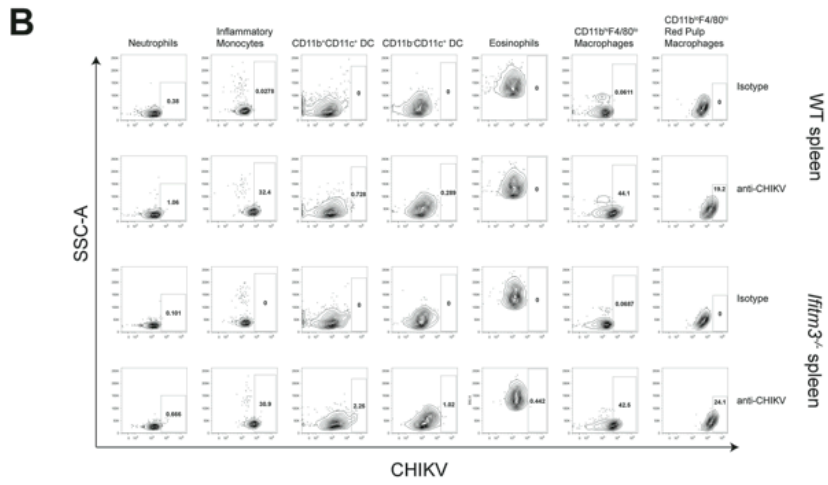


Figure 3.6. Infection of splenocyte subsets by CHIKV-LR in WT and *Ifitm3*^{-/-} mice.

Splenocytes from 4-week-old WT and *Ifitm3*^{-/-} mice were harvested 1 day after infection (10³ FFU in the footpad); stained for neutrophils, inflammatory monocytes, dendritic cells, eosinophils, macrophages, and red pulp macrophages and for surface expression of CHIKV E1 and E2 viral antigen; and analyzed by flow cytometry. **(A)** Detailed gating strategy for different cell subsets is shown. FSC, forward scatter; SSC, side scatter. **(B)** Representative contour plots of WT and *Ifitm3*^{-/-} splenocytes gated for CHIKV antigen-positive cells, stained with either isotype control or anti-CHIKV envelope protein antibody. **(C)** Scatter plots indicate the number of CHIKV antigen-positive cells for each subpopulation. Data were pooled from two independent experiments. Each dot represents one mouse ($n = 9$ to 10). Asterisks determine statistical differences by the Mann-Whitney test (*, $P < 0.05$). Note the break in the y axis. **(D)** Viral kinetics of CHIKV-LR infection in bone marrow-derived WT and *Ifitm3*^{-/-} macrophages infected at an MOI of 0.1. Data are pooled from five independent experiments performed in triplicate, and each point indicates mean and standard error of the mean. The dotted line indicates the limit of detection. Asterisks determine statistical differences by two-way ANOVA and Sidak's multiple comparisons (**, $P < 0.01$). hpi, hours postinfection.

Figure 3.7

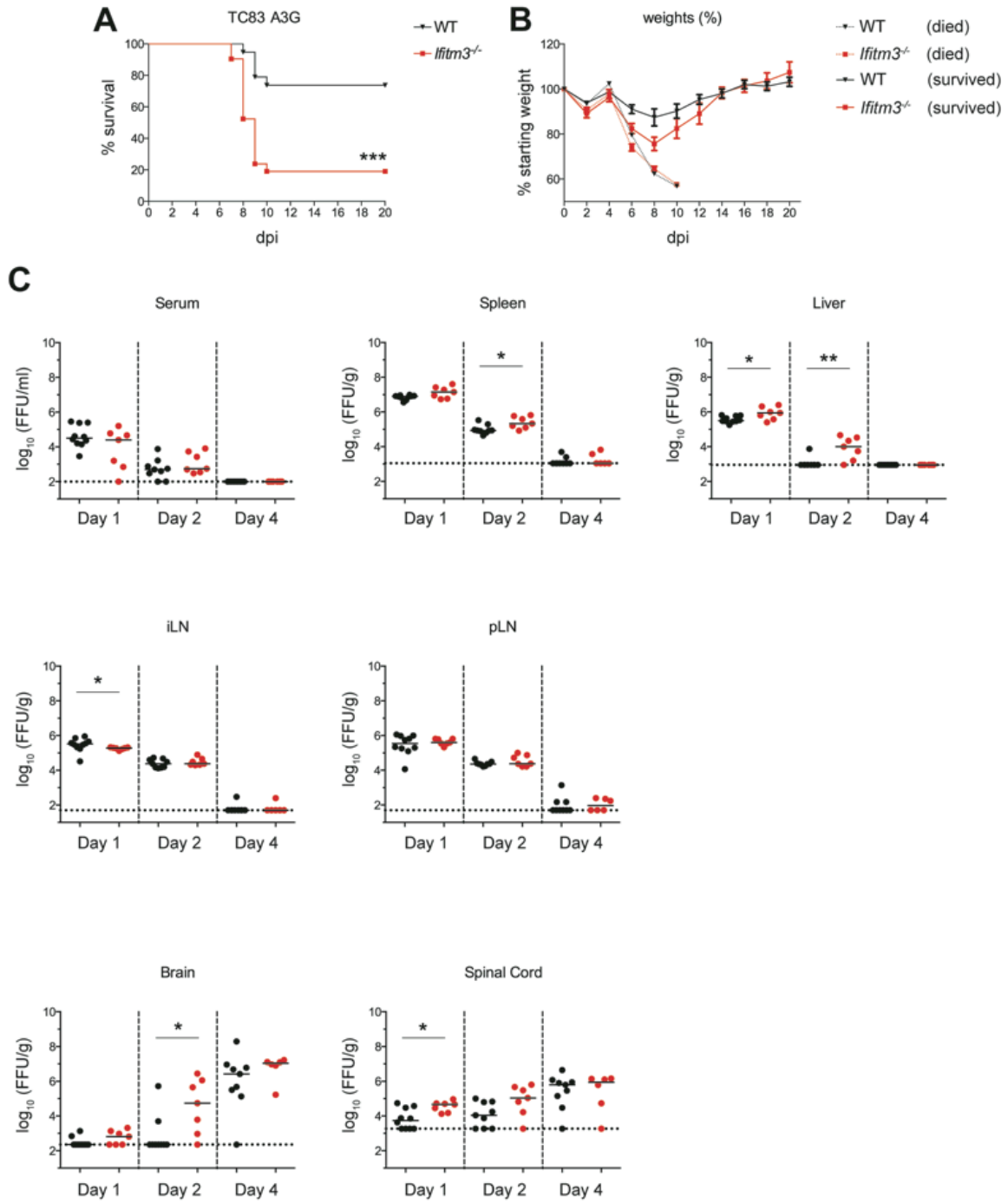


Figure 3.7. Ifitm3 protects against VEEV pathogenesis. (A and B) Four-week-old WT and *Ifitm3*^{-/-} mice were infected with 10⁶ FFU of VEEV-TC83-A3G in the footpad and followed for survival **(A)** and morbidity by weight loss **(B)**. Data are pooled from two independent experiments ($n = 19$ to 21). Asterisks denote statistical differences by log rank test (***, $P < 0.001$). **(C)** VEEV viral burden of serum, spleen, liver, inguinal lymph nodes (iLN), popliteal lymph nodes (pLN), brain, and spinal cord at days 1, 2, and 4 after infection of WT and *Ifitm3*^{-/-} mice. Data are pooled from four independent experiments, where each dot represents one mouse ($n = 6$ to 10). Dotted lines represent the limit of detection. Asterisks indicate statistical differences by the Mann-Whitney test (*, $P < 0.05$; **, $P < 0.01$).

Table 3.1: Cytokine levels in joint tissue homogenates after CHIKV infection

Cytokine	Genotype	Day +1		Day +2	
		pg/ml	P	pg/ml	P
IL-1 α	WT	7.6 (\pm 1.0)	0.2	9.8 (\pm 0.6)	0.03
	<i>Ifitm3</i> ^{-/-}	12 (\pm 2.4)		14 (\pm 1.5)	
IL-1 β	WT	52 (\pm 11)	0.3	144 (\pm 18)	0.2
	<i>Ifitm3</i> ^{-/-}	71 (\pm 14)		181 (\pm 9.2)	
IL-2	WT	11 (\pm 1.9)	0.03	15 (\pm 1.9)	0.09
	<i>Ifitm3</i> ^{-/-}	16 (\pm 1.8)		21 (\pm 3.1)	
IL-3	WT	0.33 (\pm 0.06)	0.9	0.39 (\pm 0.08)	0.006
	<i>Ifitm3</i> ^{-/-}	0.33 (\pm 0.06)		0.76 (\pm 0.06)	
IL-4	WT	3.2 (\pm 0.2)	0.3	4.2 (\pm 0.5)	0.1
	<i>Ifitm3</i> ^{-/-}	3.2 (\pm 0.5)		6.1 (\pm 1.0)	
IL-5	WT	0.6 (\pm 0.2)	0.9	3.0 (\pm 1.0)	0.7
	<i>Ifitm3</i> ^{-/-}	0.8 (\pm 0.4)		3.4 (\pm 1.0)	
IL-6	WT	1.5 (\pm 0.4)	0.8	8.8 (\pm 1.1)	0.4
	<i>Ifitm3</i> ^{-/-}	1.9 (\pm 1.0)		11 (\pm 1.9)	
IL-9	WT	22 (\pm 7.1)	0.9	31 (\pm 9.1)	0.006
	<i>Ifitm3</i> ^{-/-}	28 (\pm 16)		107 (\pm 24)	
IL-10	WT	1.1 (\pm 0.06)	0.3	3.1 (\pm 0.9)	0.02
	<i>Ifitm3</i> ^{-/-}	1.3 (\pm 0.2)		5.3 (\pm 0.8)	
IL-12 (p40)	WT	1.1 (\pm 0.2)	0.8	10 (\pm 1.6)	0.02
	<i>Ifitm3</i> ^{-/-}	1.4 (\pm 0.3)		15 (\pm 0.8)	
IL-12 (p70)	WT	2.8 (\pm 0.2)	0.1	6.2 (\pm 0.7)	0.5
	<i>Ifitm3</i> ^{-/-}	3.8 (\pm 0.5)		7.0 (\pm 0.6)	
IL-13	WT	LOD (38.7)	0.9	LOD (38.7)	0.9
	<i>Ifitm3</i> ^{-/-}	44 (\pm 5.7)		39 (\pm 0.8)	
IL-17	WT	0.3 (\pm 0.09)	0.9	0.3 (\pm 0.08)	0.8
	<i>Ifitm3</i> ^{-/-}	0.3 (\pm 0.1)		0.2 (\pm 0.06)	
Eotaxin	WT	151 (\pm 3.8)	0.5	176 (\pm 11)	0.9
	<i>Ifitm3</i> ^{-/-}	162 (\pm 8.2)		176 (\pm 12)	
G-CSF	WT	0.7 (\pm 0.1)	0.9	4.2 (\pm 1.2)	0.007
	<i>Ifitm3</i> ^{-/-}	0.9 (\pm 0.3)		8.5 (\pm 0.8)	
GM-CSF	WT	43 (\pm 4.9)	0.14	59 (\pm 6.4)	0.04
	<i>Ifitm3</i> ^{-/-}	55 (\pm 5.0)		77 (\pm 5.7)	
IFN- γ	WT	LOD (1.2)	>0.9	1.8 (\pm 0.3)	0.7
	<i>Ifitm3</i> ^{-/-}	LOD (1.2)		1.5 (\pm 0.14)	
KC	WT	16 (\pm 2.6)	0.6	81 (\pm 15)	0.8
	<i>Ifitm3</i> ^{-/-}	23 (\pm 5.6)		83 (\pm 13)	
MCP-1	WT	52 (\pm 15)	0.01	706 (\pm 119)	0.4
	<i>Ifitm3</i> ^{-/-}	118.5 (\pm 25.44)		833 (\pm 70)	
MIP-1a	WT	38 (\pm 1.4)	0.3	168 (\pm 29)	0.8
	<i>Ifitm3</i> ^{-/-}	50 (\pm 7.8)		151 (\pm 13)	
MIP-1b	WT	20 (\pm 3.9)	0.3	150 (\pm 33)	0.2
	<i>Ifitm3</i> ^{-/-}	34 (\pm 8.5)		89 (\pm 23)	
RANTES	WT	13 (\pm 2.4)	0.8	109 (\pm 28)	0.8
	<i>Ifitm3</i> ^{-/-}	12 (\pm 3.1)		88 (\pm 24)	
TNF- α	WT	17 (\pm 3.0)	0.004	48 (\pm 7.5)	0.5
	<i>Ifitm3</i> ^{-/-}	41 (\pm 6.4)		56 (\pm 7.4)	

Table 3.1. Mice were infected with 10^3 FFU of CHIKV-LR in the footpad. Ipsilateral joint tissues were collected at 1 and 2 days after infection, homogenates were prepared, and the indicated cytokines were measured by Bio-Plex array. Data represent the mean (\pm SEM) in pg/ml of 9 to 11 mice per group. Statistical significance was determined by the Mann-Whitney test. LOD indicates the limit of detection.

Chapter 4: Conclusions and Future Directions

CONCLUSIONS

This study attempted to identify novel antiviral ISGs using a high-throughput, gene knockdown system *in vitro*. Compared to screens where candidate ISGs was expressed ectopically, this shRNA based system would allow for the characterization of targets in the context of a physiological antiviral state. In addition, by testing with an attenuated virus strain and a virus not extensively studied in this context, we hoped to increase the chances of discovering ISGs with milder, or virus family specific functions. Unfortunately, though the initial premise of the screen was sound, the commercial shRNAs were not previously validated, and only 1 of every 3 shRNAs against a target were guaranteed to have a significant knockdown. In fact, for the top ranked ISGs in the screen, very few had multiple shRNAs with a Z-score higher than the cutoff of 1.5. This suggested that the library was mostly composed of ineffective shRNAs, or were allowing for other off-target effects and thus compromising the results of the screen, reducing our confidence in the overall results. Independent assessment of ISGs using CRISPR is still in progress, and generation of validated clonal lines must be done to optimize this system.

Of the top hits, we also had access to knockout mice for four of these ISGs: *Ifitm3*, *Ifit2*, *Lamp3* and *β 2m*. Using MEFs obtained from these mice, initial studies revealed that only *Ifitm3* had a potent antiviral phenotype against alphaviruses, a family that was previously considered in the literature to be in fact resistant to this ISG. *Ifitm3* mediated restriction was not limited to the attenuated strain CHIKV-181/25, but also reduced viral replication of the pathogenic CHIKV-LR strain, as well as other arthritogenic and encephalitic alphaviruses *in vitro*. Mechanistically, *Ifitm3* did not affect CHIKV binding or entry, but restricted fusion with the plasma membrane under conditions of ectopic expression. *Ifitm3* proved to be important *in vivo*, as the lack of this

ISG allowed for an increase in the early viral burden in CHIKV infected mice, an increase in foot swelling at days 3 and 7 post infection, and an increase in the viral antigen load in splenic macrophages. By growth curves, Ifitm3 restricts viral growth in bone marrow derived macrophages at basal conditions, and may therefore act as a reservoir *in vivo*. The absence of Ifitm3 also promoted increased mortality in mice infected with the encephalitic alphavirus VEEV-TC83-A3G, likely due to early increased viral burden and spread.

FUTURE DIRECTIONS

Screening for novel antiviral ISGs

Assuming that the initial shRNA screen is still worth following up on, it is necessary to continue developing clonal CRISPR knockout lines. The bulk CRISPR lines failed due to the genetic heterogeneity of the cells. Even partial expression of a target ISG could be sufficient to lose a potential protective phenotype. As we observed in the *Ifitm3* bulk CRISPR set, no variation of IFN or MOI tested could show a difference in restriction compared to scrambled negative controls, even though all the cell lines were selected for puromycin resistance. Western blot analysis revealed that *Ifitm3* protein was still being produced, especially after IFN treatment, and was clearly sufficient to restrict CHIKV. Furthermore, validated clonal lines should be developed in other permissive cells to confirm that any phenotypes are ISG specific, and not due to an artifact of the cell line. A more prudent approach would be to consider restarting the screen with a more reliable means of targeted knockdown or knockout. Whether by CRISPR, CRISPRi, or by shRNA, the reduction of gene expression should be validated at least at the mRNA level by qPCR. The generation of such a library will take a lot of time to properly generate, and would ideally be done commercially or through a core service.

ISG targets should be further tested across multiple primary and stable cell lines for their role in cell viability, basal transcription and cell cycle activity, to make sure these genes are not essential for survival. Following this, target ISGs should be re-introduced by ectopic expression to verify that viral restriction can be restored. Finally, relevance *in vivo* using knockout mouse models and studies to determine the stages and mechanism of viral restriction can proceed.

Characterizing Ifitm3 as an antiviral ISG

There are many questions left unanswered concerning the role of Ifitms in the context of alphavirus pathogenesis. In our *in vitro* studies, we noticed that *Ifitm-del* locus knockout MEFs was more susceptible against viral infection than *Ifitm3^{-/-}* MEFs. This suggests that the other Ifitms could also be involved in alphavirus restriction. While *Ifitm2^{-/-}* MEFs were just as sensitive to CHIKV as WT MEFs, the protective role of Ifitm1 and the other non-IFN stimulated Ifitms absent in the locus deletion is currently unknown. *Ifitm1^{-/-}* and *Ifitm2^{-/-}* mice have recently been backcrossed to the C57BL/6J background and are available for further *in vivo* studies. C57BL/6J backcrossed *Ifitm-del* mice tend to die at birth, which unfortunately makes *in vivo* experiments difficult. However, *Ifitm-del* MEFs can be used for *in vitro* studies. This line can be complemented to ectopically express single Ifitms or different combinations of Ifitm genes, and subsequently infect with CHIKV to look for differences in growth kinetics and replication. Identification of other individual or a combination of antiviral Ifitms can be followed up by generating and infecting new Ifitm knockout mice to determine *in vivo* relevance.

One of the most interesting phenotypes observed in the *Ifitm3^{-/-}* mouse was the rapid early viral titers in the spleen, ipsilateral foot and serum. This led to the finding that splenic macrophages were more antigen positive in these mice compared to WT controls. However, we did not study the role of Ifitm3 in stromal cells. CHIKV is known to infect muscle cells, osteoblasts, and fibroblasts, all of which express Ifitm3. Since the titers at the joints were either comparative or only slightly higher at all timepoints examined, we opted to not look too much further into these tissues. To better understand the role Ifitm3 plays in restricting CHIKV pathogenesis of stromal cells *in vivo*, we can take advantage of a newly established technique in the lab called In Situ Hybridization (ISH). With this staining protocol, we can determine

histologically how CHIKV spreads from the site of infection to the stromal and hematopoietic cells by staining for viral RNA. Combined with H&E staining, and immunofluorescence staining of known cells susceptible to CHIKV, ISH can help us better understand the early kinetics of viral spread and the possible changes in viral tropism in the stromal cells of the infected ankle joints, and may better inform us as to why we see early higher viremia and titers in the spleen of knockout mice. As our earliest virological titers were done at 1 day post infection, these studies should include shorter timepoints, starting at 4 hours post infection.

The role of *Ifitm3* in later stages of infection is a further point of interest. For example, CHIKV and other alphaviruses egress from host cells by budding, and may incorporate *Ifitm3* as part of their viral envelope, as has been observed with HIV-1 (72). If integration of *Ifitm3* to the alphavirus envelope can be confirmed, subsequent studies into the downstream effects of infectivity can be considered. In particular, does the integration of *Ifitm3* affect the ability of the virion to fuse with the endosomal membrane of host cells? Does this allow for faster viral clearance in the serum and tissues? Furthermore, it would be interesting to note if the absence of *Ifitm3* results in a greater or more sustained viral burden at late or chronic stages of infection.

As the mechanism of *Ifitm3* mediated restriction is still unclear, it would be beneficial to have an alphavirus strain that has adapted to no longer be sensitive to this ISG. Serial passages of CHIKV either in *Ifitm3*^{-/-} mice or MEFs should produce resistant variants. Genomic and structural comparisons of *Ifitm3* sensitive and insensitive strains can help us better understand how *Ifitm3* blocks endosomal viral fusion. An *Ifitm3* insensitive strain may also be useful in understanding if this ISG has any role in promoting or preventing chronic infection. In the case of HIV-1, it has been observed that while the founder population is resistant to IFITM3 function, subsequent generations become more sensitive to IFITM3 as more mutations to escape

neutralizing antibodies are made (73, 75, 123). A similar situation can be occurring in the case of CHIKV infection, where IFITM3 insensitive variants are responsible for maintaining a chronic phenotype.

The IFITM3 human polymorphism rs-12252 results in a 21 amino acid deletion of the N-terminus, which prevents localization to the endosomes. While this polymorphism was initially shown to alter sensitivity to IAV infections, subsequent studies have brought this observation into question (80–82). Recently however, an investigation into Hantaan virus suggests that the rs-12252 polymorphism is associated with greater disease severity and viral load (83). Thus, further studies on the importance and relevance of IFITM3 polymorphisms in the context of CHIKV and other viruses needs to be done. Understanding how different polymorphisms of IFITM3 do or do not affect restriction of viruses can be insightful towards deciphering the mechanism of this ISG.

Finally, it would be interesting to note the *in vivo* importance of Ifitms and in particular Ifitm3 in the context of other alphaviruses. Our studies only looked at CHIKV pathogenesis and only touched on VEEV pathogenesis *in vivo*. Further investigations into the role of Ifitm3 *in vivo* against other arthritogenic and encephalitic alphaviruses will help clarify the differences in pathogenesis and viral tropism. For example, Mayaro and Ross River are both arthritogenic alphaviruses that induce a different swelling response compared to CHIKV (unpublished observations, Diamond Lab). The absence of Ifitm3 can theoretically allow for amplification of the viral kinetics and pathogenesis of these infections. It may even be possible that there are alphaviruses that are in fact not restricted by Ifitm3 *in vivo*. Preliminary day 1 post infection analysis with Mayaro suggested that there is no difference in titer in the spleen, serum or joints (unpublished observations). The identification of natural resistant alphavirus would be beneficial

in deciphering the mechanism of Ifitm3 restriction, and also identifying possible viral mechanisms of bypass or escape.

As a point of interest, an investigation into the role of Ifitm3 restricting LACV infection *in vivo* should be initiated. If the published *in vitro* data is valid and orthobunyaviruses are restricted by Ifitm3, we can expect a survival difference in *Ifitm3*^{-/-} vs WT mice. As we have shown, Ifitm3 is protective against encephalitic alphaviruses, however the virus strain of VEEV used is resistant to the antiviral mechanism of Ifit1. LACV however is not affected by Ifit1 (51), theroretically making it a better pathogen to use in understanding how Ifitm3 protects the CNS.

REFERENCES

1. **McNab F, Mayer-Barber K, Sher A, Wack A, O’Garra A.** 2015. Type I interferons in infectious disease. *Nat Rev Immunol* **15**:87–103.
2. **Schneider WM, Chevillotte MD, Rice CM.** 2014. Interferon-stimulated genes: a complex web of host defenses. *Annu Rev Immunol* **32**:513–45.
3. **Kawai T, Akira S.** 2011. Toll-like receptors and their crosstalk with other innate receptors in infection and immunity. *Immunity* **34**:637–50.
4. **Isaacs A, Lindenmann J.** 2015. Pillars Article: Virus Interference. I. The Interferon. *Proc R Soc Lond B Biol Sci.* 1957. 147: 258-267. *J Immunol* **195**:1911–20.
5. **Lasfar A, Abushahba W, Balan M, Cohen-Solal K a.** 2011. Interferon lambda: A new sword in cancer immunotherapy. *Clin Dev Immunol* **2011**.
6. **Platanias LC.** 2005. Mechanisms of type-I- and type-II-interferon-mediated signalling. *Nat Rev Immunol* **5**:375–86.
7. **Schoggins JW, Rice CM.** 2011. Interferon-stimulated genes and their antiviral effector functions. *Curr Opin Virol* **1**:519–25.
8. **Bick MJ, Carroll JN, Gao G, Goff SP, Rice CM, MacDonald MR.** 2003. Expression of the zinc-finger antiviral protein inhibits alphavirus replication. *J Virol* **77**:11555–62.
9. **Brass AL, Huang I-C, Benita Y, John SP, Krishnan MN, Feeley EM, Ryan BJ, Weyer JL, Weyden L Van Der, Fikrig E, Adams J, Xavier RJ, Farzan M, Elledge SJ, van der Weyden L, Adams DJ.** 2009. The IFITM proteins mediate cellular resistance to influenza A H1N1 virus, West Nile virus, and dengue virus. *Cell* **139**:1243–54.
10. **Stremlau M, Owens CM, Perron MJ, Kiessling M, Autissier P, Sodroski J.** 2004. The cytoplasmic body component TRIM5alpha restricts HIV-1 infection in Old World monkeys. *Nature* **427**:848–853.
11. **Haller O, Kochs G.** 2011. Human MxA Protein: An Interferon-Induced Dynamin-Like

- GTPase with Broad Antiviral Activity. *J Interf Cytokine Res* **31**:79–87.
12. **Shu Q, Lennemann NJ, Sarkar SN, Sadovsky Y, Coyne CB.** 2015. ADAP2 Is an Interferon Stimulated Gene That Restricts RNA Virus Entry. *PLoS Pathog* **11**.
 13. **Iwasaki A.** 2012. A virological view of innate immune recognition. *Annu Rev Microbiol* **66**:177–96.
 14. **Diamond MS, Farzan M.** 2013. The broad-spectrum antiviral functions of IFIT and IFITM proteins. *Nat Rev Immunol* **13**:46–57.
 15. **Lenschow DJ, Lai C, Frias-Staheli N, Giannakopoulos N V, Lutz A, Wolff T, Osiak A, Levine B, Schmidt RE, García-Sastre A, Leib DA, Pekosz A, Knobeloch K, Horak I, Virgin HW.** 2007. IFN-stimulated gene 15 functions as a critical antiviral molecule against influenza, herpes, and Sindbis viruses. *Proc Natl Acad Sci U S A* **104**:1371–6.
 16. **Lenschow DJ, Giannakopoulos N V, Gunn LJ, Johnston C, O’Guin AK, Schmidt RE, Levine B, Virgin HW.** 2005. Identification of interferon-stimulated gene 15 as an antiviral molecule during Sindbis virus infection in vivo. *J Virol* **79**:13974–83.
 17. **Werneke SW, Schilte C, Rohatgi A, Monte KJ, Michault A, Arenzana-Seisdedos F, Vanlandingham DL, Higgs S, Fontanet A, Albert ML, Lenschow DJ.** 2011. ISG15 is critical in the control of Chikungunya virus infection independent of UBE1L mediated conjugation. *PLoS Pathog* **7**:e1002322.
 18. **Mattijssen S, Pruijn GJM.** 2012. Viperin, a key player in the antiviral response. *Microbes Infect.*
 19. **Jones PH, Maric M, Madison MN, Maury W, Roller RJ, Okeoma CM.** 2013. BST-2/tetherin-mediated restriction of chikungunya (CHIKV) VLP budding is counteracted by CHIKV non-structural protein 1 (nsP1). *Virology* **438**:37–49.
 20. **Schoggins JW, Wilson SJ, Panis M, Murphy MY, Jones CT, Bieniasz P, Rice CM.** 2011. A diverse range of gene products are effectors of the type I interferon antiviral response. *Nature* **472**:481–5.

21. **Li J, Ding SC, Cho H, Chung BC, Gale M, Chanda SK, Diamond MS.** 2013. A short hairpin RNA screen of interferon-stimulated genes identifies a novel negative regulator of the cellular antiviral response. *MBio* **4**:e00385-13.
22. **François-Newton V, de Freitas Almeida GM, Payelle-Brogard B, Monneron D, Pichard-Garcia L, Piehler J, Pellegrini S, Uzé G.** 2011. USP18-based negative feedback control is induced by type I and type III interferons and specifically inactivates interferon α response. *PLoS One* **6**.
23. **Silva JM, Li MZ, Chang K, Ge W, Golding MC, Rickles RJ, Siolas D, Hu G, Paddison PJ, Schlabach MR, Sheth N, Bradshaw J, Burchard J, Kulkarni A, Cavet G, Sachidanandam R, McCombie WR, Cleary M a, Elledge SJ, Hannon GJ.** 2005. Second-generation shRNA libraries covering the mouse and human genomes. *Nat Genet* **37**:1281–8.
24. **Liu S-Y, Sanchez DJ, Aliyari R, Lu S, Cheng G.** 2012. Systematic identification of type I and type II interferon-induced antiviral factors. *Proc Natl Acad Sci U S A* **109**:4239–44.
25. **Fusco DN, Brisac C, John SP, Huang Y-W, Chin CR, Xie T, Zhao H, Jilg N, Zhang L, Chevaliez S, Wambua D, Lin W, Peng L, Chung RT, Brass AL.** 2013. A genetic screen identifies interferon- α effector genes required to suppress hepatitis C virus replication. *Gastroenterology* **144**:1438–49, 1449–9.
26. **Metz P, Dazert E, Ruggieri A, Mazur J, Kaderali L, Kaul A, Zeuge U, Windisch MP, Trippler M, Lohmann V, Binder M, Frese M, Bartenschlager R.** 2012. Identification of type I and type II interferon-induced effectors controlling hepatitis C virus replication. *Hepatology* **56**:2082–93.
27. **Varble A, Benitez A a, Schmid S, Sachs D, Shim J V, Rodriguez-Barrueco R, Panis M, Crumiller M, Silva JM, Sachidanandam R, tenOever BR.** 2013. An in vivo RNAi screening approach to identify host determinants of virus replication. *Cell Host Microbe* **14**:346–56.
28. **Kane M, Zang TM, Rihn SJ, Zhang F, Kueck T, Alim M, Schoggins J, Rice CM,**

- Wilson SJ, Bieniasz PD.** 2016. Identification of Interferon-Stimulated Genes with Antiretroviral Activity. *Cell Host Microbe* **20**:392–405.
29. **Solignat M, Gay B, Higgs S, Briant L, Devaux C.** 2009. Replication cycle of chikungunya: A re-emerging arbovirus. *Virology*.
30. **Petersen LR, Powers AM.** 2016. Chikungunya: epidemiology. *F1000Research* **5**:1–8.
31. **Leung JY-S, Ng MM-L, Chu JJH.** 2011. Replication of alphaviruses: a review on the entry process of alphaviruses into cells. *Adv Virol* **2011**:249640.
32. **Morrison TE, Oko L, Montgomery S a., Whitmore AC, Lotstein AR, Gunn BM, Elmore S a., Heise MT.** 2011. A mouse model of chikungunya virus-induced musculoskeletal inflammatory disease: Evidence of arthritis, tenosynovitis, myositis, and persistence. *Am J Pathol* **178**:32–40.
33. **Gardner J, Anraku I, Le TT, Larcher T, Major L, Roques P, Schroder W a, Higgs S, Suhrbier A.** 2010. Chikungunya virus arthritis in adult wild-type mice. *J Virol* **84**:8021–32.
34. **Couderc T, Chrétien F, Schilte C, Disson O, Brigitte M, Guivel-Benhassine F, Touret Y, Barau G, Cayet N, Schuffenecker I, Desprès P, Arenzana-Seisdedos F, Michault A, Albert ML, Lecuit M.** 2008. A mouse model for Chikungunya: young age and inefficient type-I interferon signaling are risk factors for severe disease. *PLoS Pathog* **4**:e29.
35. **Fox JM, Diamond MS.** 2016. Immune-Mediated Protection and Pathogenesis of Chikungunya Virus. *J Immunol* **197**:4210–4218.
36. **Hawman DW, Stoermer K, Montgomery S, Pal P, Oko L, Diamond MS, Morrison TE.** 2013. Chronic joint disease caused by persistent Chikungunya virus infection is controlled by the adaptive immune response. *J Virol* **87**:13878–88.
37. **Pal P, Dowd K a, Brien JD, Edeling M a, Gorlatov S, Johnson S, Lee I, Akahata W, Nabel GJ, Richter MKS, Smit JM, Fremont DH, Pierson TC, Heise MT, Diamond**

- MS.** 2013. Development of a highly protective combination monoclonal antibody therapy against Chikungunya virus. *PLoS Pathog* **9**:e1003312.
38. **Chen W, Foo SS, Sims NA, Herrero LJ, Walsh NC, Mahalingam S.** 2015. Arthritogenic alphaviruses: New insights into arthritis and bone pathology. *Trends Microbiol* **23**:35–43.
39. **Chen W, Foo S-S, Rulli NE, Taylor A, Sheng K-C, Herrero LJ, Herring BL, Lidbury B, Li RW, Walsh NC, Sims N, Smith PN, Mahalingam S.** 2014. Arthritogenic alphaviral infection perturbs osteoblast function and triggers pathologic bone loss. *Proc Natl Acad Sci U S A* **111**:6040–5.
40. **Edelman R, Tacket CO, Wasserman SS, Bodison SA, Perry JG, Mangiafico JA.** 2000. Phase II safety and immunogenicity study of live chikungunya virus vaccine TSI-GSD-218. *Am J Trop Med Hyg* **62**:681–5.
41. **Caglioti C, Lalle E, Castilletti C, Carletti F, Capobianchi MR, Bordi L.** 2013. Chikungunya virus infection: an overview. *New Microbiol* **36**:211–27.
42. **Gorchakov R, Wang E, Leal G, Forrester NL, Plante K, Rossi SL, Partidos CD, Adams a P, Seymour RL, Weger J, Borland EM, Sherman MB, Powers AM, Osorio JE, Weaver SC.** 2012. Attenuation of Chikungunya virus vaccine strain 181/clone 25 is determined by two amino acid substitutions in the E2 envelope glycoprotein. *J Virol* **86**:6084–96.
43. **Partidos CD, Weger J, Brewoo J, Seymour R, Borland EM, Ledermann JP, Powers AM, Weaver SC, Stinchcomb DT, Osorio JE.** 2011. Probing the attenuation and protective efficacy of a candidate chikungunya virus vaccine in mice with compromised interferon (IFN) signaling. *Vaccine* **29**:3067–73.
44. **Gardner CL, Burke CW, Higgs ST, Klimstra WB, Ryman KD.** 2012. Interferon-alpha/beta deficiency greatly exacerbates arthritogenic disease in mice infected with wild-type chikungunya virus but not with the cell culture-adapted live-attenuated 181/25 vaccine candidate. *Virology* **425**:103–12.

45. **Karki S, Li MMH, Schoggins JW, Tian S, Rice CM, Macdonald MR.** 2012. Multiple interferon stimulated genes synergize with the zinc finger antiviral protein to mediate anti-alphavirus activity. *PLoS One* **7**:e37398.
46. **Ryman KD, Meier KC, Nangle EM, Ragsdale SL, Korneeva NL, Rhoads RE, Macdonald MR, Klimstra WB.** 2005. Sindbis virus translation is inhibited by a PKR/RNase L-independent effector induced by alpha/beta interferon priming of dendritic cells. *J Virol* **79**:1487–99.
47. **Zhang Y, Burke CW, Ryman KD, Klimstra WB.** 2007. Identification and characterization of interferon-induced proteins that inhibit alphavirus replication. *J Virol* **81**:11246–55.
48. **Hyde JL, Gardner CL, Kimura T, White JP, Liu G, Trobaugh DW, Huang C, Tonelli M, Paessler S, Takeda K, Klimstra WB, Amarasinghe GK, Diamond MS.** 2014. A viral RNA structural element alters host recognition of nonself RNA. *Science* **343**:783–7.
49. **Proenca-Modena JL, Sesti-Costa R, Pinto AK, Richner JM, Lazear HM, Lucas T, Hyde JL, Diamond MS.** 2015. Oropouche virus infection and pathogenesis are restricted by MAVS, IRF-3, IRF-7, and type I interferon signaling pathways in nonmyeloid cells. *J Virol* **89**:4720–37.
50. **Proenca-Modena JL, Hyde JL, Sesti-Costa R, Lucas T, Pinto AK, Richner JM, Gorman MJ, Lazear HM, Diamond MS.** 2016. Interferon-Regulatory Factor 5-Dependent Signaling Restricts Orthobunyavirus Dissemination to the Central Nervous System. *J Virol* **90**:189–205.
51. **Pinto AK, Williams GD, Szretter KJ, White JP, Proença-Módena JL, Liu G, Olejnik J, Brien JD, Ebihara H, Mühlberger E, Amarasinghe G, Diamond MS, Boon ACM.** 2015. Human and Murine IFIT1 Proteins Do Not Restrict Infection of Negative-Sense RNA Viruses of the Orthomyxoviridae, Bunyaviridae, and Filoviridae Families. *J Virol* **89**:9465–76.

52. **Bailey CC, Zhong G, Huang I-C, Farzan M.** 2014. IFITM-Family Proteins: The Cell's First Line of Antiviral Defense. *Annu Rev Virol* **1**:261–283.
53. **Jia R, Xu F, Qian J, Yao Y, Miao C, Zheng Y-M, Liu S-L, Guo F, Geng Y, Qiao W, Liang C.** 2014. Identification of an endocytic signal essential for the antiviral action of IFITM3. *Cell Microbiol* **16**:1080–93.
54. **Yount JS, Karssemeijer R a, Hang HC.** 2012. S-palmitoylation and ubiquitination differentially regulate interferon-induced transmembrane protein 3 (IFITM3)-mediated resistance to influenza virus. *J Biol Chem* **287**:19631–41.
55. **Shan Z, Han Q, Nie J, Cao X, Chen Z, Yin S, Gao Y, Lin F, Zhou X, Xu K, Fan H, Qian Z, Sun B, Zhong J, Li B, Tsun A.** 2013. Negative regulation of interferon-induced transmembrane protein 3 by SET7-mediated lysine monomethylation. *J Biol Chem* **288**:35093–103.
56. **Huang I-C, Bailey CC, Weyer JL, Radoshitzky SR, Becker MM, Chiang JJ, Brass AL, Ahmed A a, Chi X, Dong L, Longobardi LE, Boltz D, Kuhn JH, Elledge SJ, Bavari S, Denison MR, Choe H, Farzan M.** 2011. Distinct Patterns of IFITM-Mediated Restriction of Filoviruses, SARS Coronavirus, and Influenza A Virus. *PLoS Pathog* **7**:e1001258.
57. **Feeley EM, Sims JS, John SP, Chin CR, Pertel T, Chen L-M, Gaiha GD, Ryan BJ, Donis RO, Elledge SJ, Brass AL.** 2011. IFITM3 inhibits influenza A virus infection by preventing cytosolic entry. *PLoS Pathog* **7**:e1002337.
58. **Zucchi I, Prinetti a, Scotti M, Valsecchi V, Valaperta R, Mento E, Reinbold R, Vezzoni P, Sonnino S, Albertini a, Dulbecco R.** 2004. Association of rat8 with Fyn protein kinase via lipid rafts is required for rat mammary cell differentiation in vitro. *Proc Natl Acad Sci U S A* **101**:1880–5.
59. **Bailey CC, Huang I-C, Kam C, Farzan M.** 2012. Ifitm3 limits the severity of acute influenza in mice. *PLoS Pathog* **8**:e1002909.
60. **Mudhasani R, Tran JP, Retterer C, Radoshitzky SR, Kota KP, Altamura L a, Smith**

- JM, Packard BZ, Kuhn JH, Costantino J, Garrison AR, Schmaljohn CS, Huang I-C, Farzan M, Bavari S.** 2013. IFITM-2 and IFITM-3 but not IFITM-1 restrict Rift Valley fever virus. *J Virol* **87**:8451–64.
61. **Lu J, Pan Q, Rong L, He W, Liu S-L, Liang C.** 2011. The IFITM proteins inhibit HIV-1 infection. *J Virol* **85**:2126–37.
62. **Amini-Bavil-Olyae S, Choi YJ, Lee JH, Shi M, Huang I-C, Farzan M, Jung JU.** 2013. The antiviral effector IFITM3 disrupts intracellular cholesterol homeostasis to block viral entry. *Cell Host Microbe* **13**:452–64.
63. **Everitt AR, Clare S, Pertel T, John SP, Wash RS, Smith SE, Chin CR, Feeley EM, Sims JS, Adams DJ, Wise HM, Kane L, Goulding D, Digard P, Anttila V, Baillie JK, Walsh TS, Hume D a, Palotie A, Xue Y, Colonna V, Tyler-Smith C, Dunning J, Gordon SB, Smyth RL, Openshaw PJ, Dougan G, Brass AL, Kellam P.** 2012. IFITM3 restricts the morbidity and mortality associated with influenza. *Nature* **484**:519–23.
64. **Everitt AR, Clare S, McDonald JU, Kane L, Harcourt K, Ahras M, Lall A, Hale C, Rodgers A, Young DB, Haque A, Billker O, Tregoning JS, Dougan G, Kellam P.** 2013. Defining the range of pathogens susceptible to Ifitm3 restriction using a knockout mouse model. *PLoS One* **8**:e80723.
65. **Perreira JM, Chin CR, Feeley EM, Brass AL.** 2013. IFITMs restrict the replication of multiple pathogenic viruses. *J Mol Biol* **425**:4937–55.
66. **Chan YK, Huang I-C, Farzan M.** 2012. IFITM proteins restrict antibody-dependent enhancement of dengue virus infection. *PLoS One* **7**:e34508.
67. **Raychoudhuri A, Shrivastava S, Steele R, Kim H, Ray R, Ray RB.** 2011. ISG56 and IFITM1 proteins inhibit hepatitis C virus replication. *J Virol* **85**:12881–9.
68. **Chutiwitoonchai N, Hiyoshi M, Hiyoshi-Yoshidomi Y, Hashimoto M, Tokunaga K, Suzu S.** 2013. Characteristics of IFITM, the newly identified IFN-inducible anti-HIV-1 family proteins. *Microbes Infect* **15**:280–90.

69. **Anafu A, Bowen CH, Chin CR, Brass AL, Holm GH.** 2013. Interferon-inducible transmembrane protein 3 (IFITM3) restricts reovirus cell entry. *J Biol Chem* **288**:17261–71.
70. **Jiang D, Weidner JM, Qing M, Pan X-B, Guo H, Xu C, Zhang X, Birk A, Chang J, Shi P-Y, Block TM, Guo J-T.** 2010. Identification of five interferon-induced cellular proteins that inhibit west nile virus and dengue virus infections. *J Virol* **84**:8332–41.
71. **Savidis G, Perreira JM, Portmann JM, Meraner P, Guo Z, Green S, Brass AL.** 2016. The IFITMs Inhibit Zika Virus Replication. *Cell Rep* **15**:2323–30.
72. **Compton AA, Bruel T, Porrot F, Mallet A, Sachse M, Euvrard M, Liang C, Casartelli N, Schwartz O.** 2014. IFITM Proteins Incorporated into HIV-1 Virions Impair Viral Fusion and Spread. *Cell Host Microbe* **16**:736–747.
73. **Yu J, Li M, Wilkins J, Ding S, Swartz TH, Esposito AM, Zheng YM, Freed EO, Liang C, Chen BK, Liu SL.** 2015. IFITM Proteins Restrict HIV-1 Infection by Antagonizing the Envelope Glycoprotein. *Cell Rep* **13**:145–156.
74. **Stacey MA, Clare S, Clement M, Marsden M, Abdul-Karim J, Kane L, Harcourt K, Brandt C, Fielding CA, Smith SE, Wash RS, Brias SG, Stack G, Notley G, Cambridge EL, Isherwood C, Speak AO, Johnson Z, Ferlin W, Jones SA, Kellam P, Humphreys IR.** 2017. The antiviral restriction factor IFN-induced transmembrane protein 3 prevents cytokine-driven CMV pathogenesis. *J Clin Invest* **127**:1463–1474.
75. **Foster TL, Wilson H, Iyer SS, Coss K, Doores K, Smith S, Kellam P, Finzi A, Borrow P, Hahn BH, Neil SJD.** 2016. Resistance of Transmitted Founder HIV-1 to IFITM-Mediated Restriction. *Cell Host Microbe* **20**:429–442.
76. **Warren CJ, Griffin LM, Little AS, Huang I-C, Farzan M, Pyeon D.** 2014. The antiviral restriction factors IFITM1, 2 and 3 do not inhibit infection of human papillomavirus, cytomegalovirus and adenovirus. *PLoS One* **9**:e96579.
77. **Muñoz-Moreno R, Cuesta-Geijo MÁ, Martínez-Romero C, Barrado-Gil L, Galindo I, García-Sastre A, Alonso C.** 2016. Antiviral Role of IFITM Proteins in African Swine

- Fever Virus Infection. PLoS One **11**:e0154366.
78. **Li K, Markosyan RM, Zheng Y-M, Golfetto O, Bungart B, Li M, Ding S, He Y, Liang C, Lee JC, Gratton E, Cohen FS, Liu S-L.** 2013. IFITM proteins restrict viral membrane hemifusion. PLoS Pathog **9**:e1003124.
 79. **Lin T-Y, Chin CR, Everitt AR, Clare S, Perreira JM, Savidis G, Aker AM, John SP, Sarlah D, Carreira EM, Elledge SJ, Kellam P, Brass AL.** 2013. Amphotericin B increases influenza A virus infection by preventing IFITM3-mediated restriction. Cell Rep **5**:895–908.
 80. **Williams DEJ, Wu W-L, Grotefend CR, Radic V, Chung C, Chung Y-H, Farzan M, Huang I-C.** 2014. IFITM3 Polymorphism rs12252-C Restricts Influenza A Viruses. PLoS One **9**:e110096.
 81. **Weidner JM, Jiang D, Pan X-B, Chang J, Block TM, Guo J-T.** 2010. Interferon-induced cell membrane proteins, IFITM3 and tetherin, inhibit vesicular stomatitis virus infection via distinct mechanisms. J Virol **84**:12646–57.
 82. **Jia R, Pan Q, Ding S, Rong L, Liu S-L, Geng Y, Qiao W, Liang C.** 2012. The N-terminal region of IFITM3 modulates its antiviral activity by regulating IFITM3 cellular localization. J Virol **86**:13697–707.
 83. **Xu-yang Z, Pei-yu B, Chuan-tao Y, Wei Y, Hong-wei M, Kang T, Chun-mei Z, Ying-feng L, Xin W, Ping-zhong W, Chang-xing H, Xue-fan B, Ying Z, Zhan-sheng J.** 2017. Interferon-Induced Transmembrane Protein 3 Inhibits Hantaan Virus Infection, and Its Single Nucleotide Polymorphism rs12252 Influences the Severity of Hemorrhagic Fever with Renal Syndrome. Front Immunol **7**:1–13.
 84. **Schoggins JW, MacDuff D a, Imanaka N, Gainey MD, Shrestha B, Eitson JL, Mar KB, Richardson RB, Ratushny A V, Litvak V, Dabelic R, Manicassamy B, Aitchison JD, Aderem A, Elliott RM, García-Sastre A, Racaniello V, Snijder EJ, Yokoyama WM, Diamond MS, Virgin HW, Rice CM.** 2014. Pan-viral specificity of IFN-induced genes reveals new roles for cGAS in innate immunity. Nature **505**:691–5.

85. **Daffis S, Lazear HM, Liu WJ, Audsley M, Engle M, Khromykh A a, Diamond MS.** 2011. The naturally attenuated Kunjin strain of West Nile virus shows enhanced sensitivity to the host type I interferon response. *J Virol* **85**:5664–5668.
86. **Daffis S, Szretter KJ, Schriewer J, Li J, Youn S, Errett J, Lin T-Y, Schneller S, Zust R, Dong H, Thiel V, Sen GC, Fensterl V, Klimstra WB, Pierson TC, Buller RM, Gale M, Shi P-Y, Diamond MS.** 2010. 2'-O methylation of the viral mRNA cap evades host restriction by IFIT family members. *Nature* **468**:452–6.
87. **Szretter KJ, Daniels BP, Cho H, Gainey MD, Yokoyama WM, Gale M, Virgin HW, Klein RS, Sen GC, Diamond MS.** 2012. 2'-O methylation of the viral mRNA cap by West Nile virus evades ifit1-dependent and -independent mechanisms of host restriction in vivo. *PLoS Pathog* **8**:e1002698.
88. **Cho H, Shrestha B, Sen GC, Diamond MS.** 2013. A role for Ifit2 in restricting West Nile virus infection in the brain. *J Virol* **87**:8363–71.
89. **Güssow D, Rein R, Ginjaar I, Hochstenbach F, Seemann G, Kottman A, Ploegh HL.** 1987. The human beta 2-microglobulin gene. Primary structure and definition of the transcriptional unit. *J Immunol* **139**:3132–8.
90. **Lee E-J, Park K-S, Jeon I-S, Choi J-W, Lee S-J, Choy HE, Song K-D, Lee H-K, Choi J-K.** 2016. LAMP-3 (Lysosome-Associated Membrane Protein 3) Promotes the Intracellular Proliferation of *Salmonella typhimurium*. *Mol Cells* **39**:566–572.
91. **Z. Z, Q. X, Y. W, Y. Y, J. W, T. H.** 2011. Lysosome-associated membrane glycoprotein 3 is involved in influenza A virus replication in human lung epithelial (A549) cells. *Virology* **438**:1–8.
92. **Friedman RL, Manly SP, McMahon M, Kerr IM, Stark GF.** 1984. Transcriptional and Posttranscriptional Regulation of Interferon-Induced Gene Expression in Human Cells **38**:745–755.
93. **Siegrist F, Ebeling M, Certa U.** 2011. The small interferon-induced transmembrane genes and proteins. *J Interferon Cytokine Res* **31**:183–97.

94. **Chesarino NM, Mcmichael TM, Yount JS.** 2014. Regulation of the trafficking and antiviral activity of IFITM3 by post-translational modifications **9**:1151–1163.
95. **Smith R, Young J, Weis JJ, Weis JH.** 2006. Expression of the mouse fragilis gene products in immune cells and association with receptor signaling complexes. *Genes Immun* **7**:113–21.
96. **Ling S, Zhang C, Wang W, Cai X, Yu L, Wu F, Zhang L, Tian C.** 2016. Combined approaches of EPR and NMR illustrate only one transmembrane helix in the human IFITM3. *Sci Rep* **6**:24029.
97. **Perreira JM, Chin CR, Feeley EM, Brass AL.** 2013. IFITMs restrict the replication of multiple pathogenic viruses. *J Mol Biol* **425**:4937–4955.
98. **Narayana SK, Helbig KJ, McCartney EM, Eyre NS, Bull RA, Eltahla A, Lloyd AR, Beard MR.** 2015. The Interferon-induced Transmembrane Proteins, IFITM1, IFITM2, and IFITM3 Inhibit Hepatitis C Virus Entry. *J Biol Chem* **290**:25946–25959.
99. **Zhang Y-H, Zhao Y, Li N, Peng Y-C, Giannoulatou E, Jin R-H, Yan H-P, Wu H, Liu J-H, Liu N, Wang D-Y, Shu Y-L, Ho L-P, Kellam P, McMichael A, Dong T.** 2013. Interferon-induced transmembrane protein-3 genetic variant rs12252-C is associated with severe influenza in Chinese individuals. *Nat Commun* **4**:1418.
100. **Wang Z, Zhang A, Wan Y, Liu X, Qiu C, Xi X, Ren Y, Wang J, Dong Y, Bao M, Li L, Zhou M, Yuan S, Sun J, Zhu Z, Chen L, Li Q, Zhang Z, Zhang X, Lu S, Doherty PC, Kedzierska K, Xu J.** 2014. Early hypercytokinemia is associated with interferon-induced transmembrane protein-3 dysfunction and predictive of fatal H7N9 infection. *Proc Natl Acad Sci U S A* **111**:769–74.
101. **Desai TM, Marin M, Chin CR, Savidis G, Brass AL, Melikyan GB.** 2014. IFITM3 restricts influenza A virus entry by blocking the formation of fusion pores following virus-endosome hemifusion. *PLoS Pathog* **10**:e1004048.
102. **Lescar J, Roussel A, Wien MW, Navaza J, Fuller SD, Wengler G, Wengler G, Rey FA.** 2001. The fusion glycoprotein shell of Semliki Forest virus: An icosahedral assembly

- primed for fusogenic activation at endosomal pH. *Cell* **105**:137–148.
103. **Smith TJ, Cheng RH, Olson NH, Peterson P, Chase E, Kuhn RJ, Baker TS.** 1995. Putative receptor binding sites on alphaviruses as visualized by cryoelectron microscopy. *Proc Natl Acad Sci U S A* **92**:10648–52.
 104. **Holland Cheng R, Kuhn RJ, Olson NH, Rossmann^Hok-Kin Choi MG, Smith TJ, Baker TS.** 1995. Nucleocapsid and glycoprotein organization in an enveloped virus. *Cell* **80**:621–630.
 105. **Steele KE, Twenhafel N.** 2010. REVIEW PAPER: pathology of animal models of alphavirus encephalitis. *Vet Pathol* **47**:790–805.
 106. **Weston S, Czieso S, White IJ, Smith SE, Wash RS, Diaz-Soria C, Kellam P, Marsh M.** 2016. Alphavirus restriction by IFITM proteins. *Traffic*.
 107. **Lange UC, Adams DJ, Lee C, Barton S, Schneider R, Bradley A, Surani MA.** 2008. Normal germ line establishment in mice carrying a deletion of the Ifitm/Fragilis gene family cluster. *Mol Cell Biol* **28**:4688–96.
 108. **Wakeland E, Morel L, Achey K, Yui M, Longmate J.** 1997. Speed congenics: A classic technique in the fast lane (relatively speaking). *Immunol Today* **18**:472–477.
 109. **Oliphant T, Engle M, Nybakken GE, Doane C, Johnson S, Huang L, Gorlatov S, Mehlhop E, Marri A, Chung KM, Ebel GD, Kramer LD, Fremont DH, Diamond MS.** 2005. Development of a humanized monoclonal antibody with therapeutic potential against West Nile virus. *Nat Med* **11**:522–30.
 110. **Oliphant T, Nybakken GE, Engle M, Xu Q, Nelson CA, Sukupolvi-Petty S, Marri A, Lachmi B-E, Olshevsky U, Fremont DH, Pierson TC, Diamond MS.** 2006. Antibody recognition and neutralization determinants on domains I and II of West Nile Virus envelope protein. *J Virol* **80**:12149–59.
 111. **Lazear HM, Pinto AK, Vogt MR, Gale M, Diamond MS.** 2011. Beta interferon controls West Nile virus infection and pathogenesis in mice. *J Virol* **85**:7186–7194.

112. **Dora S, Schwarz C, Baack M, Graessmann A, Knippers R.** 1989. Analysis of a large-T-antigen variant expressed in simian virus 40-transformed mouse cell line mKS-A. *J Virol* **63**:2820–2828.
113. **Araki T, Sasaki Y, Milbrandt J.** 2004. Increased nuclear NAD biosynthesis and SIRT1 activation prevent axonal degeneration. *Science* (80-) **305**:1010–1013.
114. **Cho H, Proll SC, Szretter KJ, Katze MG, Gale M, Diamond MS.** 2013. Differential innate immune response programs in neuronal subtypes determine susceptibility to infection in the brain by positive-stranded RNA viruses. *Nat Med* **19**:1–8.
115. **Tsetsarkin K, Higgs S, McGee CE, Lamballerie X De, Charrel RN, Vanlandingham DL.** 2006. Infectious Clones of Chikungunya Virus (La Réunion Isolate) for Vector Competence Studies. *Vector-Borne Zoonotic Dis* **6**:325–337.
116. **Morrison TE, Whitmore AC, Shabman RS, Lidbury BA, Mahalingam S, Heise MT.** 2006. Characterization of Ross River Virus Tropism and Virus-Induced Inflammation in a Mouse Model of Viral Arthritis and Myositis Characterization of Ross River Virus Tropism and Virus-Induced Inflammation in a Mouse Model of Viral Arthritis and Myositis. *J Virol* **80**:737–749.
117. **Smith SA, Silva LA, Fox JM, Flyak AI, Kose N, Sapparapu G, Khomandiak S, Ashbrook AW, Kahle KM, Fong RH, Swayne S, Doranz BJ, McGee CE, Heise MT, Pal P, Brien JD, Austin SK, Diamond MS, Dermody TS, Crowe JE.** 2015. Isolation and characterization of broad and ultrapotent human monoclonal antibodies with therapeutic activity against chikungunya virus. *Cell Host Microbe* **18**:86–95.
118. **Wahlberg JM, Garoff H.** 1992. Membrane fusion process of Semliki Forest virus. I: Low pH-induced rearrangement in spike protein quaternary structure precedes virus penetration into cells. *J Cell Biol* **116**:339–48.
119. **Bailey CC, Kondur HR, Huang I-C, Farzan M.** 2013. Interferon-induced transmembrane protein 3 is a type II transmembrane protein. *J Biol Chem* **288**:32184–93.
120. **Edwards J, Brown DT.** 1986. Sindbis virus-mediated cell fusion from without is a two

step event. *J Gen Virol* **67**:377–380.

121. **Fros JJ, Major LD, Scholte FEM, Gardner J, Van Hemert MJ, Suhrbier A, Pijlman GP.** 2015. Chikungunya virus non-structural protein 2-mediated host shut-off disables the unfolded protein response. *J Gen Virol* **96**:580–589.
122. **Hollidge BS, Weiss SR, Soldan SS.** 2011. The role of interferon antagonist, non-structural proteins in the pathogenesis and emergence of arboviruses. *Viruses* **3**:629–658.
123. **Ding S, Pan Q, Liu S-L, Liang C.** 2014. HIV-1 mutates to evade IFITM1 restriction. *Virology* **454–455**:11–24.

SUBHAJIT PODDAR

EDUCATION

- Washington University in St. Louis**, St. Louis, MO 2017
Ph.D. Immunology
- University of California at Berkeley**, Berkeley, CA 2007
B.S. Microbial Biology

RESEARCH EXPERIENCE

- Washington University in St. Louis**, Department of Medicine 2013 – Present
Graduate Student Researcher - *Michael Diamond Lab*
- Identification and characterization of novel murine antiviral interferon-stimulated genes against alphavirus infection.
 - Employed an shRNA library to screen for antiviral interferon-stimulated genes against chikungunya virus using flow cytometry.
 - Elucidated the protective role of interferon-stimulated gene *Ifitm3* against chikungunya virus in both cell culture and murine models of infection.
 - Characterizing the role of immune cell subsets in pregnancy and testicular health upon Zika virus infection.
- National Institutes of Health**, Viral Pathogenesis Section 2007-2009
Postbaccalaureate Research Fellow (IRTA) – *Ted Pierson Lab*
- Studied the pH dependent mechanisms of West Nile virus entry from host cells.
 - Tested the hypothesis that flavivirus pH dependent fusion is directed by histidine residues of the envelope protein.
 - Generated a series of WNV mutations lacking one or more histidine residues on the envelope protein using QuikChange mutagenesis.
 - Characterized the viability and pH sensitivity of each mutant.
- University of California at Berkeley**, Department of Plant and Microbial Biology 2003-2007
Undergraduate Researcher – *Krishna Niyogi Lab*
- Honors Thesis: Characterizing the genes for LOR3 and NSY in *Chlamydomonas reinhardtii*.
 - Mutagenized wild type *Chlamydomonas* using UV radiation, and screened for carotenoid deficiencies using HPLC

PUBLICATIONS

Miner JJ, Cook LE, Hong JP, Smith AM, Richner JM, Shimak RM, Young AR, Monte K, **Poddar S**, Crowe JE, Lenschow DJ, Diamond MS. *Combination therapy with CTLA4-Ig and an antiviral monoclonal antibody controls acute chikungunya virus arthritis*. 2017 Feb 1;9(375). Sci Transl Med.

Poddar S, Hyde JL, Gorman MJ, Farzan M, Diamond MS. *The interferon-induced gene IFITM3 restricts infection and pathogenesis of arthritogenic and encephalitic alphaviruses*. J Virol. 2016 Sep 12;90(19):8780-94.

Gorman MJ, **Poddar S**, Farzan M, Diamond MS. *The interferon-stimulated gene IFITM3 restricts West Nile virus infection and pathogenesis*. J Virol. 2016 Aug 26;90(18):8212-25.

Tran PT, Sharifi MN, **Poddar S**, Dent RM, Niyogi KK. *Intragenic enhancers and suppressors of phytoene desaturase mutations in Chlamydomonas reinhardtii*. PLoS One. 2012;7(8):e42196.

Nelson S*, **Poddar S***, Lin TY, Pierson TC. *Protonation of individual histidine residues is not required for the pH-dependent entry of West Nile virus: evaluation of the "histidine switch" hypothesis*. J Virol. 2009. Dec;83(23):12631-5.

POSTERS

Poddar S*, Hyde JL, Gorman MJ, Farzan M, Diamond MS. *IFITM3 protects against arthritogenic and encephalitic alphaviruses in vitro and in vivo*. Poster presentation at the Keystone Symposia on Positive-Strand RNA Viruses. Breckenridge. 2016.

Poddar S*, Wells A, Roswit W, Yun N, Paessler S, Patel AC, Holtzman MJ. *Response to H5N1-type Influenza A Virus Using Expression Microarrays*. Poster Presentation at the Asthma and Allergic Diseases Cooperative Research Center Meeting. St Louis. 2009

Poddar S*, Nelson S, Pierson TC. *Protonation of individual histidine residues is not required for the pH-dependent entry of West Nile virus: evaluation of the "histidine switch" hypothesis*. Meeting for the American Society of Tropical Medicine and Hygiene. New Orleans. 2008

*presenter

LAB RELATED SKILLS

- Tissue culture:** Growth and maintenance of primary and immortalized cell lines.
Experience with both mammalian and insect derived cells.
- Molecular biology:** DNA and RNA isolation from cell lines and tissue.
PCR and qRT-PCR.
Mutagenesis and cloning of plasmids using QuikChange, Gateway or restriction enzyme digestion.
Transfection and transduction of cell lines. DNA sequencing and analysis.
Knockdown and knockout of target genes involving shRNA, siRNA and CRISPR.
Gel electrophoresis and Western blots.
- Immunological-based:** ELISA and ELISPOT.
Flow cytometry of cell lines, mouse organs and PBMCs.
Production and maintenance of bone marrow derived primary macrophages.
Cytokine assays from tissues and serum.
- Virology:** Production and maintenance of virus.
Quantification of virus using qRT-PCR, flow cytometry or focus forming assay.
Analysis of viral infectivity via growth curves.
Analysis of virus binding, entry, transcription and egress.
- In vivo:*** General mouse handling.
Experience in ip, tail vein, and sc injections.
Isolation and preparation of tissue and organ samples for microscopy, flow cytometry, virological analysis, or histology.

REFERENCES

Dr. Michael Diamond, M.D., Ph.D.
The Herbert S. Gasser Professor
Departments of Medicine, Molecular Microbiology, Pathology & Immunology
Associate Director, The Andrew M. and Jane M. Bursky Center for Human Immunology and Immunotherapy
Programs
Washington University School of Medicine

Email: mdiamond@wustl.edu
Phone: 314-362-2842

Dr. Deborah Lenschow, M.D., Ph.D.,
Associate Professor
Departments of Medicine, Molecular Microbiology, Pathology & Immunology
Washington University School of Medicine

Email: dlenschow@wustl.edu
Phone: 314-362-8639

Dr. Marco Colonna, M.D.
The Robert Rock Belliveau MD Professor
Departments of Pathology & Immunology
Washington University School of Medicine

Email: mcolonna@wustl.edu
Phone: 314-362-0367

Dr Jacco Boon, Ph.D.,
Assistant Professor
Departments of Medicine, Molecular Microbiology, Pathology & Immunology
Washington University School of Medicine

Email: jboon@wustl.edu
Phone: 314-286-1522